Fliri, Lukas; Heise, Katja; Koso, Tetyana; Todorov, Aleksandar R.; del Cerro, Daniel Rico; Hietala, Sami; Fiskari, Juha; Kilpeläinen, Ilkka; Hummel, Michael; King, Alistair W.T.

Solution-state nuclear magnetic resonance spectroscopy of crystalline cellulosic materials using a direct dissolution ionic liquid electrolyte

Published in:
Nature Protocols

DOI:
10.1038/s41596-023-00832-9

Published: 01/07/2023

Document Version
Peer-reviewed accepted author manuscript, also known as Final accepted manuscript or Post-print

Solution-State Nuclear Magnetic Resonance Spectroscopy of Crystalline Cellulosic Materials using a Direct Dissolution Ionic Liquid Electrolyte

Lukas Fliri,[1] Katja Heise,[1] Tetyana Koso,[2] Aleksandar R. Todorov,[2] Daniel Rico del Cerro,[2] Sami Hietala,[2] Juha Fiskari,[3] Ilkka Kilpeläinen,[2] Michael Hummel[1,*] and Alistair W. T. King[2,4,*]

[1] Department of Bioproducts and Biosystems, Aalto University, P.O. Box 16300, FI-00076, Espoo, Finland
[2] Materials Chemistry Division, Department of Chemistry, University of Helsinki, FI-00560, Helsinki, Finland
[3] Fibre Science and Communication Network (FSCN), Mid Sweden University, SE-851 70, Sundsvall, Sweden
[4] VTT Technical Research Centre of Finland Ltd, Tietotie 4e, FI-02150, Espoo, Finland

Abstract

Owing to its high sustainable production capacity, cellulose represents a valuable feedstock for the development of more sustainable alternatives to currently used fossil fuel-based materials. Chemical analysis of cellulose remains challenging and analytical techniques have not advanced as fast as the development of the proposed materials science applications. Crystalline cellulosic materials are insoluble in most solvents which restricts direct analytical techniques to lower resolution solid state spectroscopy, destructive indirect procedures or to 'old-school' derivatisation protocols. While investigating their use for biomass valorisation, tetralkylphosphonium ionic liquids (ILs) exhibited advantageous properties for direct solution-state nuclear magnetic resonance (NMR) analysis of crystalline cellulose. After screening and optimisation, the IL tetra-*n*-butylphosphonium acetate [P_{4444}][OAc], diluted with DMSO-d_6, was found to be the most promising partly deuterated solvent system for high-resolution solution-state NMR. The solvent system has been used for the measurement of both 1D and 2D experiments for a wide substrate scope, with excellent spectral quality and signal-to-noise, all with modest collection times. The procedure initially describes the scalable syntheses of an IL, in 24 to 72 hours, of sufficient purity, yielding a stock electrolyte solution. The dissolution of cellulosic materials and preparation of NMR samples is presented, with pre-treatment, concentration and dissolution time recommendations for different sample types. Also included is a set of recommended 1D and 2D NMR experiments with parameters optimized for an in-depth structural characterization of cellulosic materials. The time required for full characterisation varies between a few hours and several days.

Keywords: NMR, nanocellulose, lignocellulose, crystallinity, direct dissolution, ionic liquid

Introduction

The ongoing worldwide ambitions to develop a more sustainable future include the search for bio-based and biodegradable alternatives for fossil fuel-based materials.[1] Owing to its abundancy and already high sustainable production capacities, cellulose represents a promising feedstock in bio-based materials development.[2] The relevance of cellulose and the possibilities it can offer are evident in the wide variety of daily encountered materials, made from paper, cardboard or cotton and the economic relevance of the industries involved in producing them. Less obvious in everyday life, also different cellulose derivatives like methylcellulose, cellulose acetate, cellulose nitrate or carboxymethyl cellulose have found widespread application as chemicals in a multitude of products and processes. While native cellulose and its slightly modified, *e.g.,* surface-modified, derivatives can be used for many applications, these materials are not amenable to melt processing. This means that shaping of the materials becomes more complicated and there are many cases where direct substitution of fossil fuel-based plastics is not possible.[3,4]

To expand the area of applications on a commercial scale, further processing of crystalline cellulosics, therefore, either relies on more laborious dissolution and regeneration techniques, or on derivatizations resulting in high degrees of substitutions (DS; number of substituent groups attached per monomeric unit of cellulose). Both approaches rely on excessive disposal or recycling of expensive chemicals, which elevates the cost of cellulosics in wide application, in comparison to petrochemically-derived materials. In the case of high DS cellulose derivatives the biocompatibility of the materials can also be affected. Similar ecological and economic considerations have also led to the motivation to optimize or rethink the processes used in the isolation of technical celluloses. Consequently, while the potential of cellulose as a renewable feedstock is evident, there is still room for improvement to reduce the ecological footprint of the materials and enhance their biocompatibility, and biodegradability, all at lower cost.

Strategies to achieve these goals are intensely researched. For example, in the subjects of whole plant biomass fractionation,[5,6] biofuel or chemicals production processes;[7,8] in the utilization of nano-scaled cellulose materials;[9,10] or in the production of more environmentally benign low DS or only surface modified cellulose derivatives, for tailor-made applications.[11] These emerging research topics are accompanied with new analytical challenges, which can be difficult to overcome with the currently available analytical toolbox. Thus, there is a need for additional high resolution and broadly applicable techniques.

Cellulose and NMR

Solution-state NMR spectroscopy is widely accepted as one of the most valued spectroscopic methods for both qualitative and quantitative structural determination in various disciplines of chemistry related research.[12-14] Over an approximately 50-year period, it has drastically transformed the utility of organic chemistry for other fields of natural sciences. However, for cellulose or plant-based materials, the application of solution state NMR was so far prevented by the inherent insolubility of the crystalline moieties, in all commonly available (per)deuterated solvents.[15] This is partly due to the amphiphilic nature of the bonding patterns that hold the cellulose crystalline lattice together. It also very much depends on the polymeric backbone rigidity introduced by strong intra- and intermolecular H-bonds, requiring strongly H-bond basic media to alleviate this rigidity.[16] Consequently, the applicable NMR techniques are predominantly restricted to solid state ^{13}C Cross-Polarization Magic Angle Spinning (CP MAS NMR). As will be described in detail below, these solid state NMR techniques have substantially expanded our understanding of different cellulose related phenomena, but they do not allow for high-resolution quantitative 1D and solely scalar-dependent 2D correlation experiments.

Following the discovery that certain ionic liquids (ILs) are powerful direct-dissolution solvents for cellulose,[17] as well as various other H-bond-stabilized biopolymers, research has uncovered several systems for this purpose.[18,19] Concomitantly, attempts to utilize non-deuterated imidazolium based ILs – the archetypical cellulose solvents – for solution state NMR applications were reported.[20-22] However, despite their high dissolving capabilities, several aspects, such as high chemical reactivity, make them a poor choice as an NMR solvent. Furthermore, there is little evidence that either of these approaches were implemented in other research institutes, as a standard protocol for solution state NMR of cellulose.

In our initial investigations towards tetraalkylphosphonium acetate-based ILs for their biomass processing and NMR analysis potential,[23,24] high solvating power for cellulose was observed in the respective DMSO electrolyte solutions for longer chain-length tetraalkylphosphonium acetates, even at very low ratios of IL to DMSO (low viscosity). Further to this, we have screened different homologues with different solvent ratios, and the tetra-*n*-butylphosphonium acetate $[P_{4444}]$[OAc]:DMSO-d_6 (1:4 wt%) electrolyte showed the best properties for every day usage in cellulose related research areas. The key advantages of this electrolyte compared to other reported systems can be summarized as follows:

- Preparation of $[P_{4444}]$[OAc] in high purity by metathesis from inexpensive and commercially available chloride or bromide salts.

- Great potential for dissolving cellulose at low IL contents, in terms of molar ratio of IL *vs.* anhydroglucose unit (AGU). With 80 wt% of DMSO-d_6 as perdeuterated co-solvent the relative signal intensities of the residual IL peaks can be drastically reduced.
- No signal overlap of the residual IL peaks with the cellulose backbone signals in the ^{1}H or ^{13}C spectral regions. This includes phasing artefacts in the 2D NMR spectra.
- Less aliphatic signal overlap due to its symmetry. With all aliphatic signals in a roughly similar signal intensity, problems with dynamic range are reduced for most experiments.
- Low viscosity cellulose solutions in concentrations relevant for NMR applications can be obtained at a comparably low measuring temperature of 65 °C. Lower temperatures prevent cellulose degradation and allow implementation of the protocol on less specialised NMR spectrometers.
- Finally, tetraalkylphosphonium salts are among the most stable of all the salt analogues, minimising IL degradation artifact formation during dissolution and analysis.

Nonetheless, we do not want to claim that the presented electrolyte represents the inherent "best" solution for every imaginable cellulose or biopolymer related NMR problem. Especially, as only a fraction of the known direct-dissolution cellulose solvents is so far investigated for applications in spectroscopy. Improvements in resolution and S/N are foreseeable, once synthesis for adequately (per)deuterated ILs, in reasonable quantity and costs, are elaborated. However, no serious investigations in this regard have yet started. Given the cost effective synthesis, the already proven broad applicability and developing know-how (see **Table 1**), [P_{4444}][OAc]:DMSO-d_6 (1:4 wt%) represents an excellent solution to many spectroscopic challenges. Furthermore, the availability of one generalized and commonly applied solution state NMR procedure enhances the comparability of results and allows to build up on previously reported studies.

Motivation and Content

The motivation for this protocol originated in the transfer of the optimised method to a more technology-orientated cellulose chemistry group. Despite a detailed description of the procedure in two previous publications utilising this electrolyte,[25,26] we observed a still modest knowledge barrier required in the preparation of a high purity IL precursor and in the practical and theoretical knowledge necessary for the correct choice of NMR experiments and associated parameters. These translational barriers are addressed in detail. Special emphasis

is laid onto the preparation of high-purity, low-cost [P_{4444}][OAc], following a straightforward metathesis scheme, and avoiding hazardous chemicals or more specialized laboratory equipment. Frequently encountered problems are also highlighted. In the NMR specific part, a set of 1D and 2D experiments is presented which allows for expedient characterization of the dissolved samples. The underlying principles or guidelines for the interpretation of the different NMR-experiments are not highlighted in detail, except for the clear utility of peak-fitting in the lower-resolution quantitative 1D ^{1}H experiment. Some peculiarities of the experiments and the obtained spectra are pointed out. The future potential and wide applicability are also demonstrated in a more extensive anticipated results section. However, the parameters of the common NMR experiments are listed, briefly discussed, and summarized for experienced in-house technical NMR operators, to implement and adapt to the available spectrometers.

While the common NMR experiments can provide extensive information on their own, other types of NMR experiments, or indeed non-NMR techniques, can be employed to refine this information. For example, to improve the confidence of some signal assignments, in particular those involving reducing end modification, preparation of model compounds is clearly advantageous.[27,28] We also wish to emphasize that the purpose of this method is not to replace the alternative analytics but to complement them, with higher resolution of chemical species. However, it should be appreciated that there is now the opportunity to elevate cellulose chemistry analytics close to the same analytical standards that low molecular weight synthetic chemists have enjoyed for over 50 years.

Development of the protocol

The protocol arose out of efforts to develop more recyclable ILs for biomass processing. The now archetypical imidazolium chloride and acetate-based ILs are excellent solvents for cellulose. However, imidazolium-based ILs are known to suffer from chemical and thermal instability, which is enhanced by the strong basicity and nucleophilicity of the anion[29,30] – one of the same features that makes them such good solvents for cellulose. Meanwhile, several studies confirm that imidazolium halides and carboxylates react with cellulose and can cause notable depolymerization,[31-33] with the basic anions promoting the reaction of the imidazolium C-2 position with the reducing end. Common impurities, *e.g.,* imidazoles, further have a strong catalytic effect on the reaction of the imidazolium cation with reducing ends, or can enhance transacylation reactions.[34-36] For solution-state NMR, prolonged collection times at elevated temperatures and high dilution are often required to obtain well-resolved spectra of polymeric materials. Thus, these known instabilities limit the use of imidazolium-based ILs for artifact-free NMR analysis. Consequently, more stable and less acidic cations are required. The long

chain homologues of tetraalkylphosphonium acetates proved to be highly effective and inert solvents for cellulose, even as their electrolytes in dipolar aprotic solvents.[23] This facilitated the production of rather low-viscosity cellulose solutions (~3-8 wt%) with a majority of DMSO-d_6 as the necessary co-solvent to provide well-resolved spectra.[24] As an added benefit, the IL signals did not overlap with the cellulose backbone signals in the ^{1}H or ^{13}C spectral regions, as opposed to the dialkylimidazolium salts. As mentioned above [P_{4444}][OAc] emerged as the most promising congener in screenings among these initial phosphonium structures. So far, artifact formation through cellulose degradation can mostly be avoided, due to the increased stability of the cation, if the IL is prepared correctly. The development of the method can be followed in the already published literature, in which a wide range of substrates and methods have been applied, using this and similar electrolytes (**see Table 1**). Optimum conditions for dissolution and analysis of cellulosic materials were found to be 5 wt% (cellulose in electrolyte solution) and a sample temperature of 65 °C. The method and a set of NMR experiments were initially thoroughly described for investigations in nanocellulose modifications.[25] Furthermore, detailed spectral assignment of different model compounds was performed using these settings, useful as references for further investigations.[26]

One bottleneck preventing an expansion of the protocol, until now, was the cumbersome synthesis of the needed high-purity IL, following metathesis procedures starting from an isomerically pure form of [P_{4444}]Cl. This included working with pyrophoric tri-*n*-butylphosphine under inert atmosphere, and – owing to the high hygroscopicity of the chloride analogue – H_2O uptake during preparation had to be meticulously avoided.[25] Besides the difficult removal in the final drying steps, H_2O also influences the exact stoichiometry and the solubility of the metathesis products, leading to incomplete conversions. These metal cation-containing impurities can in turn lead to catalytic degradation of the cellulosic materials during the dissolution and data collection stages. Although the metathesis can be performed by a skilled chemist, on a smaller scale, these peculiarities have frustrated both upscaling and successful reproduction of the synthesis in less specialized laboratories. In efforts to simplify the synthesis, the commercial phase-transfer catalyst [P_{4444}]Br was identified as excellent low cost starting material (see **Fig. 1**). In contrast to other [P_{4444}] salts, isomeric impurities in the bromide congener can be removed by careful recrystallization.[37] For the transformation to the acetate salt, two metathesis schemes were elaborated. The first was adapted from a protocol reported for [P_{4444}][COO],[37] using a cost efficient and scalable two-step approach over ammonium tetrafluoroborate [NH_4][BF_4] and KOAc (see **Fig. 1a**). The second focuses on a one-step procedure using AgOAc,[25] ideal for smaller scale laboratory preparations (see **Fig. 1b**).

Table 1. Summary of original publications in which tetra-*n*-alkylphosphonium acetates were used for the acquisition of solution-state NMR spectra of cellulosic materials. The investigated material and the performed analyses are listed.

Sample Type:	**Electrolyte:**	**Analyses:**	**Ref.**
MCC	$[P_{8881}]$[OAc]:DMSO-d_6	Signal assignment – HSQC	23
Whole wood	$[P_{4444}]$[OAc]:DMSO-d_6	Comparison of wood solubility after pre-treatment from cellulose ^{1}H signal intensities – ^{1}H	38
Cellobiose, MCC, sc-H_2O extracted MCC (residue), B-Spruce-Sul pulp, B-Euca-PHK pulp, Bacterial cellulose, cotton lint., acid-hyd-cotton, enz-hyd-cotton, XYL (Oat spelt), GRX (Birch) & GGM (Spruce)	$[P_{8881}]$[OAc]:DMSO-d_6	Signal assignments (HSQC) and quantification of REGs – ^{1}H, HSQC, TOCSY, peak-fitting in Mnova for DP_n determination.	24
MCC	$[P_{8888}]$[OAc]:DMSO-d_6	Demonstration of MCC dissolution into the electrolyte – ^{1}H	39
Acetylated CNFs	$[P_{4444}]$[OAc]:DMSO-d_6	Confirmation of acetylation and partial HSQC signal assignment – diffusion-edited ^{1}H (stacked DOSY array) and HSQC	40
Esterified CNCs	$[P_{4444}]$[OAc]:DMSO-d_6	Confirmation of esterification and partial signal assignment – ^{1}H, diffusion-edited ^{1}H & ^{13}C	41,42
PMMA-*g*-CNCs	$[P_{4444}]$[OAc]:DMSO-d_6	Thorough 2D assignments, including the PMMA tacticity, C6-sulphate half ester signals. Polymer ratios, graft lengths and graft densities were also determined – ^{1}H, diffusion-edited ^{1}H, HSQC, diffusion-edited HSQC, quantitative ^{13}C	25
IL-welded CNF films	$[P_{4444}]$[OAc]:DMSO-d_6	Samples were analysed for presence of residual IL – ^{1}H	43
Esterified & IL-welded BSK pulp films	$[P_{4444}]$[OAc]:DMSO-d_6	Confirmation of esterification and presence/absence of residual IL was made – ^{1}H, diffusion-edited ^{1}H & HSQC	44
REG modified CNCs	$[P_{4444}]$[OAc]:DMSO-d_6	Confirmation and semi-quantitation of the Knoevenagel condensation at REGs. DP_n was also calculated for the starting CNCs – ^{1}H, diffusion-edited ^{1}H, HSQC, HSQC-TOCSY, band-selective TOCSY, HMBC and peak-fitting in *fityk* for DP_n determination	27
Wet-spun fibers from PHK pulp and TEMPO-oxidized pulp	$[P_{4444}]$[OAc]:DMSO-d_6	Compositional analysis of the regenerated fibers - presence of residual IL was determined using ^{1}H and HSQC	45
Acetylated BHK pulps	$[P_{4444}]$[OAc]:DMSO-d_6	DS determination (^{1}H) & signal assignment (HSQC) – ^{1}H, diffusion-edited ^{1}H, HSQC, HSQC-TOCSY and peak-fitting in *fityk* for DS determination	46
glucose, gluconic acid, glucuronic acid, cellobionic acid, sc-H_2O extracted MCC-residue, TEMPO-ox cellulose, periodate-ox cellulose, RE-ox-cellulose, MCC	$[P_{4444}]$[OAc]:DMSO-d_6	Thorough signal assignments (HSQC) and assessment of quantitative HSQC for quantifying chemical modifications – ^{1}H, diffusion-edited ^{1}H, HSQC, HSQC-TOCSY, HMBC, Q-CAHSQC, peak-fitting in *fityk* for DP_n determination	26
Acetylated-B-Beech-Sul. pulp	$[P_{4444}]$[OAc]:DMSO-d_6	Determination of DS and regioselectivity of surface acetylation - ^{1}H, diffusion-edited ^{1}H, HSQC and peak-fitting in *fityk* for DS and regioselectivity determination	42
PSS-RE-*g*-CNCs before and after reductive amination, ATRP initiator introduction and grafting steps.	$[P_{4444}]$[OAc]:DMSO-d_6	Confirmation of reaction at each stage through a combination of experiments – ^{1}H, diffusion-edited ^{1}H, HSQC, HSQC-TOCSY, HMBC, peak-fitting in *fityk* for determination of graft introduction	28
Succinylated Cellulose	$[P_{4444}]$[OAc]:DMSO-d_6	Confirmation of reaction, crude regioselectivity and DS determination	47
Acetylated CNCs, CNC aerogel, B-H-PHK pulp, B-Beech-Sul. pulp, IONCELL fibres	$[P_{4444}]$[OAc]:DMSO-d_6	Determination of DS and regioselectivity of acetylation	48

Acetylated-B-Beech-Sul. pulp – bleached beech sulphite dissolving-grade pulp; acid-hyd-cotton – acid-hydrolysed cotton; ATRP – atom transfer radical polymerization; B-Euca-PHK pulp – Bahia PHK pulp (a hardwood pulp from Eucalyptus); BHK pulps – bleached hardwood pre-hydrolysis kraft pulp; BSK pulp – bleached softwood kraft pulp; B-H-PHK pulp – bleached pre-hydrolysis hardwood (mainly birch) kraft pulp; B-Spruce-Sul pulp – Borregaard Super VS sulfite pulp (a softwood pulp from spruce); CNC – cellulose nanocrystals; CNF – cellulose nanofibers; cotton lint. – cotton linters; DOSY – Diffusion Ordered SpectroscopY; DP – degree of polymerization; DS – degree of substitution; enz-hyd-cotton – enzymatically hydrolysed cotton; GGM – birch galactoglucomannan; GRX – birch glucuronoxylan; HMBC – Heteronuclear Multiple Bond Correlation; HSQC – Heteronuclear Single Quantum Coherence; IL – ionic liquid; MCC – microcrystalline cellulose; periodate-ox cellulose – periodate oxidised cellulose; PHK pulp – Birch prehydrolysis Kraft pulp; PMMA-*g*-CNCs – poly (methyl methacrylate) grafted CNCs; PSS-RE-g-CNCs – poly (styrene sulfonate) reducing end group grafted CNCs; $[P_{8881}]$[OAc]:DMSO-d_6 – tetra-*n*-butylphosphonium acetate diluted in DMSO-d_6; Q-CAHSQC – Quantitative CPMG-Adjusted HSQC (CPMG for an evenly spaced 180° pulse train named after its inventors, Carr, Purcell, Meiboom and Gill); REGs – reducing end groups; RE-ox-cellulose – reducing end-group oxidised cellulose; sc-H_2O – supercritical water; TEMPO – 2,2,6,6-Tetramethylpiperidin-1-yl)oxyl; TOCSY – Total Correlation SpectroscopY; XYL – Xylan from oat spelt

211 ## Overview of the Protocol

212 The protocol can be separated in three distinct steps. First, the [P_{4444}][OAc] is synthesized in
213 larger quantities to provide enough IL for several measurements (**Fig. 1a** or **1b**). An aliquot
214 thereof is diluted with DMSO-d_6 (1:4 wt%) to obtain the NMR electrolyte. In the second step,
215 the cellulosic samples are prepared for measurement by dissolution in the electrolyte (2.5 – 5
216 wt%) at 65 °C and transferred to the NMR tube (**Fig. 1c** and **e**). Once the material is dissolved,
217 in the third step, the NMR experiments are performed.

218 The choice of experiments depends on the qualitative and quantitative information required.
219 We propose a set of three NMR experiments, for a preliminary analysis of both native, and
220 chemically modified cellulosic materials (**Box 1, Section I**). If needed, thorough peak
221 assignment and quantification can be performed with selected 2D heteronuclear multiple bond
222 correlated experiments and ^{13}C NMR (**Box 1, Section II**). Although not described in more
223 detail in this protocol, also other measurements can be performed with the dissolved samples
224 (**Box 1, Section III**).

225

226 **BOX 1 Overview of commonly used 1D and 2D solution-state NMR**
227 **experiments**

228 The image within this box, summarises the parameters for the most commonly used NMR
229 experiments[25,26] for cellulose samples in [P_{4444}][OAc]:DMSO-d_6 (1:4 wt%) at 65 °C. This
230 includes their recommended acquisition order and the principal information received from
231 each experiment. The listed exemplary scan numbers and collection times are based on our
232 experience to obtain workable spectral quality on a 400 MHz or 600 MHz spectrometer (see
233 Reagent and Equipment section for details). They might vary depending on the available
234 equipment. The choice of experiments strongly depends on the sample under investigation
235 and the anticipated results.

236 We recommended to always start the data collection with the quantitative ^{1}H, diffusion-edited
237 ^{1}H and multiplicity-edited HSQC experiments (**I**).

238 To aid in peak assignment and quantitation, a set of further 1D and 2D experiments have
239 proven to be very useful (**II**).

240 Other experiments can also be successfully applied if the standard experiments are not
241 sufficient for signal assignment or quantitation (**III**).

242 Experiments of sections **I** and **II** are presented in more detail in **Procedure 2**.

Suggested acquisition order, preliminary number of scans (f1 increments[a])[b] and collection times			Principle information received through the NMR technique
(I) Initial experiments			Important for initial confirmation of covalent modification, impurity determination and/or quantitation
1D – ^{1}H (quantitative)[c]	16 scans	8 min	Quantitative proton spectrum
1D – Diffusion-edited ^{1}H	32-1024	5-60 min	Confirmation of covalent attachment by editing out the fast-diffusing species (DMSO, IL or other impurities)
2D – Multiplicity-edited ^{1}H-^{13}C HSQC	8 (512 increments)	2:30 h	^{1}H-^{13}C single-bond ($^{1}J_{CH}$) correlations with identification of multiplicity
Good spectral quality			
(II) Experiments for signal assignments & quantitation			
1D – ^{13}C (qualitative)	1024	3:00 h	Qualitative carbon spectrum
1D – ^{13}C (quantitative)[d]	8192	15 h	Quantitative carbon spectrum
2D – ^{1}H-^{13}C HSQC-TOCSY[e,f]	8 (512)	2:30 h	^{1}H-^{13}C single-bond ($^{1}J_{CH}$) to ^{1}H-^{1}H multiple bond ($^{3}J_{HH}$) correlations
2D – ^{1}H-^{13}C HMBC	32 (512)	2:15 h	Long-range ^{1}H-^{13}C correlations ($^{2\text{-}4}J_{CH}$)
(III) Additional experiments			
2D – ^{1}H-^{13}C HSQC-NOESY[e-g]	32[f] (256)	5:00 h	^{1}H-^{13}C single-bond ($^{1}J_{CH}$) to through-space ^{1}H-^{1}H correlations (NOE)
2D – ^{1}H-^{13}C HSQC (quantitative)[h]	16 (256)	15 h	Quantitative ^{1}H-^{13}C single-bond ($^{1}J_{CH}$) correlations
2D – ^{1}H-^{13}C HSQC (diffusion-edited)	16 (256)	2:30 h	^{1}H-^{13}C single-bond ($^{1}J_{CH}$) correlations with significant (but incomplete) attenuation of fast-diffusing species
2D – ^{1}H-^{15}N HMBC	8 (64[i])	20 min	Long-range ^{1}H-^{15N} correlations ($^{2\text{-}4}J_{NH}$)

[a] 'td' for f1 - the number of transients (real and imaginary).

[b] S/N is proportional to the square root of the number of scans and f1 resolution is proportional to the number of f1 increments – until ~256 real increments for ^{13}C HSQC – above which the proportionality decreases as you approach the natural linewidth.

[c] Cellulose backbone ^{1}H T_1 values range between 1-2.25 s (MCC, 600 MHz)[26] – additional, more conformationally free, functionalities may have even longer T_1 values so a conservative guestimate for the relaxation delay to achieve quantitative conditions (5 × T_1), for a wide range of modifications, is ~ 20 s for a 90° flip angle or ~ 8 s for a 30 ° flip angle.

[d] Cellulose backbone ^{13}C T_1 values range between 0.27-0.53 s (cotton CNCs, 600 MHz)[25] – additional, more conformationally free or quaternary, functionalities may have even longer T_1s so a very conservative guestimate for the relaxation delay to achieve quantitative conditions (5 × T_1), for a wide range of modifications, is ~ 10 s for a 90° flip angle or ~ 5 s for a 30° flip angle.

257 [e] Short (~ 15 ms) TOCSY mixing times yield COSY-like cross-correlations (showing mainly 3-
258 bond CH correlations), whereas long (~120 ms) TOCSY mixing times give total correlation, at
259 the expense of reduced S/N.

260 [f] 2D HSQC-TOCSY/NOESY is preferred over 2D TOCSY/NOESY as the use of the ^{13}C
261 dimension in f1 affords additional resolution over using two ^{1}H dimensions, again, at the
262 expense of S/N.

263 [g] In the HSQC-NOESY experiment, short (demonstrating shorter range NOE) mixing times
264 (25 ms) yield quite low cross-peak S/N, which may be a problem for detecting correlations for
265 low abundance species or high molecular weight samples – if this is so, increasing the scans
266 may help – alternatively, HSQC-ROESY may offer better cross-peak S/N or one can resort to
267 the lower resolution 2D NOESY or ROESY experiment.

268 [h] Cellulose backbone ^{1}H T_1 values (HSQC is a ^{1}H detected experiment) range between 1-2.25
269 s (MCC, 600 MHz)[26] – additional, more conformationally free, functionalities may have even
270 longer T_1 values so a conservative guestimate for the relaxation delay to achieve quantitative
271 conditions (5 × T_1), for a wide range of modifications, is ~ 20 s and ~10 s for quantification of
272 the cellulose backbone signals – in practice the T_1 values may be much shorter than the
273 existing measured ^{1}H T_1 values,[26] as relaxation is for ^{1}H directly attached to ^{13}C (spin ½), and
274 not ^{12}C – cross-peak integral values also need correction for T_2 losses during the pulse
275 sequence[26] the number of f1 increments can typically be quite low as there are typically few
276 ^{15}N resonances that need to be resolved in such spectra, in the f1 (^{15}N) dimension.

277 **END OF BOX 1**

278

279

Comparison with other methods

Non-NMR techniques in cellulose analytics

The longstanding interest in cellulosic materials has resulted in the development of various analytical methods for the characterization of their chemical composition.[49-51] Many classic techniques originated from quality control-based analytics in the pulp and paper industries and were developed during the last century, *e.g.*, intrinsic viscosity, kappa number or alpha cellulose content. They often rely on work intensive indirect and / or destructive procedures, which were standardized, often with arbitrary scales. Although, they can be regarded as very reliable and comparable in general, when transferring these trusted techniques to currently intensively investigated novel cellulosic materials, their value can even be detrimental. As these indirect approaches would require careful and laborious adaptions of their parameters, in many cases correlation against or replacement with direct spectroscopic procedures may be advantageous.

In material-related studies using cellulose, spectroscopy is hampered by poor availability or by low spectral (chemical) resolution offered by solid-state techniques. Thus, different spectroscopic or diffraction techniques have been typically combined, *e.g.*, solid-state NMR, IR spectroscopy,[52-54] Raman spectroscopy[55-57] or X-ray photoelectron spectroscopy (XPS),[58-60] delivering more qualitative or semi-quantitative information. Chemical and spatial resolution of these methods is typically poor. Yet long-range structural ordering is often retained, which is lost in the solution-state. XPS especially is a very surface-sensitive method (top < 10 nm),[61] thus, preventing bulk quantification and making the measurement highly sensitive to the sample preparation. For example, in the emerging field of cellulose-based nanomaterials, where cellulose nanocrystals (CNCs) or cellulose nanofibrils (CNFs) are common substrates, these analytical limitations are a considerable problem. Controlled regioselective chemistry, *e.g.*, at the surface or reducing end groups of CNCs,[27] typically yield introduction of only a small bulk degree of substitution (DS). However, these regioselective chemistries can have a large contribution to supramolecular interactions and the materials properties. For quantification, the determination of DS values or surface grafting densities is commonly achieved through elemental analysis (EA).[52,59,62,63] Low degrees of surface modification commonly fall below the detection limit of classical CHN(S) EA and necessitate the introduction of either nitrogen or sulphur containing moieties to be detectable. Furthermore, IR, Raman and XPS are more limited in species resolution and may not be able to distinguish between surface adsorption of compounds or actual covalent modification. Despite this, they are often more expedient methods for certain tasks and can yield rapid results when calibrated against direct quantitative methods.[64]

315 Other widely applicable indirect approaches for quantifying functional groups, after chemical
316 modification, can be found in different titration (*e.g.,* for carboxylate[65,66] or carbonyl
317 functionalities[67,68]) or labelling protocols combined with chromatography (*e.g.*, 'FDAM' or
318 'CCOA' methods).[69-71] However, these methods rely on the presence of reactive groups and
319 are dependent on stoichiometric transformation, which may not be suitable for more
320 heterogeneous/irregular samples. Moreover, they are usually laborious and often require
321 larger sample amounts to facilitate multiple replicate measurement. In fact, these alternative
322 methods all have value and should be applied to complement each other in improving reliability
323 and speed of analysis. As mentioned previously, the main feature of the application of solution-
324 state NMR, in this context, is the drastic improvement in resolution of chemical species, offered
325 by bulk solution-state analysis.

326 **Solid-State NMR in cellulose research**

327 The aforementioned solubility issues of crystalline cellulosic materials have previously
328 restricted NMR investigations mostly to solid-state studies. These have a long reputation in
329 the analysis of crystalline cellulosics and were made experimentally accessible with the
330 application of proton-enhanced nuclear induction spectroscopy (PENIS),[72] also known as
331 cross-polarisation (CP) and magic-angle spinning (MAS).[73] In the combined technique ^{13}C CP
332 MAS NMR, CP is typically used to enhance the signal intensity of carbon resonances, with
333 protons directly attached. Different improvements of this technique have led to spectra in
334 which mainly the chemical shift variation arising from the restricted conformations in the solid-
335 state is visible, giving valuable information about crystallinity encoded into the chemical shifts.
336 Thorough assignment of the crystalline and non-crystalline phases of cellulose has been
337 performed by a combination of discrimination of chemical shifts, based on variable relaxation
338 of crystalline and non-crystalline phases, and by correct choice of model materials.[74-76] While
339 ^{13}C CP MAS has become very useful in the semi-quantitative determination of crystallinity of
340 cellulose samples, resolution and signal-to-noise ratio (S/N) are still limited in monitoring many
341 chemical modifications, especially those modifications that have low degrees of conversion,
342 *e.g*. in the direct confirmation of reducing end group modifications. True quantitation of such
343 resonances is also much more problematic as direct polarisation of ^{13}C would be required
344 (lower S/N), relying on relaxation delays (5 × T_1) based on the much longer ^{13}C T_1 values.
345 Therefore, comparing the solution vs solid-state techniques in cellulose research, solid-state
346 NMR utilising CP and MAS is useful for following changes in crystallinity,[77] or investigating
347 supramolecular phenomena like hornification,[78] and interactions with other plant
348 constituents.[79] It is also relatively sensitive towards changes in chemical species, that do not
349 overlap with the cellulose backbone signals, *e.g*., carbonyls. This can of course be adopted
350 as a relatively rapid quantitative analysis, using calibration. By contrast, all long-range material

351 ordering is lost in solution-state NMR (dissolved samples). However, the rapid signal
352 averaging that solvation affords increases resolution to such a level to allow for increased
353 peak separation (**Fig. 2**), with the further advantage of reduced collection times for quantitation
354 (compared to quantitative solid-state NMR using direct polarisation). Noteworthy, 2D NMR
355 experiments were also reported in solid-state NMR investigations of cellulose.[77,80] However,
356 these normally require specialized equipment and long collection times, thus practically
357 restricting the information obtainable from solid-state measurements to ^{13}C NMR. In turn, the
358 presented protocol allows to take advantage of high-resolution 2D experiments in reasonable
359 collection times even with commonly available NMR spectrometers.

360 **Alternative solution-state NMR procedures for cellulose**

361 Owing to the intrinsic benefits of solution-state NMR, notable investigations towards a direct
362 method for analysing whole biomass or cellulosic samples have been previously contributed
363 by several groups. Imidazolium based ILs have been used for dissolution of cellulose-rich
364 samples.[20-22, 31] However, the previously discussed inherent instability of imidazolium cations,
365 and the potential for signal-overlap makes these poor choices for artifact-free analyses. Many
366 more indirect solution-state NMR methods exist for analysis of cellulose or whole biomass,
367 after chemical derivatization (*e.g.*, phosphitylation,[81] perpropionylation[82] and acetylation[83,84])
368 to render the cellulose fractions soluble in common perdeuterated solvents. However, this
369 obviously introduces further potential for artifact formation, requires additional laborious
370 derivatization steps and has a considerable effect on the chemical shifts of nuclei near the
371 derivatization sites. In some cases, this may be beneficial as it offers an additional method to
372 resolve signals that may overlap in the underivatized state (*e.g.*, in lignin acetylation).[85,86]

373 Notably, solution-state NMR investigations were also conducted in whole plant cell-wall
374 analysis and established protocols have been reported by the groups of Ralph[87] and
375 Ragauskaus.[88] However, these methods are largely restricted to the analysis of cell-wall
376 polymers other than cellulose, as the used solvent systems are not capable of dissolving
377 cellulose without degradation.

378 Thus, there are important solutions for the analysis of various cell-wall polymers, and indeed
379 whole cell-wall material. However, none of the mentioned approaches offers rapid and artifact-
380 free direct quantitation for crystalline cellulosic materials nor have emerged as a standard to
381 follow. A general procedure would be of great value as this could drastically enhance
382 comparability and reproducibility of different investigations and methods.

383

384 ## Applications of the method

385 The protocol was developed and optimized for the direct analysis of crystalline cellulose
386 (including presence of cellulose I or cellulose II allomorph groups) and lignocellulosics, in
387 various stages of purification or chemical modification (see **Table1**). In recent investigations,
388 the electrolyte showed excellent applicability in the confirmation and quantification of chemical
389 modifications, of relatively low DP cellulosic materials (predominantly CNC and MCC).[25,26] It
390 was even possible to follow regioselective reactions on reducing end groups in nanocelluloses,
391 which is regarded as a distinctive analytical challenge.[27,28] The targeted audience includes a
392 large share of the cellulose community and we are optimistic, that the presented procedure
393 can contribute to refining our structural understanding of modified lignocellulosics and
394 generation of novel structural information, not previously attainable. We hope to promote this
395 method especially for (bio-)chemical engineers working on chemical modification of purified
396 or whole lignocellulosics, the valorisation of lignocellulosics, plant biomass analytics (*e.g.*,
397 biofuels, fractionation), chemical structural specification of lignocellulosic biomass fractions
398 (*e.g.*, chemical pulps, nanocelluloses), or on the chemical structural analysis of native or
399 purified lignocellulosics (cellulose sources or whole plant material).

400 An expansion of the protocol to other biopolymeric or biocomposite materials, regarded as
401 insoluble in common NMR solvents, is conceivable. In pretrials, the presented protocol was
402 applied to silk, textile wool, spruce galactoglucomannan (GGM), birch glucuronoxylan (GX),
403 chitin and chitosan.[25] Thereby, the electrolyte gave good quality solutions and well resolved
404 spectra for all but two (chitin and chitosan) samples. Further preliminary investigations
405 potentially target applications in whole wood analysis and fingerprint analytics and quality
406 control of insect-derived food materials (see **Example IV** in Anticipated Results Section).
407 Thus, there may also be potential for metabolomic studies, *e.g.*, using engineered plant
408 materials, fungi or insects. However, the system is not yet fully tested or optimized for other
409 biopolymers and probably needs adaptions in both the dissolution as well as the NMR specific
410 steps, to guarantee for optimal results.

411 Experimental design and limitations

412 Solubility and stability in the electrolyte

413 As was already mentioned above and as will be highlighted in more detail in the Anticipated
414 Results Section, the protocol can be applied to a broad spectrum of cellulosic materials and,
415 to a certain extent, to other polymers. After preparation of the electrolyte, solubility and stability
416 of the sample under investigation represent the major issues for the application of the
417 presented protocol. Although we observed some general trends therein, the adaptability will
418 still strongly rely on basic investigative studies.

419 In applications of the protocol focusing on the analytics of native cellulosic materials, *e.g.*, in
420 measurements to investigate differences in the composition of materials obtained from various
421 sources, problems are likely to arise in samples with very high degrees of polymerization (DP).
422 These are more difficult and slower to dissolve in the presented electrolyte. Furthermore, the
423 high viscosity of the dissolved sample might result in more challenging sample handling (*e.g.*,
424 transfer to the bottom of the NMR tube) when preparing the solution and a reduced spectral
425 resolution. The same applies to modified cellulosics that are crosslinked. Increasing the
426 temperature during dissolution and reducing the analyte concentration (*e.g.*, from 5 wt% to 2
427 wt%) can alleviate these problems to some extent. However, spectral resolution is still highly
428 dependent on molecular weight and analyte concentration. Highly cross-linked samples may
429 not dissolve at all rendering quantitation impossible. Although, even swollen samples may give
430 valuable information, after measurement, in some cases.

431 In the field of cellulose chemistry, some limitations of the protocol arise from the chemical
432 properties of the used $[P_{4444}]$[OAc]-based electrolyte. The acetate anion in DMSO-d_6
433 possesses considerable basicity, which for example led to fragmentation of dialdehyde
434 cellulose owing to *β*-elimination.[26] Additionally, its nucleophilicity may cause reactions with
435 more fragile introduced modifications, *e.g.*, in the presence of electrophiles such as tosyl
436 cellulose, leading to cellulose acetylation. In this case, an indirect determination of the
437 modification through conversion of the labile functionality to a more chemically stable and
438 spectrally unique derivative is possible. However, if full conversion to acetate is possible,
439 quantitation and regioselective assignments are already well documented.[48,84] Furthermore,
440 we observed catalytic degradation phenomena of cellulose, if trace amounts of certain
441 impurities are present in the electrolyte. Although not completely understood yet, these
442 problems were attributed to residual metal ions or excess acetic acid introduced by an
443 incomplete metathesis. However, it is likely that impurities present in the sample under
444 investigation can also cause the same phenomena. Thus, it is important to thoroughly purify
445 the substrate before conducting the protocol. Notably, we also observed insolubility of
446 cellulosics after introduction of a high anionic surface charge, *e.g.,* through TEMPO oxidation
447 and regeneration at higher pH. However, a simple acidification procedure, which was
448 summarized in the Supplementary Information of a previous article,[26] rendered the material
449 soluble and measurable.

450 When using the protocol to investigate cellulose chemistry, the introduced bulk chemical
451 modifications can render the material soluble in common perdeuterated organic NMR
452 solvents. This is strongly dependent on the nature of the derivatization and solubilisation
453 usually requires a higher degree of substitution. If full solubility in classic organic solvents is
454 observed or was reported for similarly modified derivatives, we always recommend using

455 standard NMR solvents instead of the presented electrolyte. The absence of the residual non-
456 deuterated IL peaks will increase the accessible spectral area, maximise S/N (no dynamic
457 range issues) and in general result in higher resolution spectra. Nonetheless, the NMR
458 experiments presented in **Procedure 2** can also be expediently applied to strongly derivatized
459 cellulose materials dissolved in common perdeuterated NMR solvents.

460 **Acquisition of NMR experiments**

461 A set of standard 1D and 2D NMR experiments, allowing for a full NMR structural
462 characterization of cellulosic materials, is summarized in **Procedure 2**. The experimental
463 settings described therein are optimized, according to our experience, to give comprehensive
464 spectral assignment of crystalline cellulose samples (CNC, MCC). Not all experiments are
465 needed in all cases but can be applied *ad hoc*, as the user becomes experienced with the
466 method. **Box 1** shows a preferred acquisition order and summarizes obtainable information
467 from each NMR experiment. It gives an approximate number of transients and number of f1
468 increments (for 2D experiments) leading to tractable collection times, using typical 400-600
469 MHz spectrometers and probes. Of course, these parameters may vary depending on the
470 desired results. In essence, the selection of different 1D and 2D NMR experiments relies on
471 the information required as well as the available measuring time. Due to the complexity of
472 NMR, this requires the development of some expertise from the laboratory and the NMR
473 experimentalist. For standard reaction control, the measurement of quantitative ^{1}H, diffusion-
474 edited ^{1}H and multiplicity-edited HSQC is sufficient in most cases. **Table 2** shows how different
475 measurement settings for each NMR experiment can be adapted, *e.g.*, to reach a better
476 spectral quality by improving S/N, and lists references on background information, as well as
477 on original research where they have been applied to cellulosic materials.
478 Before starting the analysis, the operator must also consider the offered ideal measuring
479 frequency range. Especially in the ^{1}H dimension (see **Procedure 2, Steps 1-3**), different areas
480 of the spectra are populated either by very intensive signals of the electrolyte (approx. 2.5 –
481 1.0 ppm) or by the rather broad peaks of the cellulose backbone (approx. 4.5 and 4.0 – 3.0
482 ppm). This can lead to problems in the assignment of the signals owing to peak superpositions,
483 *e.g.*, in cellulosic materials containing other poly- and/or oligosaccharides or in cellulosics
484 modified with aliphatic moieties. In the case of peak overlap, qualitative assignments can still
485 be performed with the diffusion-edited ^{1}H NMR experiment and the multiple bond correlated
486 2D NMR experiments (see **Box 1**). However, these more complex experiments tend to
487 incorrectly estimate the relative substituent signal intensities because the different types of
488 nuclei have different relaxation times. This leads to disproportionate signal losses prior to
489 acquisition, *i.e.*, during the pulse sequence pulse lengths/delays, and only qualitative or semi-
490 quantitative indications of chemical composition can be obtained.[26]

The presented NMR experiments can also be successfully executed on an autosampler. Owing to the applied elevated temperature, the higher viscosity and the high intensity of the IL peaks, the automated tuning and matching sequence and the shimming process can sometimes give suboptimal results. As they are normally not performed separately for each acquisition, it is advisory to schedule to measure only samples with similar chemical composition and to give special care to equal filling heights for the NMR tubes (preferably 4-5 cm). An autosampler is very practical for routine analyses of larger numbers of samples. However, manual control over all experimental parameters is generally advantageous. Additionally, this gives access to a wider range of experiments and needs, but also allows the user to learn the practicalities and theory of running NMR.

Quantitative Information

Besides the qualitative analysis, quantitative Information can also be obtained, However, it must be considered that, except for the quantitative ^{1}H (**Procedure 2, Steps 1-4**) or quantitative ^{13}C experiment (**Procedure 2, steps 17-20**), the presented experiments are not quantitative. A reliable quantification using the expedient, HSQC or diffusion-edited ^{1}H spectra can only be performed after establishment of a calibration function, using cross-validation. It is also possible to apply quantitative HSQC pulse sequences to dissolved cellulosic materials. However, both T_1 & T_2 times should be measured as relaxation during and after the pulse sequence is an ever-present problem with 2D NMR.[26] Although, requiring long measuring times to obtain the needed S/N, the quantitative ^{13}C experiment in many cases represents the easiest option for quantification of the chemical composition. The quicker and, thus, less expensive quantitative ^{1}H experiment often suffers from strong peak overlap, especially by the broad H_2O or cellulose backbone signals.

Provided accurate phasing and modest baseline correction is performed, these issues can be resolved by a simple peak-fitting using suitable software, *e.g., Fityk*.[89] For example, in investigations on non-substituted CNCs, the fitting procedure could be applied to accurately calculate their number-average degree of polymerisation (DP_N) by comparing the peak intensities of the polymeric H1 (AGU-1), non-reducing end H1 (NRE-1), reducing end α-H1 (α-RE-1) and reducing end β-H1 (β-RE-1) resonances, according to **Equation 1**.[26] Especially, in very low DP cellulose fractions this is of importance as commonly applied size exclusion chromatography procedures tend to give inconclusive results, owing to peak superposition with other eluted oligosaccharides or the mobile phase.

$$DP_{N\text{-}^{1}H} = \frac{\alpha\text{-}RE\text{-}1 + \beta\text{-}RE\text{-}1 + NRE + AGU\text{-}1}{\alpha\text{-}RE\text{-}1 + \beta\text{-}RE\text{-}1} \qquad \textbf{(Equation 1)}$$

527 Peak-fitting can also be applied for DS calculations of chemically modified cellulosics by
528 comparing the intensities of signals of the introduced derivatization with the cellulose
529 backbone peaks. Depending on the nature of the introduced modification, the signals
530 accessible for calculations can vary due to changes in frequency for the modified backbone
531 resonance positions. However, quantifications against the relatively isolated H1 signal prove
532 to be quite consistent. This also highlights the need for backbone resonance assignment, to
533 be able to distinguish these peak regions in the 1D spectra. Therefore, it should be
534 emphasised that accurate determinations can only be performed after thorough qualitative
535 peak assignment. For the same reason, initial synthetic trials or optimization studies should
536 be designed to rely on signals that would be expected to appear in the unoccupied spectral
537 region of the ^{1}H dimension, *e.g.*, utilising aryl, vinyl, and other suitable functionalities.

538

539 Expertise needed to implement the protocol

540 Before implementing the protocol, a discussion with the person responsible for the
541 maintenance and access to the NMR spectrometers should take place, as the measurements
542 require prolonged heating to 65 °C and since each probe has defined limits for application of
543 pulse power/lengths during each experiment's duty cycle. We summarized the specifics of the
544 presented pulse sequences for an NMR expert (**Procedure 2**). The presented set of NMR
545 experiments is intended to allow for a standard characterization of cellulosic materials. Of
546 course, there are plenty more advanced experiments available (see **Box 1, Section III**). A
547 possible implementation thereof should also be discussed with the responsible NMR expert.

548 To successfully implement the protocol, it is not necessary to fully understand all aspects and
549 underlying principles of NMR spectroscopy. For the more interested users, literature and
550 online lectures are available, covering the basic principles and giving a solid introduction to
551 the field.[90,91]

552 For data analysis, practical working knowledge in the Bruker Topspin software and / or
553 MestreNova is recommended.

554 Advanced knowledge in the processing and interpretation of 2D spectra is advantageous for
555 accurate assignment of the peaks. Excellent literature as well as free of charge online lectures
556 concerning these topics are available.[14,92] Common resonances for all sorts of organic
557 moieties are summarized and listed in literature.[93,94]

558 # Materials

559 ## Reagents

560 **!CAUTION:** The chemicals and solvents used for the preparation of the $[P_{4444}]$[OAc]:DMSO-
561 d_6 electrolyte are potentially hazardous. Therefore, the material safety data sheet (MSDS) for
562 each reagent should be consulted before performing the metathesis. Concerning the toxicity
563 of $[P_{4444}]$[OAc], there is preliminary toxicity data available for structurally similar short chain
564 tetra-*n*-alkylphosphonium acetate homologues, indicating the status of 'practically harmless'
565 towards human and bacterial cells.[95] Owing to the known transdermal carrier properties of
566 DMSO solutions,[96] further precautions are advisory and appropriate personal protective
567 equipment (gloves, laboratory coat and eye protection) is mandatory. The generated solid and
568 liquid waste must be disposed according to local regulation.

569

570 - Tetra-*n*-butylphosphonium bromide ($[P_{4444}]$Br; *e.g.,* 98%; Sigma Aldrich, cat. Nr:
571 189138 or 99%; ABCR, cat. Nr: 11424213; or > 99.0%, TCI Europe, cat. Nr: T1124)

572

573 **<CRITICAL>** The precipitation of $[P_{4444}][BF_4]$, as the first step of the metathesis scheme, can
574 be performed with different H_2O soluble phosphonium starting materials (*e.g.*, $[P_{4444}]$Cl,
575 $[P_{4444}]$[OAc], $[P_{4444}]$Br). $[P_{4444}][BF_4]$ is also commercially available. However, we strongly
576 recommend the synthesis starting from $[P_{4444}]$Br as it is available at reasonable prices in
577 recrystallized form and in excellent isomeric purities from different vendors. Potential
578 impurities of the commercial product can be removed during the precipitation. In case the
579 quality of the starting material varies from batch to batch, a reported recrystallization from
580 acetone was found to decrease isomeric impurities.[37] However, it might take several
581 recrystallizations to reach the desired quality. On the other hand, no purification procedures
582 for isomeric contaminations are described in the literature for $[P_{4444}][BF_4]$, $[P_{4444}]$Cl or
583 $[P_{4444}]$[OAc]. Trials to transfer reported recrystallization protocols from closely related
584 analogous $[N_{4444}]$X salts were unsuccessful.
585 **CRITICAL:** It is important to assess the purity of the starting materials by running a ^{1}H NMR
586 spectrum before performing the metathesis - isomeric impurities will not influence the solubility
587 or stability of the cellulosic material in the $[P_{4444}]$[OAc] product, but are unwanted, as they
588 reduce the accessible measuring ppm-range and might result in superposition with potential
589 peaks of the investigated cellulosic sample (*e.g.*, cellulose acetate signals).

590

591 - Ammonium tetrafluoroborate (NH_4BF_4; for synthesis; Sigma Aldrich, cat. Nr: 8.43945)
592 - Potassium acetate (KOAc; ACS reagent, ≥ 99.0 %; Sigma Aldrich, cat. Nr: 236497)
593 - Silver acetate (AgOAc, 99 %, ABCR GmbH, cat. Nr: AB108667)

- Molecular sieves, 3Å (beads, 8-12 mesh; Sigma Aldrich, cat. Nr: 208582)
- Methanol (MeOH; CHROMASOLV(TM) for HPLC, >= 99.9%, Honeywell - Riedel-de Haen, cat. Nr: 34860)
- Ethanol (EtOH; absolute for analysis; Sigma Aldrich cat. Nr.: 1.00983)
- Acetonitrile (MeCN; for HPLC, gradient grade, ≥99.9%; Sigma Aldrich, cat. Nr: 34851)
- Liquid nitrogen
- Hexadeuterodimethyl sulfoxide (DMSO-d_6; 99.80% D, H_2O < 0.02%; Eurisotop; cat. Nr: D010ES)
- Millipore-processed (Merck, resistivity 18.2 MΩ×cm) deionized (DI) water – further referred to as H_2O
- Celite(R) 545, (VWR; cat. Nr: 22552.290)
- Activated Charcoal (DARCO(R) KB-G; Sigma-Aldrich; cat. Nr: 675326)
- Avicel® PH-101 (~50mm particle size; Merck Supelco; cat. Nr: 11365)

Equipment – [P_{4444}][OAc] synthesis

- Hot plate with magnetic stirring function
- Desiccator filled with desiccant (*e.g.*, activated silica gel)
- Oil pump equipped with liquid N_2 cold trap (min. pressure < 1 mbar)
- Rotavapor equipped with membrane pump
- Standard laboratory fridge (T = 4 °C)
- Standard laboratory freezer (T = < -24 °C)
- Reflux condenser (NS 29/32)
- Oil bath or heating mantle
- Glass Beakers (1L, 500, 250 mL)
- Round Bottom flasks (NS 29/32; 500 mL, 2 × 250 mL)
- Magnetic stirring bars
- Transition piece with core and stopcock (NS 29/32)
- Stoppers with standard taper (NS 29/32)
- Joint clips
- Aluminum foil and parafilm (Sigma-Aldrich, cat. Nr. P7793-1EA)
- Minispike syringe filters (ACRODISC 13 mm with 2 µm GHP-hydrophilic polypropylene membranes; Pall Corporation; cat. Nr.: 4554)

Equipment – sample dissolution and preparation

- 4-mL screw cap glass vials (clear glass, 15 × 45 mm, optionally VWR, cat. Nr. 548-0051 or Phenomenex Verex, cat. Nr. AR0-3300-13)

628 - Screw cap (optionally PP black, closed top, with 13 mm nat. rubber/TEF fitting 1.3 mm,
629 VWR, cat. Nr. 548-0512 or PP black, closed top, 13 mm butyl/PTFE fitting 1.3 mm,
630 VWR, cat. Nr.548-0805)
631 - PTFE magnetic stirring bars (cylindrical, 10 × 6 mm, optionally VWR, cat. Nr. 442-
632 0295)
633 - Hot plate with magnetic stirring function
634 - Oil bath (Silicone oil, VRW, cat. Nr. 84542.290)
635 - 1 glass beaker (50 or 100 ml, optionally VWR, cat. Nr. 213-0462P or 213-0476P) and
636 1 crystallization glass or stainless still dish of larger size
637 - Short-necked Pasteur glass pipettes (unplugged, 150 mm, optionally Fisher Scientific,
638 cat. Nr. 1154-6963)
639 - 5-mm NMR glass tubes (Wilmad-Labglass Co., Sigma Aldrich, cat. Nr. Z565229-
640 100EA)
641 **CRITICAL!** Please, consult the local NMR specialist about the NMR tube of choice. Typically,
642 inexpensive NMR tubes are chosen, as the samples can get very viscous at ambient
643 temperature and thus difficult to remove from the sample tubes. Recycling is possible but
644 might require concentrated acids to remove last traces of previous samples. However, we
645 leave the decision to the user whether the recycling is justifiable. More precise/expensive
646 sample tubes can be used. However, the small increase in spectral quality does not
647 necessitate their implementation in everyday use. The major concern is general to NMR: Use
648 tubes that are not prone to cracking to prevent probe damage!
649

650 **Reagent and Equipment setup**

651 Except for $[P_{4444}]Br$, all other reagents were used as received, without further quality control
652 or purification.
653 **Molecular sieves** A quick control for the applicability of the molecular sieves 3Å can be
654 conducted by putting 1 g in a 50 mL round bottom flask and adding H_2O (5 mL). An exothermic
655 reaction (gentle heating of the hand) indicates that they are good to use. Otherwise, activation
656 through heating to 200 °C under vacuum is recommended. This can easily be achieved in
657 seconds using a Bunsen flame, Schlenk vacuum and then argon or nitrogen quench.
658 **Solvents** Used solvents should be sufficiently pure (preferably HPLC grade). Possible
659 contaminations with H_2O can be tolerated to a small extent as they are actively removed during
660 the metathesis by the molecular sieves 3Å.
661

662 **Dissolution setup for the cellulosic samples**

663 For the dissolution of the cellulosic materials, a simple setup using a conventional heating
664 plate with stirring function and temperature sensor and two stacked oil baths (**Fig. 3**) proved
665 to be expedient. It allows for the simultaneous preparation of several samples for NMR
666 measurement. The sample vials are equipped with a small magnetic stirring bar, inserted into
667 the upper oil-bath and stirred at 65 °C until soluble.
668
669
670 **EQUIPMENT SETUP**
671 **General** The used equipment should ideally be clean and dry but working under very
672 dry or inert conditions is not strictly necessary. The use of 'Glindemann' Teflon rings to seal
673 ground-glass joints, instead of vacuum grease, is recommended. Sintered glass filter frits are
674 stored at 105 °C before use to avoid H_2O contamination.
675 **!CAUTION:** Only use glassware that is free from cracks and stars and can withstand high
676 vacuum. Otherwise, the applied reduced pressures can result in implosions.
677
678
679 **NMR experiments**
680 The NMR experiments can be setup by adapting already available Bruker pulse programs.
681 However, several acquisition parameters are adapted to the measurement of high-molecular-
682 weight cellulose samples, or are probe-specific, and require implementation by an NMR
683 expert. For example, the suitability of the probe-head for measurement at 65 °C must be
684 confirmed, as must be the application of strong gradient and gradient pulse lengths during the
685 diffusion-edited ^{1}H experiment duty cycle. We summarized the applied parameters in
686 **Procedure 2**. If in doubt, ask the manufacturer to provide details about the extent to which
687 gradients can be applied during the duty cycle.
688 The following spectrometers were used for the acquisition of the spectra presented in this
689 protocol:
690
691 - Bruker NMR spectrometers operating at 400 (AVANCE III), 500 or 600 (AVANCE 600
692 NEO), and 850 (AVANCE III HD) MHz, equipped with 5-mm liquid-state probe-heads:
693 a (TXI 600Mz, ^{1}H/^{19}F, ^{13}C, ^{31}P inverse triple resonance), a (BBFO 500 MHz or 400 MHz
694 SmartProbe^{TM} double resonance broad band) or a (TCI cryogenically cooled 850 MHz
695 ^{1}H-^{13}C/^{15}N/D triple resonance), respectively.
696 - For some samples, a 600-MHz cryogenically cooled quadrupole resonance probe-
697 head QXI (^{1}H, ^{13}C, ^{31}P, ^{15}N) was used.
698
699

Data Analysis

- Bruker TopSpin® (version: 4.0.9, for Windows or 4.1.1 for OSX) was used for the spectral processing. Free academic licenses (processing only) are available after registration on the Bruker website: https://www.bruker.com/en/products-and-solutions/mr/nmr-software/topspin (accessed: 2022, October 05)
- Mestrelab MestReNova (version 14.02.0, for Windows or 10.0 for OSX) was used for further spectral processing and graphical representation of the spectral data. Mestrelab website: https://mestrelab.com/ (accessed: 2022, October 05)
- *Fityk* (version 1.3.1, for Windows or OSX) was used for the data processing and nonlinear curve fitting for DS determinations.[89] *Fityk* website: https://fityk.nieto.pl/ (accessed: 2022, October 05)
  The processing steps used in this protocol are described in detail in the *Fityk* manual: https://fityk.nieto.pl/fityk-manual.html (accessed: 2022, October 05)
- Microsoft® Powerpoint and Excel (various versions for Windows, OSX or Office 365 cloud versions) was used for illustrating the assigned spectra
- Chemdraw (20.0 for OSX) was used for preparing representative structures for the assigned spectra

719 # Procedure 1 – Preparation of electrolyte and NMR samples

720 ## Preparation of the [P_{4444}][OAc] - DMSO-d_6 (1:4) electrolyte

721 **1**) Synthesise [P_{4444}][OAc] as described in either option A or B. Both procedures
722 were designed to prepare approximately 6 – 8 g of ionic liquid, which is enough for the
723 dissolution of around 30 – 40 standard cellulose NMR samples (50 mg cellulose : 950 mg
724 electrolyte). At this scale both syntheses can be performed with basic laboratory equipment.
725 Option A was adapted from our previously reported metathesis scheme[25] and results in the
726 desired IL in a one-step reaction. We generally recommend using option A for smaller scales,
727 as it is less laborious. However, depending on the available equipment filtration of formed
728 nanoparticles and drying can become tedious. Furthermore, the starting materials for option
729 A are not commercially available in the highest purities, possibly leading to unwanted
730 contaminations. While option B is more laborious, we found it to be very robust and easier to
731 perform with less specialized equipment. The intermittent precipitation in the two-step
732 procedure also can tackle potential contaminations of the commercial starting materials.
733 Although upscaling is possible, especially following option B, vacuum drying of the end-
734 product gets rather difficult, requiring more advanced equipment to reach sufficient vacuum
735 (preferably < 5 mbar). Furthermore, the [P_{4444}][OAc] product is hygroscopic and bigger batches
736 might need additional drying steps after longer storage. In humid climates, we recommend
737 storing the prepared electrolyte under inert gas.
738

739 **A) Preparation of [P_{4444}][OAc] following the AgOAc metathesis approach Timing: 70**
740 **h with drying**

741 **i.** Dissolve [P_{4444}]Br (6.79 g, 20.0 mmol, 1.01 eq) in MeOH (50 mL) in a 100 mL round
742 bottom flask, at room temperature (20 °C). Vigorously stir using a medium-sized
743 magnetic stirring bar until a clear, colourless solution is obtained.

744 **CRITICAL STEP:** Use a slight molar excess of [P_{4444}]Br over AgOAc. Excess silver salts have
745 the tendency to reduce over time to form silver nanoparticles and residual silver (I) or (0),
746 which can act as a catalyst for degradation of cellulose. Residual bromide anion does not
747 affect the dissolution or cause degradation artefacts.
748

749 **ii.** Add AgOAc (3.33 g, 19.8 mmol, 1.00 eq) in one portion to the [P_{4444}]Br solution, at
750 room temperature (20 °C). Flush the head of the flask with argon and stopper until
751 sealed. Then wrap the flask completely with aluminium foil and stir at room temperature
752 (20 h).

753 **CRITICAL STEP:** Neither AgOAc nor AgBr are fully soluble in MeOH. However, the
754 metathesis of [P_{4444}]Br to [P_{4444}][OAc] occurs slowly over this period, without heating.

755
756 **iii.** Remove the white solid by filtration under reduced pressure using a fritted glass filter
757 (Porosity 3) under reduced pressure. Further wash the precipitate with MeOH (3 × 20
758 mL) and combine the methanolic solutions, containing the crude $[P_{4444}][OAc]$.
759
760 **iv.** Concentrate the methanolic phase to a volume of ~20 mL using a rotary evaporator
761 (40 °C; 30 min). Let the solution cool to room temperature and additionally filter using
762 a 0.2 μm GHP-hydrophilic polypropylene membrane syringe filter, to remove any
763 residual silver metal or salts.
764
765 **v.** Evaporate the recovered solution to dryness on a rotary evaporator (50 °C down to 2
766 mbar) and flush the head of the flask with argon and stopper until sealed. Let the liquid
767 solidify at room temperature (18 h).
768
769 **vi.** Redissolve the formed solid in MeOH (20 mL) and add activated charcoal (1 g; one
770 portion) to adsorb and remove unfilterable contaminations (discolorations, Ag-
771 nanoparticles). Reflux the mixture in one portion (3h, 70 °C).
772
773 **vii.** Let the mixture slowly cool for ~ 5 min and filter the still hot to warm reaction mixture
774 (~ 50 °C) through a Celite® plug, in a glass sintered filter, to remove the charcoal.
775
776 **viii.** Let the solution cool to room temperature and additionally filter using a 0.2 μm GHP-
777 hydrophilic polypropylene membrane syringe filter, to remove any residual charcoal,
778 silver metal or salts.
779
780 **CRITICAL STEP:** From step **iii** - **viii** residual silver (I) salts may convert to silver (0)
781 nanoparticles, which results in a greyish hue of the recovered materials or solutions.
782 The syringe filtrations are designed to remove these nanoparticles. If the final product
783 still turns grey over time, these filtration steps may be repeated. Residual silver salts
784 can catalyse degradation reactions during the dissolution; thus, it is important to check
785 the quality of the resulting electrolyte in **steps 2-7**.
786
787 **ix.** Evaporate the recovered solution to dryness on a rotary evaporator (60 °C down to 2
788 mbar) and flush the head of the flask with argon and stopper until sealed. Let the liquid
789 solidify at room temperature (18 h). Store the obtained slightly yellow solid in the
790 freezer at –24 °C.
791

792 **CRITICAL STEP:** To remove all traces of solvent, the sample should be melted and
793 slowly turned during evaporation. This is best achieved using a well-maintained rotary
794 evaporator with a highly efficient pump. Drying of the sample below the melting
795 temperature (44 - 46 °C) or without turning of the sample takes much longer. Limit
796 exposure of the IL product to the atmosphere to avoid potential rapid H_2O uptake!
797
798 **x.** In an typical experiment 6.3 g (99%) of [P_{4444}][OAc], as a clear crystalline material, are
799 obtained.
800
801 **PAUSE POINT** When solid and cold [P_{4444}][OAc] shows only little hygroscopicity and can be
802 stored in the freezer for several months.
803
804
805 **B) Preparation of [P_{4444}][OAc] following the NH_4BF_4 / KOAc metathesis**
806 **approach <TIMING>** Preparation of [P_{4444}][BF_4] takes 24 h with drying. Conversion to
807 [P_{4444}][OAc] takes 72 hours with drying.
808 **<CRITICAL>** This is a two stage process. The first stage is to prepare [P_{4444}][BF_4]
809 (steps i- viii) which is further transformed to [P_{4444}][OAc] (steps ix-xxi).
810 **i.** Dissolve [P_{4444}]Br (30 g, 88.4 mmol, 1 eq) in H_2O (500 mL) in a 1-L glass beaker, at
811 room temperature. Vigorously stir using a medium-sized magnetic stirring bar until a
812 clear, colourless solution is obtained. If bigger crystals dissolve too slowly, use an
813 ultrasonic bath. If an insoluble residue is observed, filter the solution.
814 **CRITICAL STEP:** Don't heat! It will lead to the formation of an oily precipitate, which
815 is more difficult to dry and might lead to inclusions of H_2O and the NH_4Br side product.
816 **ii.** Dissolve NH_4BF_4 (12 g, 115 mmol, 1.3 eq) in H_2O (300 mL) in a 500-mL glass beaker,
817 at room temperature (20 °C). Stir using a medium sized magnetic stirring bar until a
818 clear, colourless solution is obtained. If bigger crystals dissolve too slowly, use an
819 ultrasonic bath. If an insoluble residue is observed, filter the solution.
820 **CRITICAL STEP:** Don't heat! It will lead to the formation of an oily precipitate, which
821 is more difficult to dry and might lead to inclusions of H_2O and the NH_4Br side product.
822 **iii.** Over 1 min, add the NH_4BF_4 solution into the 1-L beaker containing the dissolved
823 [P_{4444}]Br, under vigorous stirring by a medium sized magnetic stirring bar. A fine, white
824 precipitate is obtained immediately. Stirring is continued for 30 min.
825 **iv.** Cover the beaker with aluminium foil and keep it in a refrigerator (4 °C, 2 h). The formed
826 precipitate should float on top of the solution.

827 **v.** Separate the white precipitate under reduced pressure using a fritted glass filter
828 (Porosity 2) and wash with cold H_2O (4 °C, 200 mL).
829 **CRITICAL STEP:** To reduce the time in the subsequent drying step, keep the reduced
830 pressure on the suction flask for several minutes after the washing step, to remove
831 excess H_2O.
832 **vi.** Dry the precipitate overnight (ca. 16 h) in a desiccator filled with drying agent (activated
833 silica gel), under reduced pressure (< 1 mbar, oil pump equipped with liquid N_2 cold
834 trap).
835 **vii.** Check the obtained white, powdery solid for impurities and H_2O content by running a
836 ^{1}H NMR experiment in DMSO-d_6.
837 **CRITICAL STEP:** A small residual H_2O content is acceptable for the subsequent conversion.
838 Otherwise, repeat the drying step.
839 **viii.** In an typical experiment 26-28 g (85 – 90%) of a fine, white powder of $[P_{4444}][BF_4]$ are
840 obtained. Store in a closed vessel or a desiccator
841
842 **PAUSE POINT** The dried $[P_{4444}][BF_4]$ is stable and can be stored for … without further
843 precautions.
844
845 **ix.** Dissolve $[P_{4444}][BF_4]$ (10 g, 28.9 mmol, 1 eq) in MeCN (45 mL) in a 250-mL glass
846 beaker with the aid of an ultrasonic bath. **NOTE:** Depending on the used educts and
847 residual H_2O content, white particles or emulsified drops might be visible in the
848 colourless solution. The reaction can be performed successfully in either case.
849
850 **x.** Suspend KOAc (3 g, 30.3 mmol, 1.05 eq) in EtOH (15 mL) in a 250-mL round-bottom
851 flask under vigorous stirring (magnetic stirring bar). Connect a reflux condenser and
852 heat under reflux (85 °C, 30 min) until a clear colourless solution is obtained.
853
854 **xi.** Disconnect the reflux condenser and quickly add the $[P_{4444}][BF_4]$ solution into the 250-
855 mL round-bottom-flask containing the hot ethanolic KOAc solution. A white precipitate
856 of KBF_4 forms immediately.
857
858 **xii.** Connect the reflux condenser and keep the formed suspension under reflux (30 min)
859 under vigorous stirring. Afterwards, let the mixture slowly cool to room temperature.
860
861 **xiii.** Add molecular sieves (3Å, 15 g) to the cooled solution and keep the closed vessel at
862 –24 °C overnight (16 h).
863

CRITICAL STEP: Do not stir solutions that contain molecular sieves! It will result in their disintegration leading to formation of fine particles difficult to remove by filtration.

xiv. Remove the solids by filtration under reduced pressure using a fritted glass filter (Porosity 4) into a 250-mL round-bottom flask and wash with cold MeCN (–24 °C, 20 mL).

xv. Evaporate the solvent from the filtrate by means of a rotary evaporator (first at 60 °C for 1h; then 90 °C for 3h)

CRITICAL STEP! When most of the solvent is removed, apply lowest pressure possible, ideally < 5 mbar.

xvi. A slightly orange viscous liquid with a visible crystalline solid residue of KOAc is obtained. Add MeCN (20 mL) and molecular sieves (10 g, 3Å) to remove the last traces of KOAc and H_2O.

CRITICAL STEP! H_2O is effectively trapped in the ionic liquid matrix due to strong hydrogen-bonding. Thus, it is difficult to remove in the subsequent distillation steps. It proved to be more expedient to remove H_2O by molecular sieves 3Å while the IL is still dissolved in MeCN.

xvii. Keep the vessel in the freezer (–24 °C, at least 2h) before removing the solids by filtration under reduced pressure using a fritted glass filter (Porosity 4) into a 250-mL round-bottom flask. Wash with cold MeCN (–24 °C, 10 mL).

xviii. Evaporate the solvent from the filtrate by means of a rotary evaporator (first at 60 °C for 1h, then 90 °C for 3h)

CRITICAL STEP! When most of the solvent is removed, apply lowest pressure possible, ideally < 5 mbar. Limit exposure of the IL product to the atmosphere to avoid potential rapid H_2O uptake.

xix. Additionally, remove last traces of EtOH from the slightly viscous, orange liquid by distillation. Connect the round-bottom flask with a transition piece with core and stopcock to a high vacuum oil pump (pressure < 1 mbar), equipped with a liquid N_2 cold trap. Keep the solution at 90 °C under slight stirring overnight (12- 16 h).

902 **CRITICAL STEP!** This step is necessary to remove last traces of EtOH that are
903 adsorbed inside the IL structure. Check the obtained product by running an ^{1}H NMR
904 spectrum. Continue drying until no EtOH peaks are visible.
905
906 **CAUTION:** Use appropriate and undamaged glassware to avoid potential implosion.
907 Perform the drying step in a closed fume hood.
908
909 **xx.** After drying, slowly cool the product to room temperature under vacuum. Seal the
910 round-bottom flask with a stopper and parafilm and store the obtained slightly yellow
911 solid in the freezer at –24 °C **CRITICAL STEP!** Limit exposure of the IL product to the
912 atmosphere to avoid potential rapid H_2O uptake.
913
914 **xxi.** In a typical experiment approximately 8.5 g (~ 90%) of a white to slightly yellow
915 crystalline mass of $[P_{4444}]$[OAc] is obtained.
916
917 **PAUSE POINT:** When solid and cold $[P_{4444}]$[OAc] shows only little hygroscopicity and
918 can be stored in the freezer for several months.
919
920 **?TROUBLESHOOTING**
921
922 **Characterization and quality control**
923 **<TIMING>** 24-72 h with sample preparation
924 **2.** Perform NMR to check that the correct product has been obtained, and that the material is
925 sufficiently pure.
926 **Tetra-*n*-butylphosphonium acetate ($[P_{4444}]$[OAc]).** Pale yellow crystalline mass, mp = 44 -
927 46 °C (from the melt).
928 ^{1}H NMR (600 MHz, DMSO-d_6) δ 2.27 – 2.17 (m, 8H), 1.61 (s, 3H), 1.50 – 1.36 (m, 16H), 0.91
929 (t, J = 7.2 Hz, 12H) ppm.
930 $^{13}C\{^{1}H\}$ NMR (150 MHz, DMSO-d_6) δ 13.14 (CH_3), 17.26 (CH_2, d, J = 47.3 Hz), 22.70 (CH_2, d,
931 J = 4.4 Hz), 23.32 (CH_2, d, J = 15.7 Hz), 26.20 (CH_3), 171.86 (CO) ppm.
932
933
934 ***Prepare a stock solution of NMR electrolyte.***
935 **3|** Check that the $[P_{4444}]$[OAc] and DMSO-d_6 are not contaminated with H_2O before use,
936 especially after longer storage. This is easiest to achieve by ^{1}H NMR or optionally Karl-Fischer
937 titration.

938 <CRITICAL STEP> The presence of H_2O or methanol will lead to peak overlap and can
939 affect the solubility of the cellulosics. If water or methanol is present, then dry [P_{4444}][OAc] at
940 elevated temperatures under vacuum, or add molecular sieves to the electrolyte – 3Å for
941 presence of water or 4Å for presence of methanol.
942 **4|** Weigh solid [P_{4444}][OAc] (ca. 3 g) and dissolve it in a four-fold weight of DMSO-d_6
943 (approx. 12 g or 10 mL) in a closed Schott bottle.
944 **CRITICAL STEP:** Work quickly! The frozen IL will start to melt during transfer at RT; when it
945 melts it is more likely to take up water when it is exposed to the atmosphere.
946
947 **5|** Homogenize the mixture (*e.g.*, with the aid of a vortex apparatus or an ultrasonic bath)
948 to obtain a 20 wt%, slightly yellow, stock electrolyte solution. Close the bottle carefully, wrap
949 the cap with parafilm and store it at RT until use.
950 **CRITICAL STEP:** Owing to hygroscopicity, preparation of much larger batches is not
951 recommended, as they are difficult to sufficiently dry and absorb water over time. The addition
952 of molecular sieves 3 or 4Å is recommended if the electrolyte is stored for longer periods or at
953 elevated humidity.
954
955 **6|** Check the quality of the prepared electrolyte. Prepare a sample of a known cellulosic
956 material (*e.g.,* Avicel® PH-101 MCC) (as described in **steps 8 – 11**). After dissolution leave
957 the vial at 65 °C for longer periods (24-72 h) to check the long-term stability of cellulose in the
958 prepared electrolyte.
959
960 **7|** Run a ^{1}H NMR and a diffusion edited ^{1}H NMR experiment as described in **Procedure**
961 **2** and check for unusual signs of degradation.
962 **?TROUBLESHOOTING**
963
964 **Sample preparation for NMR measurement**
965 **<TIMING>** 1-18 h with sample preparation
966 <**CRITICAL**> Depending on the material under investigation, the complete dissolution process
967 might take anything from 5 min to overnight. We therefore recommend either starting the
968 sample preparation process the day before the scheduled measurement or conducting
969 preliminary solubility tests.
970
971 **8|** Weigh 25 to 50 mg of dry (ideally freeze-dried) cellulosic material in a 4-mL screw cap
972 vial and add [P_{4444}][OAc]:DMSO-d_6 stock electrolyte (950 – 975 mg) with a Pasteur pipette
973 until a final weight of approximately 1.0 g.

9| Add a small magnetic stirring bar, tightly close the vial, and transfer it to an oil bath preheated to 65 °C (see **Fig. 3**).

10| Stir the solution until it is clear and visually homogenous. The dissolution is often accompanied by a colour change from slightly yellow to orange / brown.
<**CRITICAL STEP**> This is the step that might take between 5 minutes and 12 hours.

11| Transfer the still hot solution to a 5-mm NMR tube using a short-necked Pasteur pipette.
Slightly shake the NMR tube during the transfer to homogeneously fill the tube with the viscous sample solution. Take care that there are no visible air-bubbles in the sample and that the material is at the bottom of the tube.
<CRITICAL STEP> Work quickly! Once the sample reaches room temperature it is very difficult to transfer.

PAUSE POINT: Solutions of standard cellulosic materials (*e.g.*, MCC) can be stored in the dark at room temperature for several days. The stability of the solution is, of course, strongly dependent on the nature of the sample under investigation.

?TROUBLESHOOTING

995 **Acquisition of the NMR spectra and data processing**

996 **<TIMING>** 1-72 h

997 **CRITICAL:** Ask the NMR technician in your laboratory what the appropriate workflow should
998 be for the respective available spectrometers; the workflow might depend on what equipment
999 is used and in many cases some kind of formal training is required prior to use. Detailed
1000 instructions on setting up the NMR spectrometer for measurement are summarized in a
1001 Beginners Guide in the Supplementary Information.

1002 **CRITICAL:** Once the cellulosic sample is successfully dissolved, in principle every NMR
1003 experiment can be performed. However, when choosing which experiments to perform you
1004 should always consider the anticipated information and the limits set by resolution. Always
1005 keep in mind that measuring time on NMR spectrometers is expensive! For standard reaction
1006 control of routinely prepared samples, acquisition of ^{1}H or diffusion edited ^{1}H spectra in under
1007 1h are usually sufficient. Confirmation of regioselective modifications in novel cellulosics by,
1008 double quantum correlation experiments or quantitation over ^{13}C NMR can require measuring
1009 times of several days. Recommended NMR experiments are summarized in **Box 1** and
1010 presented in more detail in **Procedure 2**.

1011

1012 **12|** Insert the sample tube to the NMR spectrometer and prepare the device for
1013 measurement. Detailed instructions for beginners are provided in the Supplementary
1014 Information.

1015

1016 **13|** Choose the NMR experiments according to your required information. Consult **Box 1**
1017 or **Procedure 2** if in doubt.

1018 **<CRITICAL STEP>** For the diffusion-edited ^{1}H experiment, the gradient strengths and
1019 durations presented in this protocol are specific to the 50 G/cm Smartprobe™ but can be
1020 optimized for other probes. This requires careful implementation by an NMR expert, because
1021 it is important to not exceed the recommended overall pulse lengths at specific gradient
1022 strengths during the duty cycle. In addition, care should be taken not to apply too long
1023 acquisition periods, for those experiments that apply ^{13}C decoupling during acquisition, *e.g.,*
1024 HSQC-based experiments. If in doubt, always consult the NMR technician that is responsible
1025 for looking after your equipment.

1026

1027 **14|** Collect the obtained data and perform initial data processing on the spectra. Detailed
1028 instructions for beginners for the necessary steps in TopSpin® are provided in the
1029 Supplementary Information.

1030

15| (**optional**) Perform additional data analysis if needed. This includes for example visualisation of spectra for presentations or integration following peak deconvolution and fitting. Detailed instructions for peak deconvolution with the open access program *Fityk* are provided in the Supplementary Information.

?TROUBLESHOOTING

1040 # PROCEDURE 2 – NMR Experiments

1041 **<CRITICAL>** This Procedure gives an overview of selected NMR experiments we found useful
1042 in the characterization of cellulosic materials. It contains the information necessary to choose
1043 which experiments to perform. For each experiment, the following information is provided:

1044 - A short introduction including advice on when it should be performed.
1045 - The Bruker Pulse sequence and optimized parameters for an NMR expert to
1046 implement.
1047 - An example spectrum.
1048 - A summary of the characteristics of the spectra and the obtainable information.

1049 ## Standard, quantitative ^{1}H experiment:

1050 **<TIMING>** 8 min

1051 **1.** The standard quantitative ^{1}H experiment gives a solid first overview of the sample's
1052 composition with a short measuring time. Perform this experiment at the start of every
1053 measurement.

1054

1055 **2.** We suggest using the Bruker Pulse sequence '***zg30***' with the following parameters:

1056 - A 30° pulse flip angle.
1057 - 2 dummy scans (ds) and 16 transient scans (ns) to deliver a sufficient spectral quality.
1058 - Relaxation delay (d1) of 10 s to ensure quantitative acquisition of data, with a short
1059 collection time.

1060

1061 **3.** An example spectrum is presented in **Figure 4**.

1062

1063 **4.** Characteristics of the standard, quantitative ^{1}H spectra and obtainable information:

1064 - All protons of the polymeric materials and the low molecular weight components of the
1065 electrolyte ([P_{4444}][OAc]; DMSO-d_6; H_2O) and impurities are visible. Exceptions may be
1066 fast exchanging ^{1}H nuclei present, *e.g.*, in H_2O, —OH, —NH_2 or —COOH functionalities,
1067 which may appear as broad signals or not at all.
1068 - The spectra are dominated by the [P_{4444}][OAc] peaks (**Fig. 4**, highlighted in yellow).
1069 However, they only occupy areas up-field of the cellulose signals.
1070 - Owing to the higher molecular weights, the peaks of the polymeric constituents show
1071 peak broadening and are not well-resolved.

- Residual H_2O shows a very broad absorption between approx. 7 and 4 ppm, which varies between different measurements and might overlap with peaks of cellulose or introduced modifications (**Fig. 5**, top).
- The ^{1}H experiment is highly sensitive but offers poor resolution compared to the 1D ^{13}C experiment. Nonetheless, the cellulose backbone signals are still quite well resolved, as are lower abundance resonances, such as the RE and NRE signals.
- In investigations on introduced derivatizations, the preoccupied spectral areas must be considered. Generally, information can be obtained from the chemical shifts and quantitation can be performed more accurately than simple integration, by using peak-fitting, provided suitable baseline correction is applied.
- When applying a relaxation delay, d1, of 10 s (> 5 T_1, where T_1 is the spin-lattice relaxation constant for the proton, typically falling into the range of 0.5-2 s for these systems), quantitative information can be obtained from the experiment.
- Due to the overlap of peaks, mostly with the broad H_2O signal, peak-fitting after suitable baseline correction may be necessary to yield close-to quantitative analysis (see **Section 3.3. in the Supplementary Information**).

1091 **Diffusion-edited ^{1}H experiment:**

1092 **<TIMING>** 5-60 min

1093 **5.** The diffusion edited ^{1}H experiment resembles a standard ^{1}H experiment, with the peaks of
1094 fast-moving species (low molecular weight) removed from the spectra. Perform this
1095 experiment if signals are overlapping with low molecular weight compounds, especially in the
1096 IL and DMSO resonance region (2.6-0.7 ppm) or to determine if a particular resonance is
1097 polymeric or polymer-bound, *i.e.*, attached to cellulose.
1098 Set up the pulse sequence
1099

1100 **6.** We suggest using the Bruker Pulse sequence '***ledbpgp2s1d***' with the following parameters:

1101 - A 1D bipolar-pulse pair with stimulated echo (BPPSTE).[97]
1102 - A diffusion-ordered spectroscopy (DOSY) pulse sequence, with a relaxation delay (d1)
1103 of 3 s.
1104 - An acquisition time (aq) of 0.5 s.
1105 - 16 dummy scans (ds) and multiples of 16 transient scans (ns).
1106 - A sweep-width (sw) of 20 ppm with the transmitter offset on 6.1 ppm (o1p).
1107 - A diffusion time (d20) of 200 ms.
1108 - A gradient recovery delay (d16) of 0.2 ms.
1109 - An eddy current delay (d21) of 5 ms.
1110 - A diffusion gradient pulse duration (p30) of 2.5 ms.
1111 - A z-gradient strength (gpz6) of 70-90% at ≥ 50 G/cm (probe z-gradient strength) – the
1112 NMR technician should approve the maximum current-time applied during the duty
1113 cycle.
1114

1115 **7.** An example spectrum is presented in **Figure 5**.
1116

1117 **8.** Characteristics of the diffusion edited ^{1}H spectra and obtainable information:

1118 - The spectrum shows the same peaks as in the standard ^{1}H experiment. However, low
1119 molecular weight (fast diffusing) species are 'edited out' of the spectra, leaving only
1120 higher molecular weight (polymeric) resonances visible (**Fig. 5**).
1121 - Resolution is artificially increased due to T_2 losses during the pulse sequence, prior to
1122 the acquisition period. For the same reason, experiments are not quantitative as
1123 different functionalities have different T_2 values and, thus, experience variable signal
1124 loss prior to acquisition.
1125 - This experiment also suffers from reduced S/N. However, for identification of low
1126 abundance resonances, the diffusion-edited experiment is typically better than the

standard ^{1}H experiment, as receiver gain is maximized due to the absence of any dynamic range issues afforded by the presence of the large $[P_{4444}]^{+}$ signals.

- There is a molecular weight limit to how well the fast-diffusing species are 'edited out' of the spectra. This editing is more effective as the diffusion delay is increased, at the expense of overall S/N.

Multiplicity-edited ^{1}H-^{13}C Heteronuclear Single-Quantum Correlation (HSQC)

<TIMING> 2.5 h

9. The ^{1}H-^{13}C HSQC experiment shows the peaks of protons bonded to carbon. Perform this experiment if chemical modification is expected. Resolution of 1D ^{1}H NMR experiments is typically too poor to immediately identify the reactions and modifications that occurred. The signal to noise (S/N) for 1D ^{13}C NMR spectra is also typically too poor to detect low degrees of modification, despite its higher resolution. Thus, the ^{1}H-detected HSQC has good sensitivity and excellent resolution to identify the potential for application of further methods of resonance identification or quantification.

10. We suggest using the Bruker Pulse sequences '***hsqcedetgpsisp2.2***' or '***hsqcedetgpsisp2.3***'.[98-101] The HSQC experiments use a sensitivity-improved, multiplicity-edited phase-sensitive HSQC sequence, with echo/antiecho-TPPI gradient selection and adiabatic pulses with the following parameters:

- Spectral widths (sw) of 13.03 and 165 ppm, with transmitter offsets (o1p) of 6.18 and 75 ppm, for ^{1}H and ^{13}C dimensions, respectively.
- The time-domain size (td1) in the indirectly detected ^{13}C-dimension (f1) was typically 512 or 1024, corresponding to 256 or 512 t_1-increments for the real spectrum.
- Typically, 16 dummy scans (ds), minimum 1 (preferably 4 or multiples of 4) scans (ns) are recorded with an acquisition time (aq) of 0.065 s for f2 and a relaxation delay of 1.5 s.
- Window functions are typically sine squared (90°) in f1 and f2.

11. An example spectrum is presented in **Figure 6**.

12. Characteristics of the multiplicity-edited ^{1}H-^{13}C HSQC spectra and obtainable information:

- Single-bond H-C bond correlations ($^{1}J_{CH}$) are critically important.
- Multiplicity-editing allows for determination of CH_2 groups versus CH and CH_3 moieties, at the expense of peak cancelation for overlapping peaks (not typical in 2D NMR). This

1163 occurs when a CH_2 (negative signal intensity after phasing) overlaps with CH or CH_3
1164 (positive signal intensity after phasing) resonances, resulting in a net reduction in
1165 signal intensity potentially close to zero.
1166 • Besides the cellulose backbone peaks and the strong electrolyte signals phasing
1167 artifacts are usually observed (**Fig. 6**, yellow). In the f1 dimension, they can be
1168 effectively removed by spectral processing (see **Section 3.2. in the Supplementary**
1169 **Information**).
1170 • These phasing artefacts are also common in the other 2D NMR spectra. Therefore,
1171 special care is advisory if peak assignments in the up-field spectral area are performed.
1172

1173 **Qualitative ^{13}C experiment**

1174 **<TIMING>** 3 h

1175 **13**. The qualitative ^{13}C experiment gives a classic 1D ^{13}C NMR spectrum. Perform this
1176 experiment if you suspect that moieties with isolated carbon might be present. As the ^{13}C shifts
1177 for all carbons with attached protons are already obtained by the higher resolution HSQC
1178 experiment (**Procedure 2**, **Steps 9 - 12**), the acquisition of the ^{13}C NMR can often be avoided.
1179 If moieties with isolated carbons are suspected (*e.g.*, carboxylates, ketones, tertiary carbons),
1180 the ^{13}C experiment can deliver valuable information, not easily attainable through other
1181 experiments.
1182

1183 **14.** We suggest using the Bruker Pulse sequence '***zgpg30***' with the following parameters:
1184 • A 30° pulse flip angle with power-gated decoupling.,
1185 • Typically, 4 dummy scans (ds) and 1024 scans (ns) are recorded, with more applied
1186 for improved S/N.
1187

1188 **15.** An example spectrum is presented in **Figure 7**.
1189

1190 **16.** Characteristics of the qualitative ^{13}C spectra and obtainable information:

1191 • ^{13}C offers much higher resolution of species than ^{1}H spectra, at the expense of much
1192 lower S/N. Thus, accurate peak separation can be obtained, at the expense of much
1193 longer collection times.
1194 • The spectra are dominated by the IL peaks (**Fig. 7**), which occupy areas up-field of the
1195 cellulose resonances. However, resolution is still good in this region.
1196
1197

1198 **Quantitative ^{13}C experiment**

1199 **<TIMING>** 15 h

1200 **17**. Perform this experiment if quantitative information is needed from moieties that strongly
1201 superimpose in the ^{1}H dimension of the standard, quantitative ^{1}H experiment (**Procedure 2**,
1202 **Steps 1-4**). As very long acquisition times are required to assure quantitative signals, we
1203 recommend quantitating species from the ^{1}H spectra by integration or peak-fitting – if possible.
1204

1205 **18.** We suggest using the Bruker Pulse sequence '***zgig30***' with the following parameters:

1206 - A 30° pulse flip angle with inverse-gated decoupling.
1207 - 4 dummy scans (ds) and as many transients (ns) as possible within the available time,
1208 but preferably no less than 8000 (overnight collection).
1209 - A relaxation delay (d1) of 5 times the T_1, of the species under investigation, must be
1210 set for accurate quantitation.
1211 - For 5 wt% cellulose in $[P_{4444}]$[OAc]:DMSO-d_6 at 65 °C, some T_1 values have been
1212 measured previously,[25,26] giving cellulose backbone ^{13}C signals from ca. 0.2-0.6 s. For
1213 a 30° pulse flip angle this would require ca. 1 s of relaxation delay (0.6 × 5/3) for full
1214 relaxation. However, more mobile species, *e.g.*, methyl groups, or quaternary carbons
1215 typically have much longer T_1 values so higher values should be set preferably after
1216 measurement of the T_1 values for the species to be quantified. For a 30° pulse flip
1217 angle, 5s of relaxation delay is a much more reasonable number to give accurate
1218 quantitation of polymer bound species.
1219

1220 **19.** An example spectrum is presented in **Figure 8**.
1221

1222 **20.** Characteristics of the quantitative ^{13}C spectra and obtainable information:

1223 Similar to the qualitative ^{13}C experiment, quantitative ^{13}C offers excellent resolution of species.
1224 Thus, accurate peak separation and quantitation (not involving peak-fitting) can be obtained,
1225 at the expense of longer collection times (typically overnight or over the weekend).
1226
1227

1228 **2D ^{1}H-^{13}C HSQC-total correlation spectroscopy (TOCSY)**

1229 **<TIMING>** 2.5 h

1230 **21.** Perform this experiment if spin-system correlation is needed. Cellulose backbone systems
1231 are already quite well described for unmodified and esterified systems.[84] However, it is useful
1232 to perform TOCSY correlation for new functionalities and substituents.
1233

1234 **22.** We suggest using the Bruker Pulse sequence '***hsqcdietgpsisp.2***'[98]. HSQC-TOCSY
1235 experiments use a phase-sensitive HSQC-TOCSY pulse program with the DIPSI-2 isotropic
1236 mixing sequence and echo/antiecho-TPPI gradient selection with the following typical
1237 parameters:

1238 - Spectral widths (sw) are 13.0 and 200 ppm, with transmitter offsets (o1p) of 6.18 and
1239 90 ppm for ^{1}H and ^{13}C dimensions, respectively.
1240 - The time-domain size (td1) is 512 or 1024 in the indirectly detected ^{13}C-dimension (f1)
1241 dimension.
1242 - Typically, 16 dummy scans (ds), 4 (or multiples of 4) transient scans (ns), with an
1243 acquisition time (aq) of 0.107 s for f2 and a relaxation delay of 1.5 s are recorded.
1244 - The TOCSY mixing delay (d9) is 0.015 s to yield a short-range TOCSY experiment or
1245 0.12 s to yield a long-range TOCSY experiment, where the full spin-system can be
1246 typically observed. The latter experiment requires typically 2-4 times the scans (ns) to
1247 yield similar signal-to-noise as the short-range experiment.
1248 - Window functions are typically sine squared (90°) in f1 and f2.
1249

1250 **23.** An example spectrum is presented in **Figure 9**.
1251

1252 **24.** Characteristics of the ^{1}H-^{13}C HSQC-TOCSY spectra and obtainable information:

1253

1254 - Combination of HSQC with TOCSY, will return not only single-bond H-C HSQC
1255 correlations but also correlations for neighbouring J-coupled protons ($^{>1}J_{CH}$ couplings).
1256 - Extended TOCSY mixing times will allow to stretch magnetization over the whole spin-
1257 system, allowing for identification of almost all CH-XH connected species, at the
1258 expense of S/N.
1259 - Shorter mixing times restrict the TOCSY correlations to only the closest XH pairs,
1260 typically giving COSY-like correlations, except with the increased resolution that the
1261 additional ^{13}C f1 dimension affords (see **Fig. 9**).
1262 - If HSQC gives good signal-to-noise, HSQC-TOCSY (15 ms mixing time) will also.

1263 **^{1}H-^{13}C Heteronuclear Multiple Bond Correlation (HMBC)**

1264 **<TIMING>** 2.5 h

1265 **25**. Perform this experiment when you suspect that the material might contain moieties with
1266 isolated carbons or if you want to find out the regioselectivity of introduced modifications.
1267 Correlations over multiple bonds are useful when moieties with isolated carbons are suspected
1268 (*e.g.*, carboxylates, ketones, tertiary carbons).

1269

1270 **26.** We suggest using the Bruker Pulse sequence '***hmbcgplpndqf***'.[102] The HMBC
1271 experiments use a magnitude-mode gradient-enhanced HMBC sequence with a low-pass J-
1272 filter and the following typical parameters:

1273 - Spectral widths (sw) are 13.0 and 250 ppm, with transmitter offsets (o1p) of 6.3 and
1274 100 ppm for ^{1}H and ^{13}C dimensions, respectively.
1275 - The time-domain size (td1) in the indirectly detected ^{13}C-dimension (f1) is typically 512.
1276 For magnitude-mode HMBC, this directly corresponds to 512 t_1-increments for the real
1277 spectrum.
1278 - Typically, 16 dummy scans (ds) and multiples of 4 scans (ns) should be recorded with
1279 an acquisition time (aq) of 0.131 s for f2 and a relaxation delay of 1.5 s.
1280 - A $^{1}J_{CH}$ coupling constant value (cnst2) of 145 Hz is used for the low-pass filter.
1281 - The polarization transfer delay is optimized for a $^{n}J_{CH}$ long-range coupling constant
1282 value of 10 Hz (cnst13).
1283 - Window functions were typically sine bell (0°) in f1 and f2.

1284

1285 **27.** An example spectrum is presented in **Figure 10**.

1286

1287 **28.** Characteristics of the ^{1}H-^{13}C HMBC spectra and obtainable information:

1288 - Two to four bond CH correlations are expected if the molecular weight or functionality
1289 mobility is low enough. This may not always be the case, especially for
1290 conformationally stable hexoses, as some bond angles can render coupling values
1291 and correlation intensities out of reach.
1292 - An important potential is the correlation of carbonyl with aliphatic functionalities.
1293 - It is also noteworthy that correlations between the 1 and 4 positions ($^{3}J_{CH}$) on adjacent
1294 AGUs can be made (see **Fig. 10**).
1295 - Only low molecular weight and conformationally free substituents will allow for decent
1296 quality HMBC spectra; for higher molecular weight or conformationally restricted
1297 substituents there will be considerable T_2 losses during the HMBC mixing period.

Table 2. Bruker pulse programs and variable parameters of standard 1D and 2D NMR experiments for the structural determination of crystalline celluloses in $[P_{4444}]$[OAc]:DMSO-d_6 at 65 °C.

Experiment	Bruker pulse program[a]	Important parameters	Expected improvement	Additional info and T_1-values
Standard, quantitative ^{1}H	zg30	- Number of transient scans (ns) - Relaxation delay (d1)	- Increasing ns improves signal-to-noise (S/N)[e] - Sufficiently long d1 is required to give quantitative conditions[f]	26
Qualitative ^{13}C	zgpg30	- ns	- S/N	
Quantitative ^{13}C	zgig30	- ns - d1	- S/N - Quantitivity	25
Diffusion-edited ^{1}H (DOSY)	ledbpgp2s1d	- ns - Diffusion time (d20) - Gradient pulse length (p30)	- S/N - Optimization of p30 and d20 is needed to allow for efficient removal of fast-diffusion species, without compromising S/N too much[g]	25
Multiplicity-edited ^{1}H-^{13}C HSQC	hsqcedetgp hsqcedetgpsisp2.2[b] hsqcedetgpsisp2.3[b]	- ns - f1 increments (td (f1))[c]	- S/N - Increase in td (f1) gives improved f1 resolution[h]	25,26,103,104
2D ^{1}H-^{13}C HSQC-TOCSY	hsqcdietgpsisp.2	- ns - f1 increments - TOCSY mixing time (d9)[d]	- S/N - f1 resolution - Increase in d9 allows for further correlations along the spin-system, at the expense of S/N	26
^{1}H-^{13}C HMBC	hmbcgplpndqf	- ns - f1 increments	- S/N - f1 resolution	104

[a] Bruker TopSpin® version 4.0; [b] for increased sensitivity; [c] time-domain size (TD1) in ^{13}C-domain; [e] S/N increases as the square root of the number of scans – hence, to double S/N, the number of scans must be increased by 4 times compared to the original data collection; [f] sufficient delay is required for full relaxation of signals, prior to further acquisitions – this is most relevant for quantitative ^{13}C where T_1 values can be rather long and require measuring; [g] care must be taken to make sure the application of strong gradients does not exceed that which can be tolerated during the duty cycle – this is probe specific and, if in doubt, the user should definitely contact the manufacturer for advice – once these parameters have been confirmed for the probe, there should be no need to change them in further experiments; [h] f1 resolution is proportional to td (f1), until the natural line width is approached (see **Supplementary Figure 2**).

1298 # Troubleshooting

1299

1300 **Possible problems in the preparation of the [P_{4444}][OAc]:DMSO-*d*$_6$ (1:4 wt%)**
1301 **electrolyte**

1302 ***Drying:***

1303 **[P_{4444}][OAc]:** It is difficult to dry the IL, because H_2O or the short chain alcohols used as
1304 solvents in the metathesis steps are actively adsorbed in the final product. This not only leads
1305 to solvent artefacts in the spectra, but also negatively influences the complete precipitation of
1306 the inorganic by-products. The stated drying conditions in the protocol were sufficient to
1307 remove all residual solvents in our experience.
1308 However, we recommend applying the strongest vacuum available and checking the
1309 associated pumps for potential leakage (tubing connection) before application. Increasing the
1310 temperature above 90 °C during drying is not recommended, as [P_{4444}][OAc] will start to slowly
1311 decompose, leading to another source of impurities. If possible, a lower temperature should
1312 be applied.

1313

1314 **[P_{4444}][BF_4]:** Strong vacuum (<10 mbar) at room temperature is sufficient to dry the white
1315 precipitate in the last step of the metathesis. Elevated temperatures are not recommended,
1316 owing to the potential instability of the anion. In the subsequent steps, KOAc is used in excess.
1317 Thus, smaller amounts of H_2O will not influence stoichiometry. If drying issues are observed,
1318 add a larger amount of molecular sieves during the drying in the next metathesis step (**Step**
1319 **1B – xiii**).

1320

1321 ***Impurities:***

1322 In the final [P_{4444}][OAc] product, minor contaminations with silver or potassium (detected by
1323 ICP-MS)[25] or [BF_4] (detected by ^{19}F NMR) stemming from the educts are usually observed.
1324 However, they can be tolerated if there are no signs of degradation in the spectra of the
1325 cellulose model substance (*e.g.*, Avicel® PH-101 MCC) obtained in **Procedure 1, step 7**.
1326 In a correctly prepared electrolyte, usually only a very small peak of formate [$HCOO^-$] (8.61
1327 ppm) is visible. With larger amounts of residual silver or potassium ions (after metathesis), this
1328 species becomes more prominent after heating at 65 °C overnight, concomitant with sample
1329 colourisation. The mechanistic background of its formation is still unclear. However, one
1330 potential hypothesis is a combined reverse and forward Cannizzaro reaction, which would also
1331 be dependent on the presence of water in the sample.[27] We added ^{1}H spectra of a cellulose
1332 sample obtained in such a poor-quality electrolyte to the Supplementary information for clarity
1333 (see **Supplementary Figure 1**).

1334 Furthermore, minor peaks of cellulose acetate (2.02 ppm) may occur, which originate from an,
1335 as yet poorly understood reaction between cellulose and poor-quality electrolyte impurities.
1336 If degradation is observed, [P_{4444}][OAc] can be recrystallized by dissolving it in hot MeCN (1
1337 mL per g) or warm MeCN / Et_2O (1:1; 2 mL per g) and placing the solution in the freezer
1338 overnight (-24 °C, 16 h). Owing to the low melting point of the compound, the excess solvent
1339 must be removed with a Pasteur pipette while still cold (-24 °C) - an additional drying step is
1340 then necessary (rotavapor, 60 °C, 2h).
1341 In case of silver impurities, exposure to air as described in a previous metathesis scheme can
1342 also help to mitigate the problem - by conversion of residual salts to nanoparticles, which can
1343 be removed by filtration.[25]
1344 If the recrystallization is insufficient to increase purity, the metathesis reaction must be
1345 repeated. For all starting materials recrystallization protocols were described.[37]
1346

1347 **Possible problems in the dissolution of cellulosic materials and NMR sample**
1348 **preparation in Procedure I, steps 8-11**

1349 ***Insoluble samples:***

1350 - Increase temperature to increase the dissolution rate. It is generally not advisable to go
1351 above 80 °C as the IL slowly starts to decompose and solute decomposition will also be
1352 more rapid.
1353 - Check H_2O content of the used electrolyte and the sample under investigation
1354 - Decrease concentration to 1-3 wt%.
1355 - If high ionic charge is present on the polymer backbone, the sample may need
1356 neutralisation *via* acidification.

1357 If the sample dissolves only partially, spectral acquisition might still be possible. However, the
1358 suspended particles will negatively influence the shimming process and the spectral
1359 resolution. Furthermore, it will not be possible to characterize the sample entirely, as the
1360 obtained information only shows the dissolved constituents. Thus, complementary analyses
1361 with other techniques are advisable.
1362 Complete or partial insolubility is usually observed for pulps with high hemicellulose contents,
1363 highly cross-linked species or anionically charged samples. For the anionically charged
1364 samples, an acidification protocol was found to render the material soluble in the electrolyte.[26]
1365

1366 ***High viscosity of sample solution:***

1367 - Decrease the concentration to 1-3 wt%.

1368 - Increase temperature to decrease viscosity. It is generally not advisable to go above 80 °C,
1369 unless necessary, as the IL slowly starts to decompose at 100 °C. Non-ceramic spinnerets
1370 (the plastic versions) have an upper temperature limit of 80 °C.
1371 - Mechanically pre-treat your sample, *i.e.*, by ball milling

1372 High viscosity samples are more challenging to work with, but they can still be processed if
1373 their transfer into the bottom of the NMR tube (to the required level) is still possible. This type
1374 of problem is usually observed with high-DP pulps or strongly cross-linked modified cellulosics.
1375 In general, low-resolution spectra can be expected when investigating high viscosity samples.
1376 If the sample is fully dissolved but the viscosity is too high to transfer it to the NMR tube, it is
1377 usually possible to dilute the sample with pure DMSO-d_6 and still keep the cellulose in solution.
1378 **CRITICAL:** When using the protocol to monitor cellulose modification, it is advisable to visually
1379 compare the solution viscosities of the modified samples with the original substrate. If the
1380 viscosity of the product is much lower, this is an indicator of depolymerization; a much higher
1381 viscosity is an indicator of cross linking reactions. If the NMR linewidth is lower than in the
1382 starting material, this is also an indication of depolymerisation.
1383
1384 ***Transfer to the NMR tube:***
1385 If the solution is too viscous for transfer to the NMR tube, decrease the viscosity according to
1386 the points listed above. If the sample gets stuck at the top of the NMR tube or bubbles are
1387 visible in the solution, gentle shaking or manual spinning might force the solution to the bottom.
1388 A warm water bath can also help to reduce the viscosity temporarily. Application of a heat-gun
1389 is also possible, provided the temperature of the sample is kept below 100 °C to avoid
1390 degradation. In case of very viscous samples, further dilution with DMSO-d_6 or electrolyte may
1391 be preferred.
1392 Depending on the sample under investigation, the volume of the solution that can be
1393 transferred to the bottom of the NMR tube might be much lower than the volume of added
1394 electrolyte. This can be due to handling losses (material stuck in the vial or the glass pipette)
1395 and the contraction of highly viscous solutions. For optimal results it is important to keep a
1396 constant filling height of 4-5 cm. Preparing more sample or further dilution with DMSO-d_6 can
1397 alleviate this problem. We recommend aiming to prepare ~1g of cellulose-electrolyte solution.
1398

1399 ## Possible problems in the spectral acquisition

1400

1401 **S/N is poor**: The preferred way to improve S/N is to increase the sample concentration in the
1402 electrolyte, if the sample viscosity and the available sample amount allow.
1403 Alternatively:

1404 i) Ensure the receiver gain is maximised (without causing ADC overflow).
1405 ii) Increase the number of transients (S/N is proportional to the square root of the
1406 number of transients).
1407 iii) Move to higher field or more suitable probes, *e.g.*, cryogenically-cooled probes.
1408
1409 **No signal**: Check that the tube has not broken inside the probe and make sure the probe is
1410 tuned correctly.
1411
1412 **Poor shimming or line-shape**: Check that the solvent level is sufficiently high (just above the
1413 detection window) and re-shim the spectrometer. Line shape is also strongly affected by the
1414 presence of paramagnetic species. If the cellulosic samples have been treated with transition
1415 metals, *e.g.,* chromium (III) or copper (II), or there is a possibility that paramagnetic species
1416 are present as a contamination - make sure to remove these from the sample before
1417 measurement. Furthermore, suspended particles in the sample solution can introduce
1418 lineshape issues.
1419
1420 **Possible problems in the spectral interpretation:**
1421 **Dominant and overlapping H_2O peak**: Determine the H_2O content of the used electrolyte
1422 and thoroughly dry the sample. It is possible to remove small quantities of water from the
1423 electrolyte by adding dry 3 Å molecular sieves and letting the mixture sit overnight.
1424
1425 **Low-molecular-weight impurities**: Can be present in samples after insufficient work-up of
1426 prepared cellulose derivatives and lead to peak superpositions with the cellulose backbone.
1427 Perform another purification step, *e.g.*, trituration, dialysis or Soxhlet extraction. In our
1428 experience, a dispersion step in DMSO, as a part of the purification protocol (*e.g.,* after
1429 modification of CNCs), sufficiently removes impurities from the cellulose surface. But this may
1430 also remove modified cellulose surface chains. Thus, care should be taken, employing
1431 perdeuterated molecular solvents and simple ^{1}H NMR to observe what low molecular-weight
1432 impurities are present, to confirm possible exfoliation of surface cellulose chains.
1433 **CRITICAL!** If inorganic impurities are present in the sample, they can lead to a catalytic
1434 degradation, as described for the impurities stemming from insufficient IL purity.
1435
1436 **Sample instability:** Some evidence of sample instability may be observed in modified
1437 cellulosic materials. Look at the derivatizations or functionalities that have been introduced
1438 and consider whether they might undergo reactions with the acetate anion (potential
1439 nucleophile) or in presence of DMSO (oxo-transfer source).

1440 Side-reactions with the electrolyte may be apparent from the diffusion-edited ^{1}H experiment;
1441 look for the presence of additional acetate signals (~2 ppm). Oxo-transfer reactions, *e.g.*,
1442 Swern-type or Kornblum oxidations, are also apparent by the formation and odour of dimethyl
1443 sulphide. If oxo-transfer is possible, it is possible to replace DMSO-d_6 in the electrolyte with
1444 *N,N*-dimethylformamide-d_7. Another potential electrolyte-induced side-reaction, is base-
1445 induced degradation; evidence for this reaction would be the presence of new low-molecular-
1446 species.
1447 In the case of complete instability of the sample, try to understand the unwanted side-reactions
1448 by performing experiments with model compounds and by thorough attention to the literature.
1449 A good example of a well-documented side-reaction is *β*-elimination induced depolymerisation
1450 of periodate-oxidised cellulose.[26,105]
1451 In the case of partial instability try to reduce the temperature during the sample dissolution
1452 and the spectral acquisition.
1453 **CRITICAL:** If instability is suspected, as with oxidised celluloses,[26,113] and longer
1454 measurements are performed (*e.g.*, HMBC or quantitative ^{13}C), record an additional ^{1}H and
1455 diffusion edited ^{1}H spectrum at the end of the set of experiments and compare them with the
1456 spectra measured at the beginning of the collection. This helps to assure that the measuring
1457 conditions have been constant, and no chemical modification has occurred, during the
1458 collection period.
1459
1460 ***Fityk* processing:**
1461
1462 **Baseline correction:** Baseline correction using the spline baseline fitting function in *Fityk* is
1463 rather straight forward. However, care must be taken to correctly place the spline points in the
1464 spectra. For fitting the full spectrum, to allow for integration of 2 regions of interest, a minimum
1465 of 8 points should be fitted. Comparison of samples requires consistent positioning of spline
1466 points from sample to sample.
1467
1468 **Insufficient fit:** If the fitted Gaussian guess functions do not give representative fitting or high
1469 residual baseline error, they can be added, deleted, adjusted manually, and/or re-fitting can
1470 be applied with constraints, to give improved fitting and better representation of the different
1471 resonance regions, *i.e.,* H1-6 peak positions. If the obtained set of Gaussian functions
1472 describes the active region well (low residual baseline error), further Gaussian guesses can
1473 be applied to reduce the error to required levels, with extra fitting steps if needed. After this,
1474 activate the disactivated regions in 'Data-range mode' or using the command "A = a or (-2 < x
1475 and x < 20)" and disactivate new regions for fitting. After the first region is fitted sufficiently,
1476 we strongly recommend saving the session into a separate file.

Gaussians with negative values: Sometimes after application of the automatic fitting algorithms, functions with “negative” areas appear (with overall positive fitting area for the linear combination of all functions). In this case, just delete the “negative” function from the list and apply the “fit” command again. If the problem persists, the Levenberg–Marquardt (mpfit) algorithm supports the application of ‘domains’ during fitting, *i.e.*, positive value ranges can be set. Further information is available through the *Fityk* manual.

Validation of calculation: The whole processing procedure affords several manual manipulations, which inherently can bias the results. If there are several separated peaks available, it is advantageous to conduct the calculations with different fitted areas. For example, the integral of the relatively isolated C1 peak in many cases can be used to conduct the DS calculations instead of the whole cellulose backbone area.

TIMING

Procedure I:

Step 1, option A: 70 h with drying

Step 1 option B (i- viii) 24 h with drying

Step 1, option B (ix-xxi): 72 hours with drying

Steps 2-7: 24- 72 h

Steps 8-11: 1-18 h

Steps 12-14: 1-72h

Procedure II:

Steps 1-4: 8 min

Steps 5-8: 5-60 min

Steps 9-12: 2.5 h

Steps 13-16: 3 h

Steps 17-20: 15 h

Steps 21-24: 2.5 h

Steps 25-28: 2.5 h

1508 # Anticipated results

1509 ## Example I: Characterization of different cellulosic substrates – effect of degree
1510 of polymerization (DP) and the spectrometer field strength

1511 As can be seen in the comparison of quantitative ^{1}H spectra of different crystalline celluloses
1512 and pulp samples (**Fig. 11**), the presented protocol allows for the dissolution and quick
1513 characterization of a wide variety of cellulosic substrates. These examples show that the H1
1514 region is most important when it comes to analysis of different pulp samples. In samples with
1515 DP_N values below ~200, the peaks are relatively well resolved and even signals of moieties
1516 with low abundance, including reducing and non-reducing ends, or surface grafted sulphate
1517 groups, become visible. This enables quantitative analyses like DP and DS calculations. In
1518 samples with higher DP values, *e.g.,* chemical pulps or cotton cellulose, the resolution is
1519 reduced and substantial peak broadening and overlap in the NMR spectra is observed.
1520 Nonetheless, it is still possible to get valuable information about their chemical composition
1521 *e.g.*, a good estimation of their hemicellulose content can be obtained through peak-fitting.
1522 Screenings were conducted to optimise the measuring conditions for best results in resolution
1523 and S/N. It is not possible to enhance the spectral quality by increasing the concentration of
1524 cellulosic material, as the resolution will suffer from the sample's higher viscosity. Increasing
1525 the measuring temperature is also not recommended, to avoid degradation of the cellulosic
1526 material and potential probe degradation. However, further dilution with DMSO-d_6 and small
1527 increases in temperature are possible, if the responsible NMR technician approves these
1528 changes (depends on probe temperature limits and spinneret melting temperature range).
1529 Solubility problems or high viscosities often even require a reduction of the samples measuring
1530 concentration. We have found that for chemical pulp samples (DP_N typically > 200), 2.5 wt%
1531 solutions are required to improve resolution and even to allow for transfer of the dissolved
1532 samples to the NMR tube.
1533 This limitation regarding sample concentration means that it is important to use as high field-
1534 strength spectrometers as possible, if qualitative determinations of low abundancy
1535 constituents are anticipated. This, of course depends on the availability of the hardware and
1536 needs to be balanced against the cost of the analysis. For example, a high-quality HSQC
1537 spectrum was achievable for MCC using an 850 MHz spectrometer, with liquid helium-cooled
1538 cryoprobe, in only one transient scan (**Fig. 11a**). Reducing end signals and xylan signals were
1539 clearly visible. Additionally, resonances, that would not be immediately observable at the lower
1540 fields, were discernible revealing novel unassigned structural features. Moreover, increasing
1541 the field strength from 400 to 850 MHz, resolved the coupling values for the overlapping AXU-
1542 1 and AGU-RE-β-1 (**Fig. 11b**). However, one draw-back of the use of the cryoprobe is that,
1543 for the 1D ^{1}H experiment, both receiver gain and pulse-flip angle needed to be substantially

lower to avoid audio-to-digital conversion (ADC) overflow artifacts, *e.g*. receiver gain should be set to minimum and pulse-flip angle to less than 15 °. Thus, dynamic range becomes a problem when sensitivity increases, due to the presence of the intense $[P_{4444}]^+$ signals; this limits the sensitivity of this useful 1D ^{1}H experiment.

1549 **Example II: Solution-state NMR spectroscopy in cellulose chemistry – reaction**
1550 **control using the diffusion-edited ^{1}H NMR experiment**

1551 Surface modification by covalent derivatization is one of the main routes for changing the
1552 properties of cellulosic materials. In order to properly characterise the product, it is important
1553 to be able to distinguish between species that are covalently attached and those that are
1554 adsorbed or present as a result of insufficient purification (organic impurities). With
1555 investigations involving low degrees of derivatization, *e.g.,* on the surface or reducing end
1556 groups of CNCs, this represents a major analytical challenge, which is difficult to resolve using
1557 available techniques.[64] The absence of a quick and reliable analytical tool can frustrate
1558 preliminary reaction screenings and optimizations.
1559 With the aid of the presented diffusion-edited experiment (see **Procedure 2, steps 5-8**), these
1560 questions can be resolved rather quickly. In the diffusion-edited ^{1}H experiment, which is
1561 basically a 1D DOSY experiment, we exploit the difference in solution-state diffusion
1562 coefficients of high-molecular-weight (polymeric) and low-molecular-weight (*e.g.*, adsorbed
1563 impurities) compounds; by application of a single strong diffusion gradient and long diffusion
1564 delay, where only fast-diffusing species are fully attenuated.[25] By that, we can identify which
1565 resonances from the previous standard ^{1}H experiment result from covalent attachment to our
1566 slow-diffusing cellulose polymer (**Fig. 12a**) or from simple non-covalent adsorption to the dried
1567 cellulose surface (**Fig. 12b**). Hence, by comparing the spectra of the standard ^{1}H experiment
1568 with the diffusion-edited experiment, the peaks visible in both spectra can be attributed to
1569 covalent modifications.
1570 Owing to peak overlap, a combination of the technique with the high-resolution HSQC
1571 experiment, is very effective for signal assignment. As an example, the differences between
1572 the spectra of a surface benzylated MCC sample and MCC mixed with benzyl alcohol are
1573 shown in **Fig.12**. The standard ^{1}H and the HSQC spectra of high- and low-molecular weight
1574 species are similar to each other, except for the peak widths (polymer-bound species being
1575 broader than non-bound species) and the previously assigned chemical shifts for the benzylic
1576 CH_2 (compare **Fig. 12a** and **b**). However, when comparing with the diffusion-ordered ^{1}H
1577 spectra (**Fig. 12a** and **b**, lower traces), the differences become apparent. As no peaks are
1578 visible in the aromatic region for the benzyl alcohol-doped sample (**Fig. 12b**), covalent bonding
1579 to the polymer can be excluded.
1580 Furthermore, diffusion-editing allows for the investigation of modifications where some of the
1581 peaks are superimposed with the IL residual signals (*e.g.,* common cellulose alkylesters and
1582 alkylethers). For example, its application has facilitated clear confirmation of the reaction and
1583 rough assessment of regioselectivity of modification for a series of reactions involving
1584 acetylation.[40,42,46,48] Cellulose acetate peaks are difficult to assign in the ^{1}H or the HSQC

spectra (**Extended Data Figure 1**), because many of the peaks are overwhelmed by the signals from [P_{4444}][OAc] resonance region. However, in the diffusion-edited ^{1}H experiment, the acetate signals (~ 2 ppm) are clearly and quickly discernible (**Extended Data Figure 2**).

1590 **Example III: Long-range correlations and connectivity with 2D HSQC-TOCSY**
1591 **and HMBC**

1592 When applying the presented protocol in cellulose chemistry in many cases, the initial
1593 experiments suggested in **Section I** of **Box 1** are sufficient to obtain a solid overview of the
1594 chemical composition and occurred transformations. Nonetheless, there are reactions that
1595 necessitate the application of further 2D NMR experiments to properly assign the peaks. One
1596 example is TEMPO-oxidation[106] which leads to the introduction of carboxylate functionalities
1597 at the C6 position. It is ubiquitously employed in a synthetic capacity and often to introduce
1598 electrostatic charge to pulps, to reduce the specific energy requirements for fibrillation to
1599 cellulose nanofibers, or to aid in dispersion of nanocelluloses into aqueous media.
1600 Furthermore, carboxylate functionalities introduced through TEMPO oxidation or
1601 carboxylmethylation[107] are a key synthetic entry point for the attachment of chemical
1602 functionalities, often achieved *via* application of 'peptide coupling' agents.[108] commonly
1603 through or, followed by amide formation.[109] While these reactions are frequently used, they
1604 are inherently prone to by-product formation, especially through the introduction of isoureas,
1605 which are difficult to detect and quantify using commonly used methods.
1606
1607 These valuable TEMPO oxidized cellulose species are more difficult to examine using NMR
1608 as the characteristic carboxyl functionalities do not show correlations in HSQC, owing to the
1609 absence of a directly attached proton at the carbonyl carbon (*i.e.*, no $^{1}J_{CH}$ coupling).
1610 Furthermore, as only partial conversion is anticipated, the peaks of the formed
1611 anhydroglucopyranosiduronic acid (AGA) units are superimposed on the residual AGUs in the
1612 relevant spectral area (see **Fig 13a**). However, the problems can be resolved using 2D
1613 experiments where multiple bonds can be correlated. In the presented example of a TEMPO-
1614 oxidised cellulose nanocrystal[25] the application of HMBC showed clear $^{2}J_{CH}$ and minor $^{4}J_{CH}$
1615 correlations from a carboxylate functionality (~170 ppm) into the polysaccharide region. In
1616 combination with the diffusion edited ^{1}H experiment this proved the presence of polymeric
1617 AGA units (see **Fig. 13b**). Starting from characteristic and isolated peaks (usually in the acetal
1618 C1 region) the application of HSQC- TOCSY allowed to fully assign all peaks in the spin
1619 system (see **Extended Data Figure 3**).
1620 It is noteworthy that the CNC compound used as starting material in the presented study
1621 represents a model compound for applications of 2D experiments, owing to its extremely low
1622 DP and high purity. In HMBC experiments where longer-range correlations are measured, it
1623 is more difficult to obtain information for high DP samples. The 2D experiments of modified
1624 cellulosics can result in very crowded and complex spectra, even when using model substrates
1625 (**Extended Data Figure 3**). In investigations using more industrially interesting starting
1626 materials like different pulps, the additional hemicellulose signals, and peak broadening due

1627 to overall higher DP (see **Fig. 11**) will add even more complexity to the spectra. In many cases,
1628 it is therefore advisable to use MCC or CNCs that have a low degree of polymerisation as
1629 model substrates to assess the success of new cellulose chemistry with 2D NMR
1630 spectroscopy. Choosing starting materials that have a lower degree of polymerisation avoids
1631 peak superpositions with hemicelluloses correlations and generally will improve S/N for both
1632 short and long-range correlation experiments. Once the chemistry is established and peaks of
1633 the modified cellulosics have been assigned, analysis can be quickly performed using cross
1634 validation with HSQC or diffusion edited ^{1}H experiments. In some cases, in addition to the use
1635 of MCC or CNCs as model substrates, glucose or cellobiose may be required as model
1636 substrates, before implementing the chemistry and analysis on higher DP technical
1637 materials/pulps.
1638
1639
1640
1641 **Example IV: Expansion of the NMR protocol to other (bio)polymers**
1642 Aside from cellulose, other non-polysaccharide polymers proved to be soluble in the
1643 electrolyte mixture and yielded high resolution spectra in so far unpublished screening studies.
1644 On the synthetic side, it has been possible to dissolve poly(methyl methacrylate) (PMMA),
1645 poly(N-isopropylacrylamide) (PNIPAM), poly(styrene sulphonate) (PSS) and poly(ethylene
1646 glycol) (PEG). On the biopolymer side, purified spruce lignin (dioxane-extracted), softwood
1647 kraft lignin (Lignoboost^{TM}), and lignosulphonate (provided by Borregaard AS, Norway) were
1648 sufficiently dissolved in the IL NMR solvent, as were common purified hemicelluloses (from
1649 hot water extraction). The broad applicability of the electrolyte is very promising, as it facilitates
1650 investigation of composite materials.
1651
1652 ***Wood***
1653 One of the most complex and probably the most abundant composite materials – wood – also
1654 showed solubility in the presented NMR solvent. Cellulose-dissolving ILs and homologous
1655 tetraalkylphosphonium acetate:DMSO electrolytes are known to dissolve wood and all-wood
1656 biopolymers.[23,81,110] However, these type of samples typically require pre-treatment by heavy
1657 mechanical (planetary or vibratory) milling before dissolution, using direct-dissolution cellulose
1658 solvents.[81,111] If mild pressurized hot-water pre-treatment is applied,[38] even wood chips can be
1659 fully dissolved. Quite recently, we tested the dissolution of whole spruce fibres which were
1660 produced using a low-energy thermomechanical refining.[112,113] This yielded complete
1661 dissolution and very high-quality ^{1}H spectra (**Fig. 14**). From the diffusion-edited ^{1}H spectrum
1662 residual acetates are clearly visible. These mainly correspond to the retained
1663 galactoglucomannan in the sample (~2 ppm). Extractive aliphatic signals (0.5-2 ppm) are also

visible, as are the common lignin signals. Hence, this method is an excellent tool for both structural characterization of wood samples but also as a rapid method of assessing mechano-chemical pre-treatment methods for homogeneous wood processing.

Protein based materials (polymers)

It is also possible to dissolve protein-based polymers, such as, silkworm silk or wool in the electrolyte mixture, allowing for accurate assignment of the amino acids that these polymers contain.[25] Furthermore, the protocol was successfully applied to whole, milled insects (**Extended Data Figure 4**), which allowed for rapid 'finger-printing' of their contained proteins, through diffusion-edited ^{1}H NMR. However, consistent with our previous findings, chitin was not fully soluble.[25] While the application of this method may be limited, compared to traditional protein NMR analyses yielding dynamics and 3D structure, the potential for profiling in metabolism studies or quality control of food-based feedstocks may be highly important.

Competing interests:

The authors declare that they have no competing financial interests.

Acknowledgements:

The authors want to acknowledge the fundamental contributions of Ashley Holding, Valtteri Mäkelä and Sami Heikkinen in the early stages of the development of this method. **A.W.T.K.** gratefully acknowledges funding by the Academy of Finland (project # 311255, 'WTF-Click-Nano'). **K.H.** gratefully acknowledges the postdoctoral grant received from the Academy of Finland (project # 333905).

Author contributions statement:

A.W.T.K & T.K., designed and developed the workflows presented in this protocol. L.F., K.H. and M.H. implemented the protocol in a more technology orientated environment and addressed the occurring translational barriers. L.F. and A.R.T. contributed optimised metathesis schemes for the ionic liquid starting from commercial sources. S.H. provided solid state NMR spectra and expertise. D. RdC & J.F. provided samples, discussion & experimentation regarding the adaptation of the protocol to other substrates, as presented in the anticipated results section. L.F. and A.W.T.K. drafted, reviewed, and edited the manuscript with significant input from K.H., T.K. and M.H. I.K. provided funding for the basic research (initial articles) and advice on presentation of the subject matter. All authors have read through and agreed on the final version of the manuscript.

Additional information:

Supplementary information: The online version contains supplementary material available at

Correspondence and requests for materials should be addressed to Alistair W.T. King.

Related links:

Key references using this protocol:

King, A. W. T. *et al.* *Biomacromolecules* **19**, 2708–2720 (2018). https://www.sciencedirect.com/org/science/article/pii/S1525779721017797

Koso, T. *et al.* *Cellulose* **27**, 7929–7953 (2020). https://link.springer.com/article/10.1007/s10570-020-03317-0

References:

1. MacLeod, M., Arp, H. P. H., Tekman, M. B. & Jahnke, A. The global threat from plastic pollution. *Science* **373,** 61–65 (2021).

2. Sixta, H. *Handbook of pulp* (Wiley-VCH, Weinheim, 2006).

3. Szcześniak, L., Rachocki, A. & Tritt-Goc, J. Glass transition temperature and thermal decomposition of cellulose powder. *Cellulose* **15,** 445–451 (2008).

4. Li, C. *et al.* Fiber-Based Biopolymer Processing as a Route toward Sustainability. *Advanced Materials* **34 (1)**, 2105196 (2022).

5. Ning, P. *et al.* Recent advances in the valorization of plant biomass. *Biotechnol. Biofuels* **14,** 102 (2021).

6. Mussatto, S.I. *Biomass Fractionation Technologies for a Lignocellulosic Feedstock Based Biorefinery* (Elsevier, Amsterdam, 2016).

7. Robertson, G. P. *et al.* Cellulosic biofuel contributions to a sustainable energy future: Choices and outcomes. *Science* **356**, 1349 (2017).

8. Hassan, N. S., Jalil, A. A., Hitam, C. N. C., Vo, D. V. N. & Nabgan, W. Biofuels and renewable chemicals production by catalytic pyrolysis of cellulose: a review. *Environ. Chem. Lett.* **18,** 1625–1648 (2020).

9. Dufresne, A. Nanocellulose: a new ageless bionanomaterial. *Mater. Today* **16,** 220–227 (2013).

10. Li, T. *et al.* Developing fibrillated cellulose as a sustainable technological material. *Nature* **590,** 47–56 (2021).

11. Eyley, S. & Thielemans, W. Surface modification of cellulose nanocrystals. *Nanoscale* **6,** 7764–7779 (2014).

12. Rule, G.S. & Hitchens, T.K. *Fundamentals of Protein NMR Spectroscopy* (Springer-Verlag, Berlin/Heidelberg, 2006).

13. Chary, K.V.R. & Govil, G. *NMR in Biological Systems* (Springer Netherlands, Dordrecht, 2008).

14. Claridge, T. D. W. *High-Resolution NMR Techniques in Organic Chemistry* (Elsevier, Amsterdam, 2016).

15. Medronho, B., Romano, A., Miguel, M. G., Stigsson, L. & Lindman, B. Rationalizing cellulose (in)solubility: reviewing basic physicochemical aspects and role of hydrophobic interactions. *Cellulose* **19**, 581–587 (2012).

16. Heinze, T. & Koschella, A. Solvents applied in the field of cellulose chemistry: a mini review. *Polímeros* **15**, 84–90 (2005).

17. Swatloski, R. P., Spear, S. K., Holbrey, J. D. & Rogers, R. D. Dissolution of cellulose with ionic liquids. *J. Am. Chem. Soc.* **124**, 4974–4975 (2002).

18. Zhu, S. et al. Dissolution of cellulose with ionic liquids and its application: a mini-review. *Green Chem.* **8**, 325 – 327 (2006).

19. Liebert, T. F., Heinze, T. J. & Edgar, K. J. (eds.). Cellulose Solvents: For Analysis, Shaping and Chemical Modification (American Chemical Society, Washington, DC, 2010).

20. Cheng, K., Sorek, H., Zimmermann, H., Wemmer, D. E. & Pauly, M. Solution-state 2D NMR spectroscopy of plant cell walls enabled by a dimethylsulfoxide-d_6/1-ethyl-3-methylimidazolium acetate solvent. *Anal. Chem.* **85**, 3213–3221 (2013).

21. Kuroda, K., Kunimura, H., Fukaya, Y. & Ohno, H. ^{1}H NMR analysis of cellulose dissolved in non-deuterated ionic liquids. *Cellulose* **21**, 2199–2206 (2014).

22. Moulthrop, J. S., Swatloski, R. P., Moyna, G. & Rogers, R. D. High-resolution ^{13}C NMR studies of cellulose and cellulose oligomers in ionic liquid solutions. *Chem. Commun.* 1557–1559 (2005).

23. Holding, A. J., Heikkilä, M., Kilpeläinen, I. & King, A. W. T. Amphiphilic and phase-separable ionic liquids for biomass processing. *ChemSusChem* **7**, 1422–1434 (2014).

24. Holding, A. J. *et al.* Solution-State One- and Two-Dimensional NMR Spectroscopy of High-Molecular-Weight Cellulose. *ChemSusChem* **9**, 880–892 (2016).

25. King, A. W. T. *et al.* Liquid-State NMR Analysis of Nanocelluloses. *Biomacromolecules* **19**, 2708–2720 (2018).

26. Koso, T. *et al.* 2D Assignment and quantitative analysis of cellulose and oxidized celluloses using solution-state NMR spectroscopy. *Cellulose* **27**, 7929–7953 (2020).

27. Heise, K. *et al.* Knoevenagel Condensation for Modifying the Reducing End Groups of Cellulose Nanocrystals. *ACS Macro Lett.* **8**, 1642–1647 (2019).

28. Delepierre, G. *et al.* Challenges in Synthesis and Analysis of Asymmetrically Grafted Cellulose Nanocrystals via Atom Transfer Radical Polymerization. *Biomacromolecules* **22**, 2702–2717 (2021).

29. King, A. W. T. *et al.* Relative and inherent reactivities of imidazolium-based ionic liquids: the implications for lignocellulose processing applications. *RSC Adv.* **2**, 8020–8026 (2012).

30. Clough, M. T., Geyer, K., Hunt, P. A., Mertes, J. & Welton, T. Thermal decomposition of carboxylate ionic liquids: trends and mechanisms. *Phys. Chem. Chem. Phys.* **15**, 20480–20495 (2013).

31. Ebner, G., Schiehser, S., Potthast, A. & Rosenau, T. Side reaction of cellulose with common 1-alkyl-3-methylimidazolium-based ionic liquids. *Tetrahedron Lett.* **49**, 7322–7324 (2008).

32. Clough, M. T. *et al.* Ionic liquids: not always innocent solvents for cellulose. *Green Chem.* **17**, 231–243 (2015).

33. Liebert, T. & Heinze, T. INTERACTION OF IONIC LIQUIDS WITH POLYSACCHARIDES OF CELLULOSE. 5. SOLVENTS AND REACTION MEDIA FOR THE MODIFICATION. *Bioresources* **3**, 576–601 (2008).

34. Rico Del Cerro, D. *et al.* On the Mechanism of the Reactivity of 1,3-Dialkylimidazolium Salts under Basic to Acidic Conditions: A Combined Kinetic and Computational Study. *Angew. Chem. Int. Edit.* **57**, 11613–11617 (2018).

35. Zweckmair, T. *et al.* On the mechanism of the unwanted acetylation of polysaccharides by 1,3-dialkylimidazolium acetate ionic liquids: part 1—analysis, acetylating agent, influence of water, and mechanistic considerations. *Cellulose* **22**, 3583–3596 (2015).

36. Abushammala, H. *et al.* On the mechanism of the unwanted acetylation of polysaccharides by 1,3-dialkylimidazolium acetate ionic liquids: part 2—the impact of lignin on the kinetics of cellulose acetylation. *Cellulose* **24**, 2767–2774 (2017).

37. Yasaka, Y., Ueno, M. & Kimura, Y. Chemisorption of Carbon Dioxide in Carboxylate-Functionalized Ionic Liquids: A Mechanistic Study. *Chem. Lett.* **43**, 626–628 (2014).

38. Deb, S. *et al.* Application of mild autohydrolysis to facilitate the dissolution of wood chips in direct-dissolution solvents. *Green Chem.* **18**, 3286–3294 (2016).

39. Holding, A. J. *et al.* Efficiency of hydrophobic phosphonium ionic liquids and DMSO as recyclable cellulose dissolution and regeneration media. *RSC Adv.* **7**, 17451–17461 (2017).

40. Laaksonen, T. *et al.* WtF-Nano: One-Pot Dewatering and Water-Free Topochemical Modification of Nanocellulose in Ionic Liquids or γ-Valerolactone. *ChemSusChem* **10**, 4879–4890 (2017).

41. Khanjani, P. *et al.* Superhydrophobic Paper from Nanostructured Fluorinated Cellulose Esters. *ACS Appl. Mater. Inter.* **10**, 11280–11288 (2018).

42. Beaumont, M. *et al.* Unique reactivity of nanoporous cellulosic materials mediated by surface-confined water. *Nat. Commun.* **12**, 2513 (2021).

43. Reyes, G., Borghei, M., King, A. W. T., Lahti, J. & Rojas, O. J. Solvent Welding and Imprinting Cellulose Nanofiber Films Using Ionic Liquids. *Biomacromolecules* **20**, 502–514 (2019).

44. Niu, X. *et al.* Plasticized Cellulosic Films by Partial Esterification and Welding in Low-Concentration Ionic Liquid Electrolyte. *Biomacromolecules* **20**, 2105–2114 (2019).

45. Reyes, G. *et al.* Coaxial Spinning of All-Cellulose Systems for Enhanced Toughness: Filaments of Oxidized Nanofibrils Sheathed in Cellulose II Regenerated from a Protic Ionic Liquid. *Biomacromolecules* **21**, 878–891 (2020).

46. del Cerro, D. R., Koso, T. V., Kakko, T., King, A. W. T. & Kilpeläinen, I. Crystallinity reduction and enhancement in the chemical reactivity of cellulose by non-dissolving pre-treatment with tetrabutylphosphonium acetate. *Cellulose* **27**, 5545–5562 (2020).

47. Beaumont, M. *et al.* Assembling Native Elementary Cellulose Nanofibrils via a Reversible and Regioselective Surface Functionalization. *J. Am. Chem. Soc.* **143**, 17040–17046 (2021).

48. Koso, T. *et al.* Highly regioselective surface acetylation of cellulose and shaped cellulose constructs in the gas-phase. *Green Chem.* **24**, 5604–5613 (2022).

49. Klemm, D., Philipp, B., Heinze, T., Heinze, U. & Wagenknecht, W. Comprehensive Cellulose Chemistry (Wiley, 1998).

50. Klemm, D., Philipp, B., Heinze, T., Heinze, U. & Wagenknecht, W. Comprehensive Cellulose Chemistry (Wiley, 1998).

51. Rosenau, T., Potthast, A. & Hell, J. (eds.). Cellulose science and technology. Chemistry, analysis, and applications (John Wiley & Sons, Hoboken NJ, 2018).

52. Follain, N., Marais, M.-F., Montanari, S. & Vignon, M. R. Coupling onto surface carboxylated cellulose nanocrystals. *Polymer* **51**, 5332–5344 (2010).

53. Lavoine, N., Bras, J., Saito, T. & Isogai, A. Improvement of the Thermal Stability of TEMPO-Oxidized Cellulose Nanofibrils by Heat-Induced Conversion of Ionic Bonds to Amide Bonds. *Macromol. Rapid Comm.* **37**, 1033–1039 (2016).

54. Sadeghifar, H., Filpponen, I., Clarke, S. P., Brougham, D. F. & Argyropoulos, D. S. Production of cellulose nanocrystals using hydrobromic acid and click reactions on their surface. *J. Mater. Sci.* **46**, 7344–7355 (2011).

55. Wei, L. *et al.* Chemical modification of nanocellulose with canola oil fatty acid methyl ester. *Carbohyd. Polym.* **169**, 108–116 (2017).

56. Hettrich, K., Pinnow, M., Volkert, B., Passauer, L. & Fischer, S. Novel aspects of nanocellulose. *Cellulose* **21**, 2479–2488 (2014).

57. Chen, J., Huang, M., Kong, L. & Lin, M. Jellylike flexible nanocellulose SERS substrate for rapid in-situ non-invasive pesticide detection in fruits/vegetables. *Carbohyd. Polym.* **205**, 596–600 (2019).

58. Benkaddour, A., Journoux-Lapp, C., Jradi, K., Robert, S. & Daneault, C. Study of the hydrophobization of TEMPO-oxidized cellulose gel through two routes: amidation and esterification process. *J. Mater. Sci.* **49**, 2832–2843 (2014).

59. Bendahou, A., Hajlane, A., Dufresne, A., Boufi, S. & Kaddami, H. Esterification and amidation for grafting long aliphatic chains on to cellulose nanocrystals: a comparative study. *Res. Chem. Intermed.* **41**, 4293–4310 (2015).

60. Le Gars, M., Delvart, A., Roger, P., Belgacem, M. N. & Bras, J. Amidation of TEMPO-oxidized cellulose nanocrystals using aromatic aminated molecules. *Colloid. Polym. Sci.* **298**, 603–617 (2020).

61. Shard, A. G. X-ray photoelectron spectroscopy. in *Characterization of Nanoparticles* (eds. Hodoroaba, V.-D., Unger, W. E.S. & Shard, A. G.) 349–371 (Elsevier Amsterdam, 2020).

62. Vaca-Garcia, C., Borredon, M. E. & Gaseta, A. Determination of the degree of substitution (DS) of mixed cellulose esters by elemental analysis. *Cellulose* **8**, 225–231 (2001).

63. Filpponen, I. & Argyropoulos, D. S. Regular linking of cellulose nanocrystals via click chemistry: synthesis and formation of cellulose nanoplatelet gels. *Biomacromolecules* **11**, 1060–1066 (2010).

64. Heise, K. *et al.* Chemical Modification of Reducing End-Groups in Cellulose Nanocrystals. *Angw. Chem. Int. Edit.* **60**, 66–87 (2021).

65. Montanari, S., Roumani, M., Heux, L. & Vignon, M. R. Topochemistry of Carboxylated Cellulose Nanocrystals Resulting from TEMPO-Mediated Oxidation. *Macromolecules* **38**, 1665–1671 (2005).

66. Saito, T. & Isogai, A. TEMPO-mediated oxidation of native cellulose. The effect of oxidation conditions on chemical and crystal structures of the water-insoluble fractions. *Biomacromolecules* **5**, 1983–1989 (2004).

67. Zhao, H. & Heindel, N. D. Determination of degree of substitution of formyl groups in polyaldehyde dextran by the hydroxylamine hydrochloride method. *Pharm. Res.* **8**, 400–402 (1991).

68. Azzam, F., Galliot, M., Putaux, J.-L., Heux, L. & Jean, B. Surface peeling of cellulose nanocrystals resulting from periodate oxidation and reductive amination with water-soluble polymers. *Cellulose* **22**, 3701–3714 (2015).

69. Bohrn, R. *et al.* The FDAM method: determination of carboxyl profiles in cellulosic materials by combining group-selective fluorescence labeling with GPC. *Biomacromolecules* **7**, 1743–1750 (2006).

70. Röhrling, J. *et al.* A novel method for the determination of carbonyl groups in cellulosics by fluorescence labeling. 2. Validation and applications. *Biomacromolecules* **3**, 969–975 (2002).

71. Röhrling, J. *et al.* A novel method for the determination of carbonyl groups in cellulosics by fluorescence labeling. 1. Method development. *Biomacromolecules* **3**, 959–968 (2002).

72. Pines, A., Gibby, M. G. & Waugh, J. S. Proton-Enhanced Nuclear Induction Spectroscopy. A Method for High Resolution NMR of Dilute Spins in Solids. *J. Chem. Phys.* **56**, 1776–1777 (1972).

73. Schaefer, J. & Stejskal, E. O. Carbon-13 nuclear magnetic resonance of polymers spinning at the magic angle. *J. Am. Chem. Soc.* **98**, 1031–1032 (1976).

74. Newman, R. H., Davies, L. M. & Harris, P. J. Solid-State ^{13}C Nuclear Magnetic Resonance Characterization of Cellulose in the Cell Walls of Arabidopsis thaliana Leaves. *Plant Physiol.* **111**, 475–485 (1996).

75. Larsson, P. T., Wickholm, K. & Iversen, T. A CP/MAS^{13}C NMR investigation of molecular ordering in celluloses. *Carbohyd. Res.* **302**, 19–25 (1997).

76. Kono, H. *et al.* CP/MAS ^{13}C NMR study of cellulose and cellulose derivatives. 1. Complete assignment of the CP/MAS ^{13}C NMR spectrum of the native cellulose. *J. Am. Chem. Soc.* **124**, 7506–7511 (2002).

77. Foston, M. Advances in solid-state NMR of cellulose. *Curr. Opin. Biotech.* **27**, 176–184 (2014).

78. Newman, R. H. Carbon-13 NMR evidence for cocrystallization of cellulose as a mechanism for hornification of bleached kraft pulp. *Cellulose* **11**, 45–52 (2004).

79. Simmons, T. J. *et al.* Folding of xylan onto cellulose fibrils in plant cell walls revealed by solid-state NMR. *Nat. Commun.* **7**, 13902 (2016).

80. Knicker, H., Velasco-Molina, M. & Knicker, M. 2D Solid-State HETCOR ^{1}H-^{13}C NMR Experiments with Variable Cross Polarization Times as a Tool for a Better Understanding of the Chemistry of Cellulose-Based Pyrochars—A Tutorial. *Appl. Sci.* **11**, 8569 (2021).

81. King, A. W. T., Kilpeläinen, I., Heikkinen, S., Järvi, P. & Argyropoulos, D. S. Hydrophobic interactions determining functionalized lignocellulose solubility in dialkylimidazolium chlorides, as probed by ^{31}P NMR. *Biomacromolecules* **10**, 458–463 (2009).

82. Liebert, T., Hussain, M. A. & Heinze, T. Structure Determination of Cellulose Esters via Subsequent Functionalization and NMR Spectroscopy. *Macromol. Symp.* **223**, 79–92 (2005).

83. Goodlett, V. W., Dougherty, J. T. & Patton, H. W. Characterization of cellulose acetates by nuclear magnetic resonance. *J. Polym. Sci. A1* **9**, 155–161 (1971).

84. Kono, H., Hashimoto, H. & Shimizu, Y. NMR characterization of cellulose acetate: chemical shift assignments, substituent effects, and chemical shift additivity. *Carbohyd. Polym.* **118**, 91–100 (2015).

85. Ludwig, C. H., Nist, B. J. & McCarthy, J. L. Lignin. XIII. 1 The High Resolution Nuclear Magnetic Resonance Spectroscopy of Protons in Acetylated Lignins. *J. Am. Chem. Soc.* **86**, 1196–1202 (1964).

86. Nimz, H. H., Robert, D., Faix, O. & Nemr, M. Carbon-13 NMR Spectra of Lignins, 8. Structural Differences between Lignins of Hardwoods, Softwoods, Grasses and Compression Wood. *Holzforschung* **35**, 16–26 (1981).

87. Mansfield, S. D., Kim, H., Lu, F. & Ralph, J. Whole plant cell wall characterization using solution-state 2D NMR. *Nat. Protoc.* **7**, 1579–1589 (2012).

88. Jiang, N., Pu, Y. & Ragauskas, A. J. Rapid determination of lignin content via direct dissolution and ^{1}H NMR analysis of plant cell walls. *ChemSusChem* **3**, 1285–1289 (2010).

89. Wojdyr, M. Fityk: a general-purpose peak fitting program. *J. Appl. Crystallogr.* **43**, 1126–1128 (2010).

90. ANZMAG. (2014, June 06). *Introduction to the lectures series "Understanding NMR spectroscopy" by Dr James Keeler* [Video]. YouTube. https://www.youtube.com/watch?v=A502rWNKZyI.

91. Keeler, J. (2002). Understanding NMR Spectroscopy. [Learning Object]. https://doi.org/10.17863/CAM.968

92. UCI Media. (2011, November 30). *Lecture 7. Introduction to NMR Spectroscopy: Concepts and Theory, Part 1.* [Video]. YouTube. https://www.youtube.com/watch?v=vRHfYWg9GXM&list=PLC86CC98DDF0CDDAC&index=10.

93. Pretsch, E., Bühlmann, P. & Affolter, C. *Structure Determination of Organic Compounds.* (Springer-Verlag, Berlin/Heidelberg, 2000).

94. Organic Chemistry Data. *"Hans Reich's Collection. NMR Spectroscopy."* (last updated: 2020, February 14; accessed: 2022, March 29). Available at https://organicchemistrydata.org/hansreich/resources/nmr/?index=nmr_index%2F1H_shift.

95. Ruokonen, S.-K. *et al.* Correlation between Ionic Liquid Cytotoxicity and Liposome-Ionic Liquid Interactions. *Chem. Eur. J.* **24**, 2669–2680 (2018).

96. Marren, K. Dimethyl sulfoxide: an effective penetration enhancer for topical administration of NSAIDs. *Physician Sportsmed.* **39**, 75–82 (2011).

97. Wu, D. H., Chen, A. D. & Johnson, C. S. An Improved Diffusion-Ordered Spectroscopy Experiment Incorporating Bipolar-Gradient Pulses. *J. Magn. Reson. Ser. A* **115**, 260–264 (1995).

98. Willker, W., Leibfritz, D., Kerssebaum, R. & Bermel, W. Gradient selection in inverse heteronuclear correlation spectroscopy. *Magn. Reson. Chem.* **31**, 287–292; (1993).

99. Palmer, A. G., Cavanagh, J., Wright, P. E. & Rance, M. Sensitivity improvement in proton-detected two-dimensional heteronuclear correlation NMR spectroscopy. *J. Magn. Reson.* **93**, 151–170 (1991).

100. Kay, L., Keifer, P. & Saarinen, T. Pure absorption gradient enhanced heteronuclear single quantum correlation spectroscopy with improved sensitivity. *J. Am. Chem. Soc.* **114**, 10663–10665 (1992).

101. Schleucher, J. *et al.* A general enhancement scheme in heteronuclear multidimensional NMR employing pulsed field gradients. *J. Biomol. NMR* **4**, 301–306 (1994).

102. Bax, A. & Summers, M. F. Proton and carbon-13 assignments from sensitivity-enhanced detection of heteronuclear multiple-bond connectivity by 2D multiple quantum NMR. *J. Am. Chem. Soc.* **108**, 2093–2094 (1986).

103. Kono, H., Oka, C., Kishimoto, R. & Fujita, S. NMR characterization of cellulose acetate: Mole fraction of monomers in cellulose acetate determined from carbonyl carbon resonances. *Carbohyd. Polym.* **170**, 23–32 (2017).

104. Kono, H., Fujita, S. & Tajima, K. NMR characterization of methylcellulose: Chemical shift assignment and mole fraction of monomers in the polymer chains. *Carbohyd. Polym.* **157**, 728–738 (2017).

105. Hosoya, T., Bacher, M., Potthast, A., Elder, T. & Rosenau, T. Insights into degradation pathways of oxidized anhydroglucose units in cellulose by *β*-alkoxy-elimination: a combined theoretical and experimental approach. *Cellulose* **25**, 3797–3814 (2018).

106. Isogai, A., Hänninen, T., Fujisawa, S. & Saito, T. Review: Catalytic oxidation of cellulose with nitroxyl radicals under aqueous conditions. *Prog. Polym. Sci.* **86**, 122–148 (2018).

107. Li, M.-C., Mei, C., Xu, X., Lee, S. & Wu, Q. Cationic surface modification of cellulose nanocrystals: Toward tailoring dispersion and interface in carboxymethyl cellulose films. *Polymer* **107**, 200–210 (2016).

108. El-Faham, A. & Albericio, F. Peptide coupling reagents, more than a letter soup. *Chem. Rev.* **111**, 6557–6602 (2011).

109. Mackin, R. T. *et al.* Synthesis and characterization of TEMPO-oxidized peptide-cellulose conjugate biosensors for detecting human neutrophil elastase. *Cellulose* **29**, 1293–1305 (2022).

110. Kilpeläinen, I. et al. Dissolution of wood in ionic liquids. *J. Agr. Food Chem.* **55**, 9142–9148 (2007).

111. Kyllönen, L. *et al.* On the solubility of wood in non-derivatising ionic liquids. *Green Chem.* **15**, 2374–2378 (2013).

112. Fiskari, J. *et al.* Deep Eutectic Solvent Delignification to Low-energy Mechanical Pulp to Produce Papermaking Fibers. *Bioresources* **15**, 6023–6032 (2020).

113. Pérez, A. D., Fiskari, J. & Schuur, B. Delignification of Low-Energy Mechanical Pulp (Asplund Fibers) in a Deep Eutectic Solvent System of Choline Chloride and Lactic Acid. *Front. Chem.* **9**, 688291 (2021).

FIGURES

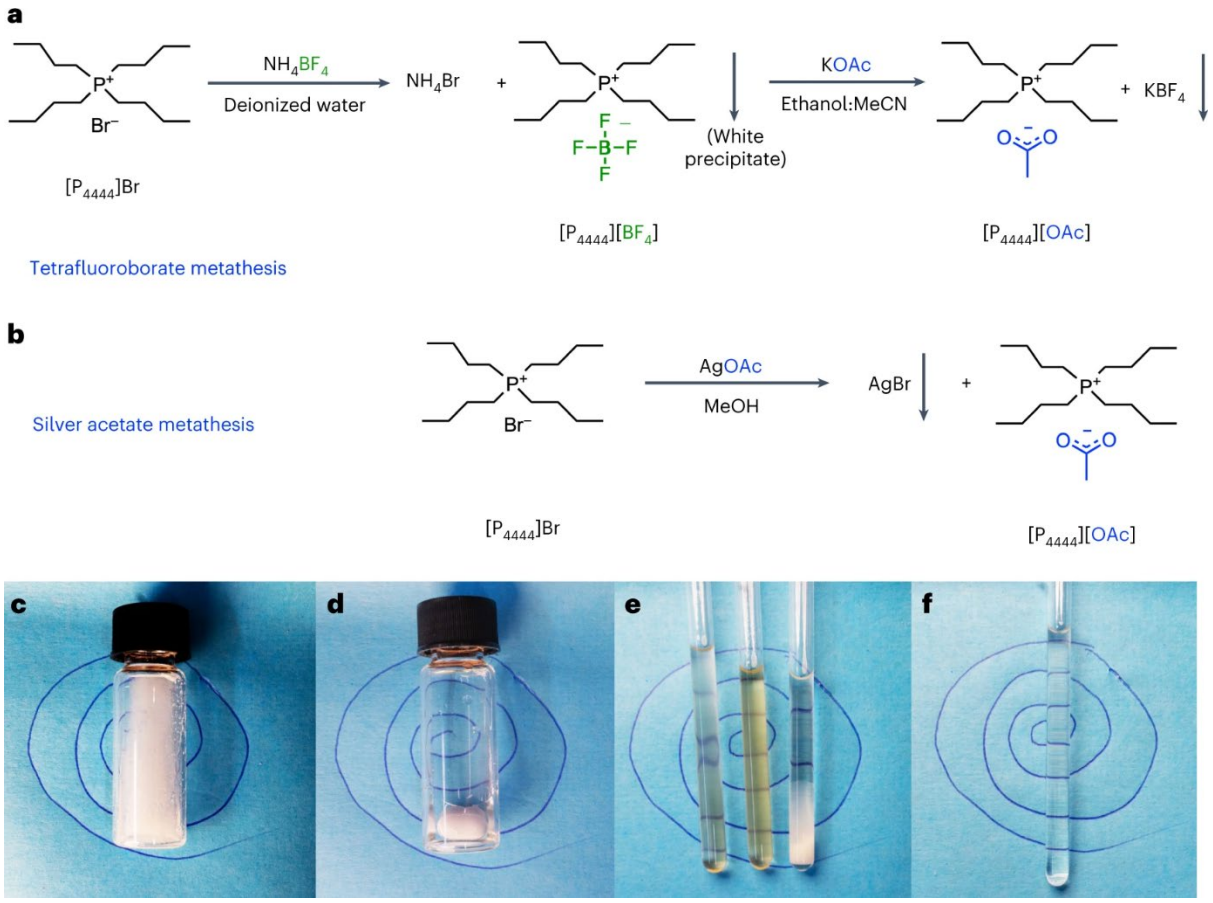

Fig. 1. Preparation of the ionic liquid (IL) electrolyte [P_{4444}][OAc]:DMSO-d_6 (1:4 wt%) and dissolution of cellulose samples. **(a)** Metathesis steps in the synthesis of [P_{4444}][OAc], using ammonium tetrafluoroborate and potassium acetate; **(b)** metathesis steps in the synthesis of [P_{4444}][OAc], using silver acetate. Photographs of the dissolution steps during sample preparation for NMR measurement: (**c**) Undissolved cellulosic sample after addition of the prepared [P_{4444}][OAc]:DMSO-d_6 stock electrolyte. (**d**) Fully dissolved sample after 18 h of stirring at 65 °C. (**e**) Examples of partly and/or undissolved samples in 5 mm NMR tubes, which will give suboptimal spectra, provided that acquisition is possible at all. (**f**) An example of a fully soluble sample, in a 5 mm NMR tube, ready for NMR measurement. Note: the colour of measurable samples can vary, depending on the investigated compound.

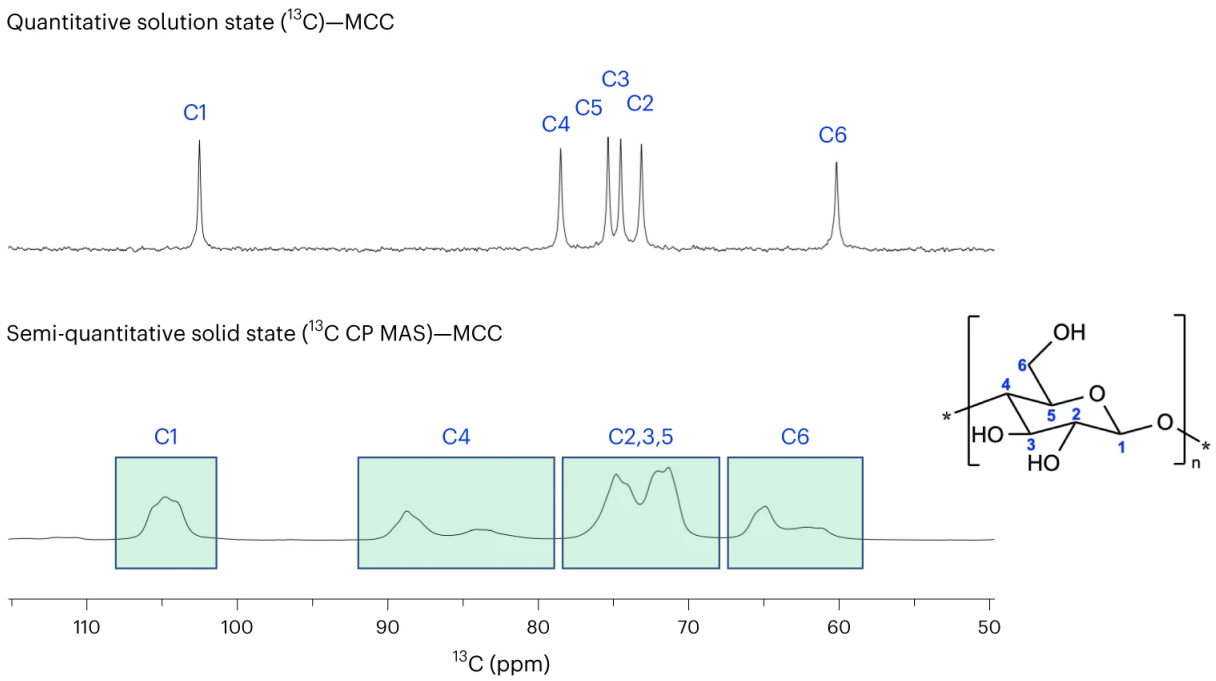

Fig. 2. Comparison of the obtainable resolution in cellulose NMR investigation of the presented quantitative solution-state NMR protocol and commonly performed solid-state CP MAS NMR protocol for MCC (Avicel® PH-101). **Top**: *Quantitative* solution-state ^{13}C NMR spectrum (5 wt% MCC in [P_{4444}][OAc]:DMSO-d_6 (1:4 wt%), 150 MHz, probe temp. = 65 °C, 8192 transients, 16 h collection time, 6 s relaxation delay for a 30° pulse flip angle, pulseprog = 'zgig30', exponential line broadening = 10 Hz). **Bottom**: *Semi-quantitative* solid-state ^{13}C NMR spectrum (MCC hydrated with 40 wt% water, 125 MHz, probe temp. = RT, MAS rotor speed = 8 kHz, 2700 transients, 2 h collection time, 2.5 s relaxation delay, pulseprog = 'cp', exponential line broadening = 10 Hz).

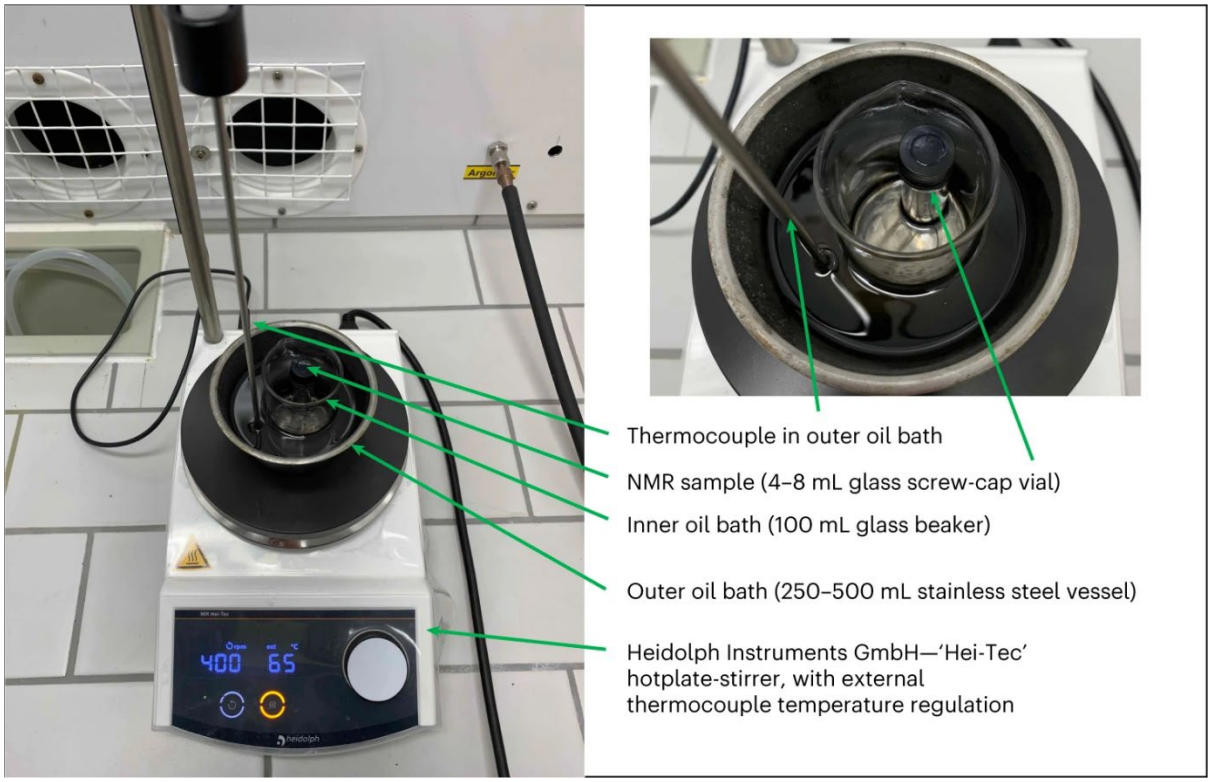

Fig. 3. Preferred dissolution setup for the NMR sample preparation.

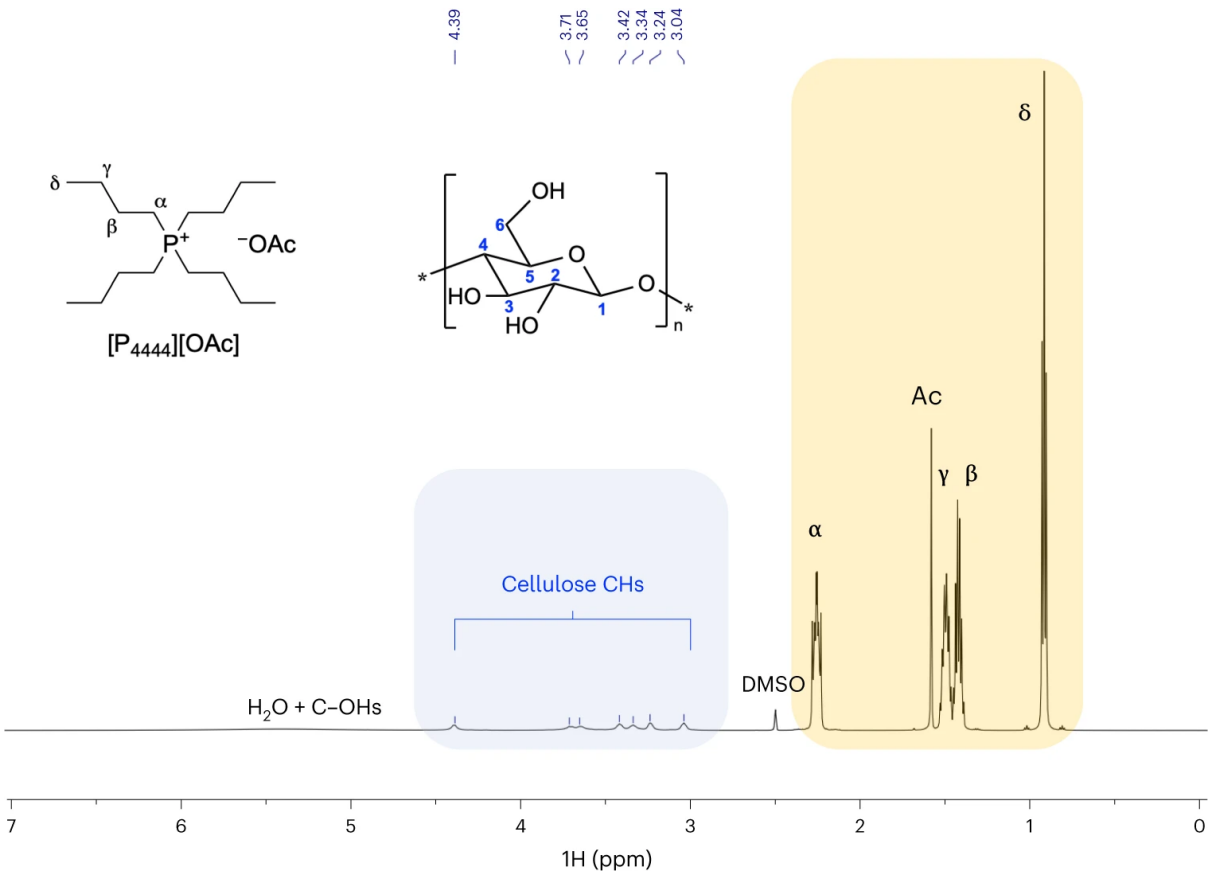

Fig. 4: Quantitative ^{1}H spectrum ([P_{4444}][OAc]:DMSO-d_6 1:4 wt%, 65 °C, 600 MHz) of MCC (Avicel® PH-101, 5 wt%) – full spectral region.

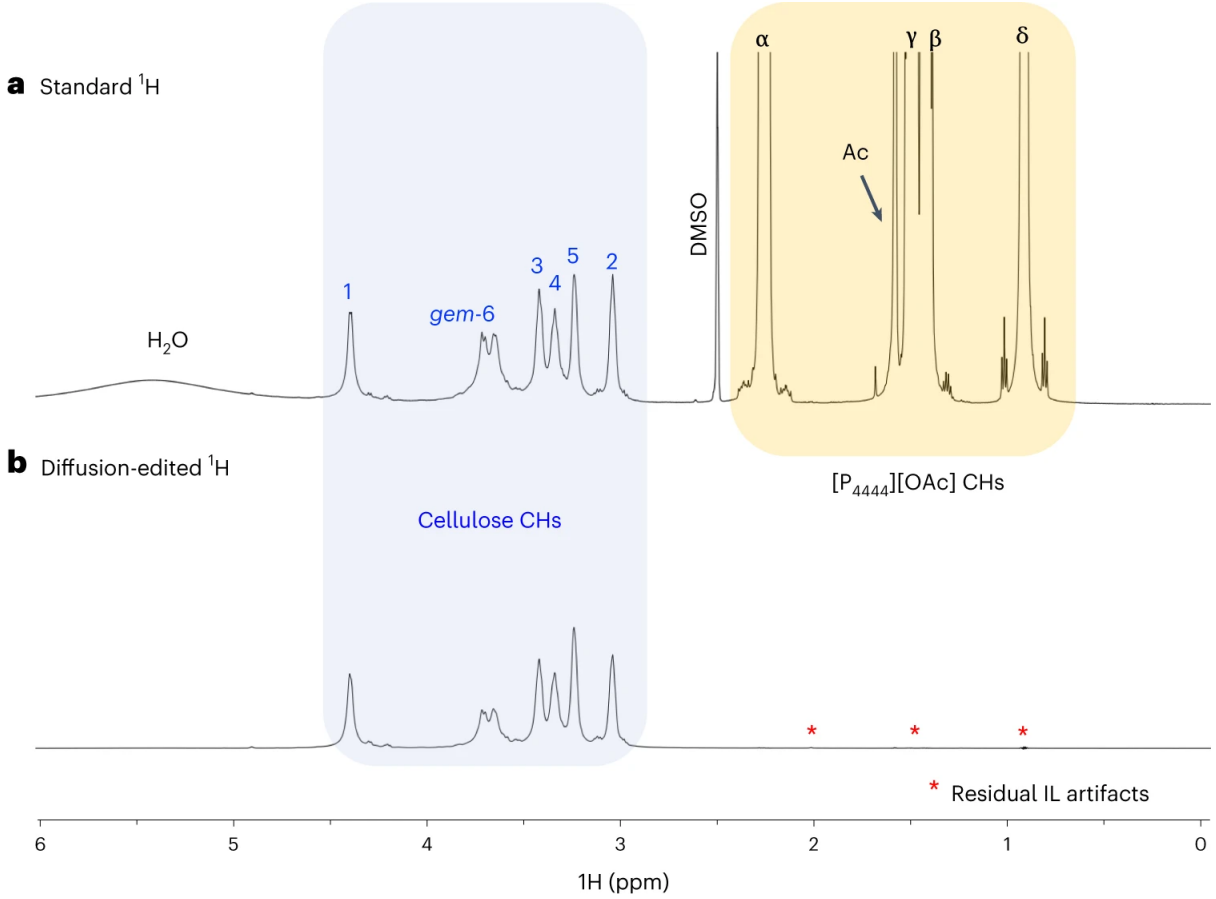

Fig. 5: Suppressing (editing-out) resonances of low molecular weight compounds in the ^{1}H spectra by diffusion-editing. Comparison of quantitative ^{1}H spectrum (**a**) and diffusion-edited ^{1}H spectrum (**b**) ([P_{4444}][OAc]:DMSO-d_6 1:4 wt%, 65 °C, 600 MHz) of MCC (Avicel® PH-101, 5 wt%).The spectral region from 6 -0 ppm is shown.

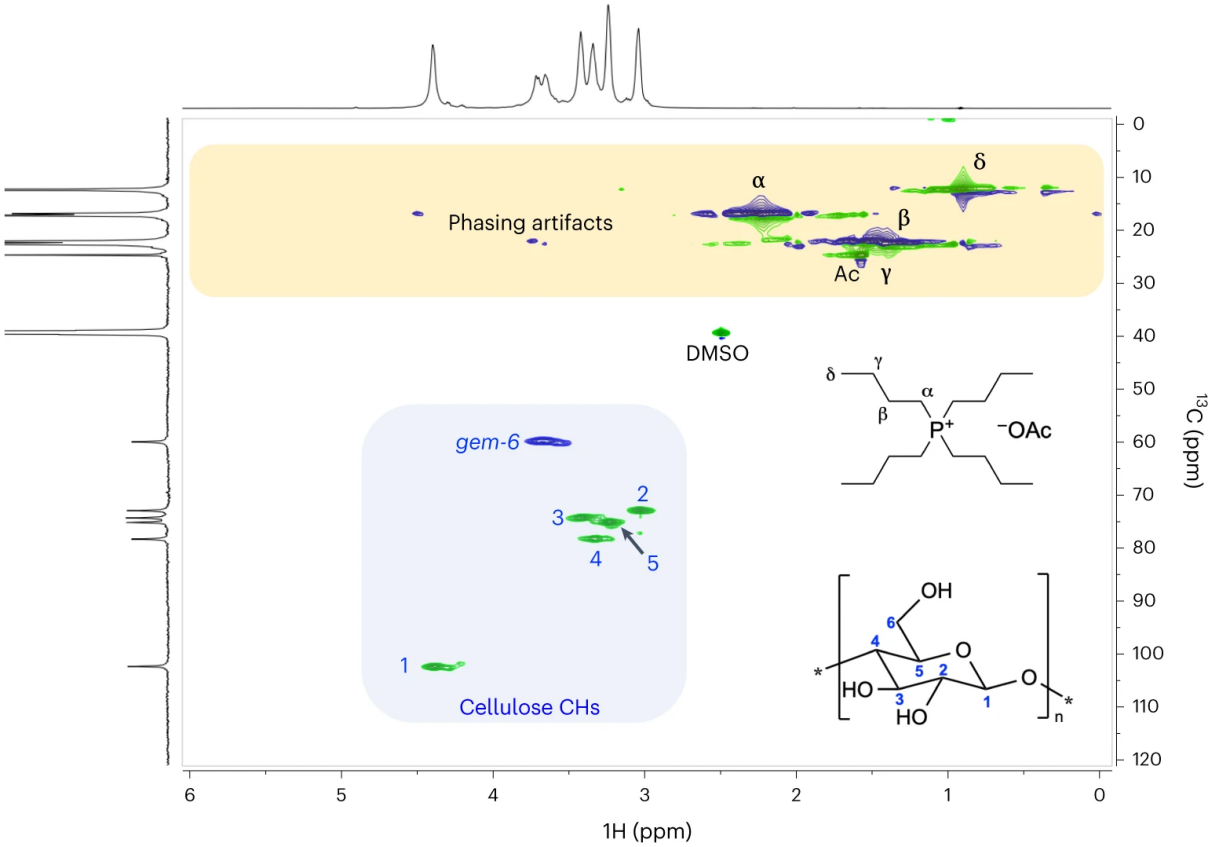

Fig. 6. Multiplicity-edited HSQC spectrum ([P_{4444}][OAc]:DMSO-d_6 1:4 wt%, 65 °C) of MCC (Avicel® PH-101, 5 wt%). CH_2 resonances are shown in blue, CH / CH_3 signals are shown in green. On top the diffusion-edited ^{1}H spectrum is shown and on the left the qualitative ^{13}C experiment was inserted.

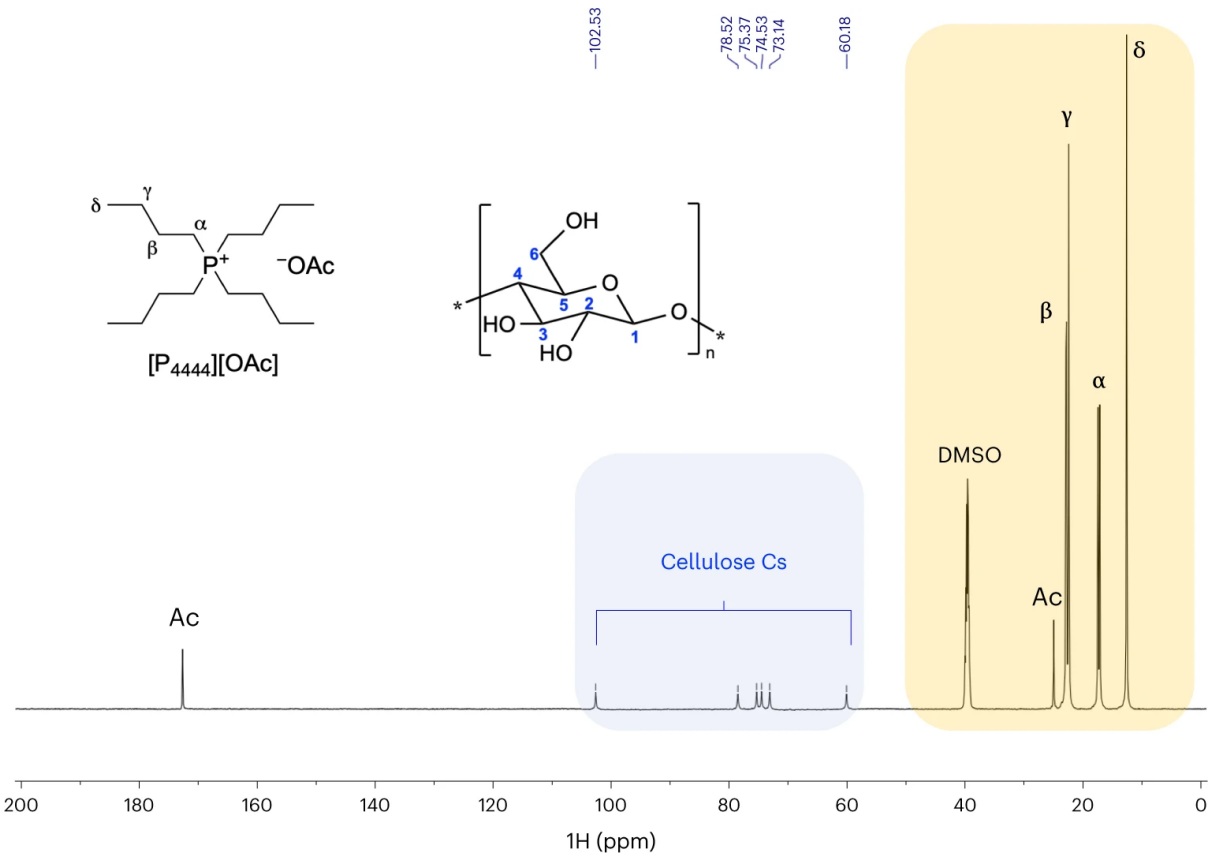

Fig. 7. Qualitative ^{13}C spectrum ([P_{4444}][OAc]:DMSO-d_6 1:4 wt%, 65 °C, 150 MHz) of MCC (Avicel® PH-101, 5 wt%) – full spectral region.

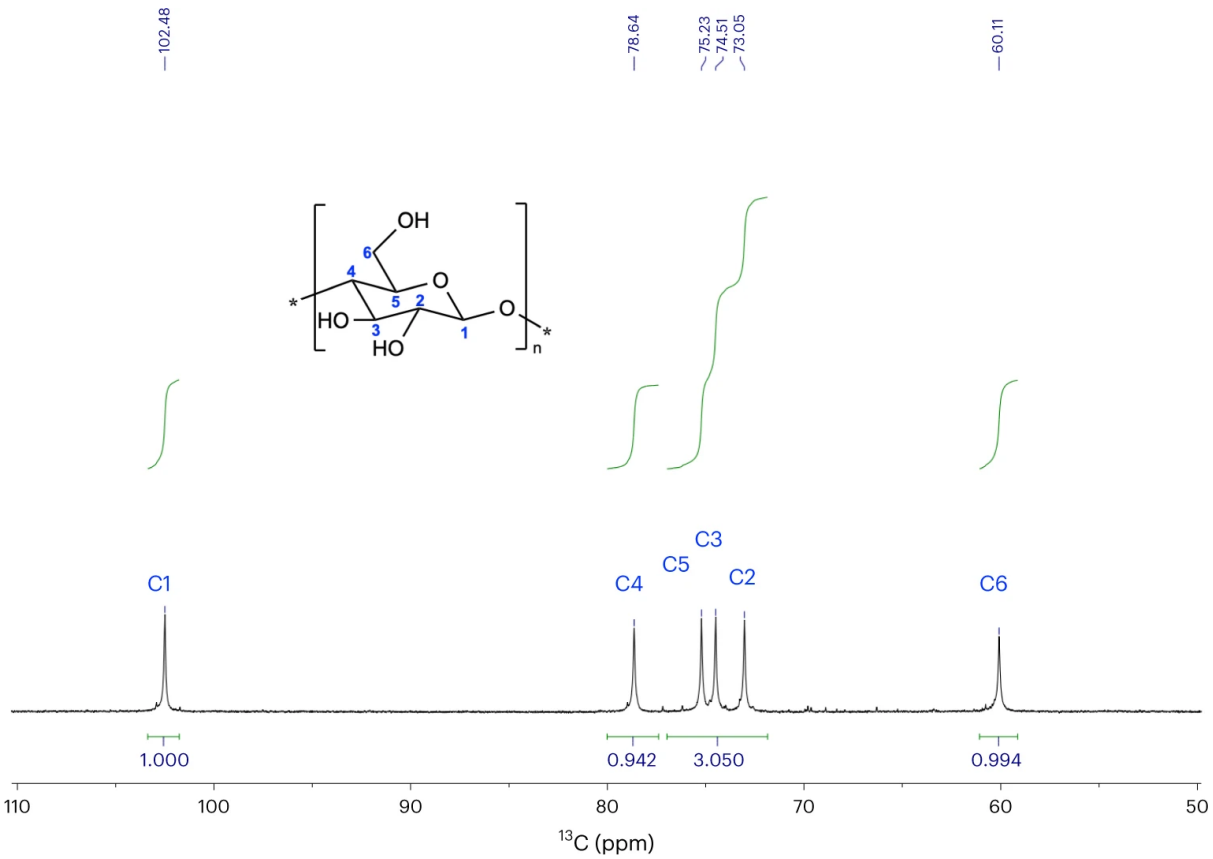

Fig. 8. Quantitative ^{13}C spectrum ([P_{4444}][OAc]:DMSO-d_6 1:4 wt%, 65 °C, 150 MHz) of MCC (Avicel® PH-101, 5 wt%). The spectral region of the cellulose backbone is shown.

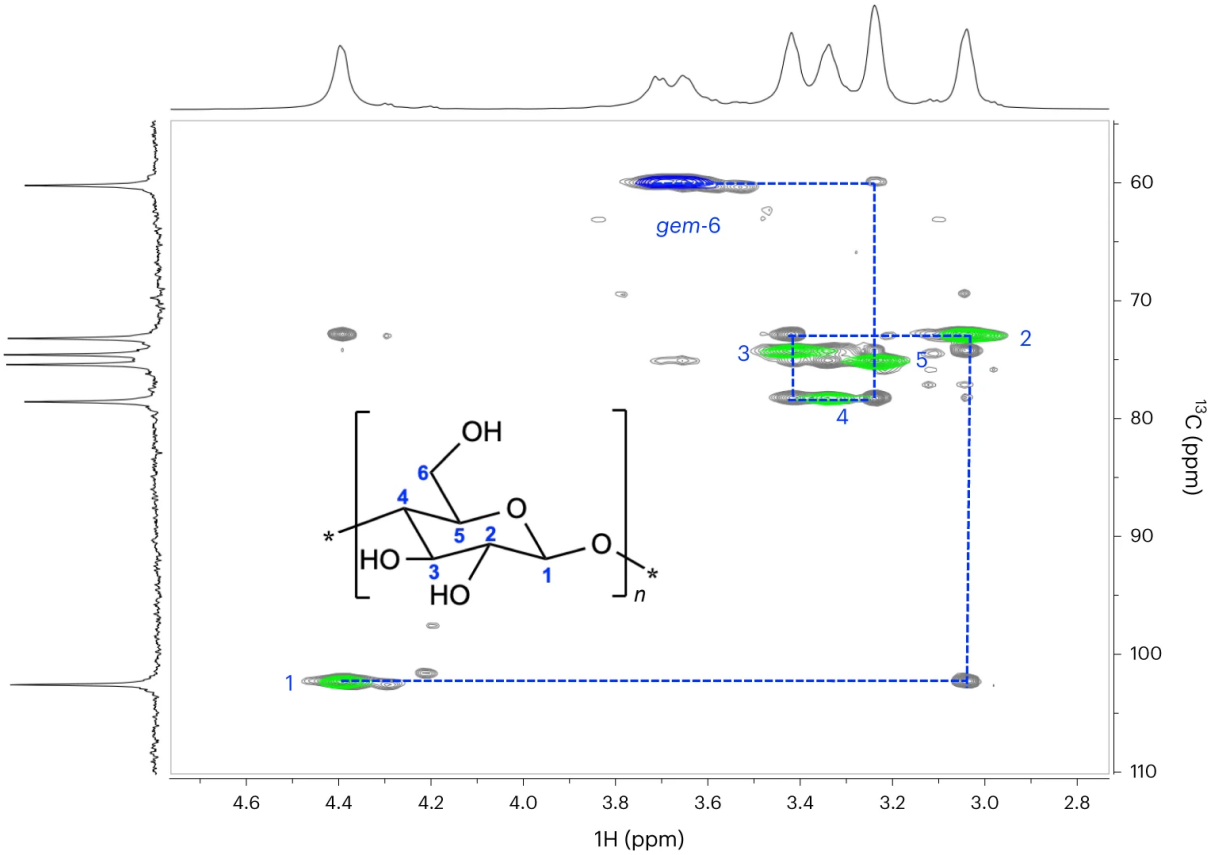

Fig. 9: HSQC-TOCSY spectrum (short-range, 15 ms TOCSY mixing time) with a multiplicity-edited HSQC overlay ([P_{4444}][OAc]:DMSO-d_6 1:4 wt%, 65 °C) of MCC (Avicel® PH-101, 5 wt%). CH_2 resonances are shown in blue, CH signals in green and TOCSY correlations in grey. The blue lines and numerical positional assignments are introduced to illustrate how the spin-system can be traced and assigned through the TOCSY correlations. The spectral region of the cellulose backbone is shown.

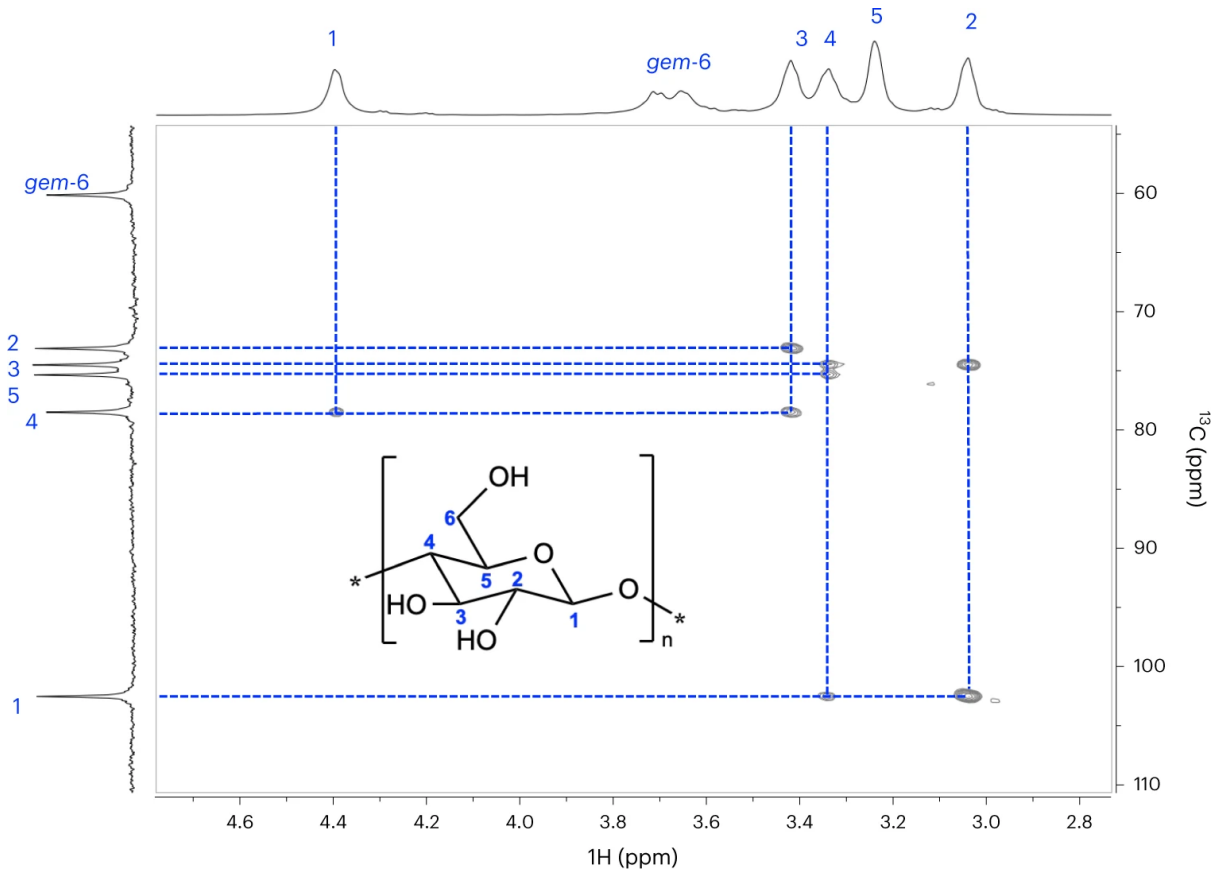

Fig. 10: HMBC spectrum ([P_{4444}][OAc]:DMSO-d_6 1:4 wt%, 65 °C) of MCC (Avicel® PH-101, 5 wt%). HMBC correlations are shown in grey, the blue lines and numerical positional assignments are introduced to illustrate how the spin-system can be traced and assigned. The spectral region of the cellulose backbone is shown.

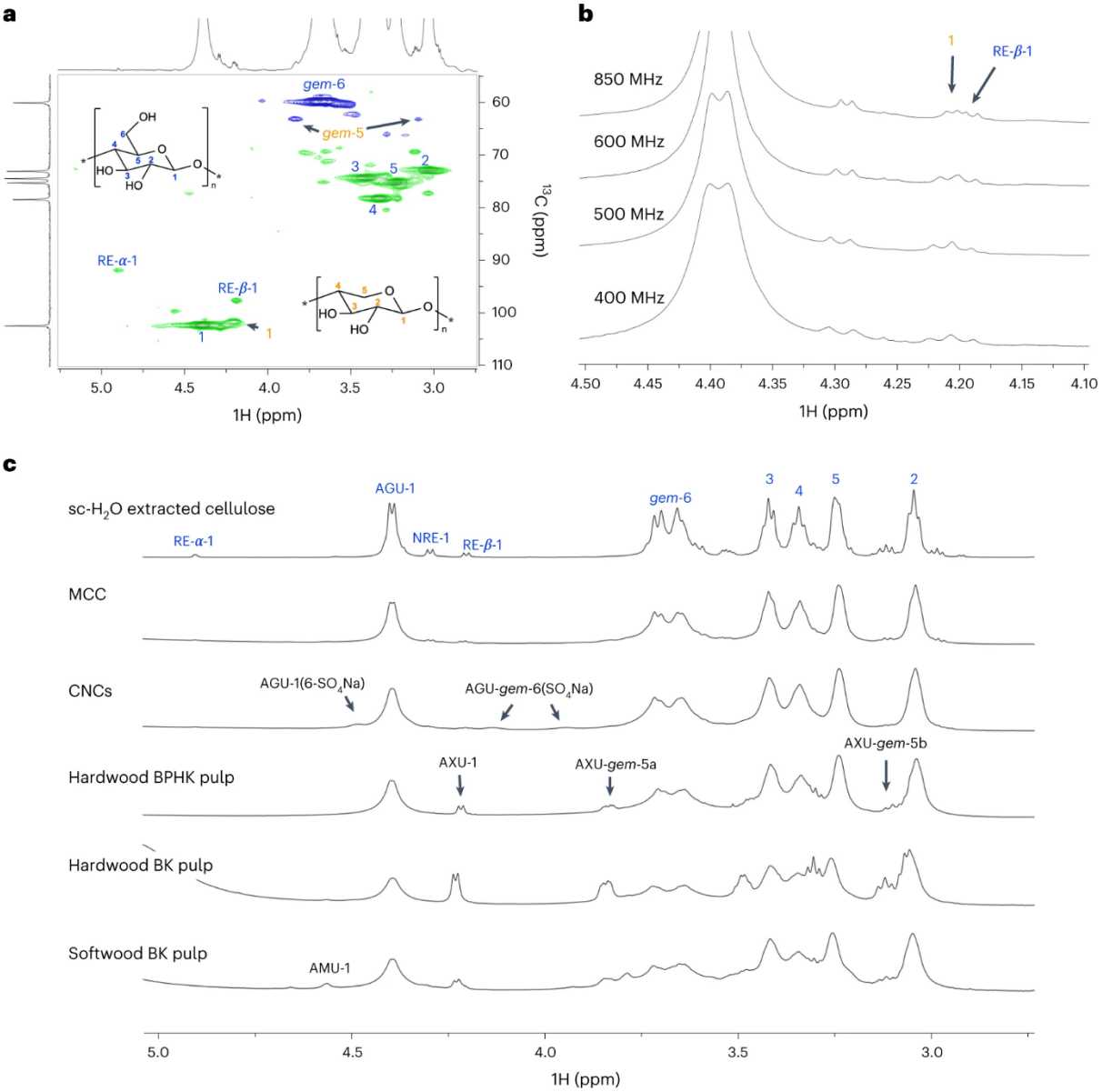

Fig. 11. Resolution of key signals in the technical cellulose backbone spectral regions. (**a**) Multiplicity-edited HSQC for MCC (1 transient using a cryoprobe and 850 MHz ^{1}H-frequency spectrometer, 65 °C; green = CH, blue = CH_2), (**b**) H1 region for MCC at different ^{1}H spectrometer frequencies at 65 °C, (**c**) Comparison of different pulp samples using ^{1}H NMR (600 MHz ^{1}H-frequency, 65 °C); AGU – anhydroglucose unit, AXU – anhydroxylose unit, AMU – anhydromannose unit, BPHK – bleached pre-hydrolysis kraft, BK – bleached kraft, sc – super/sub-critical.

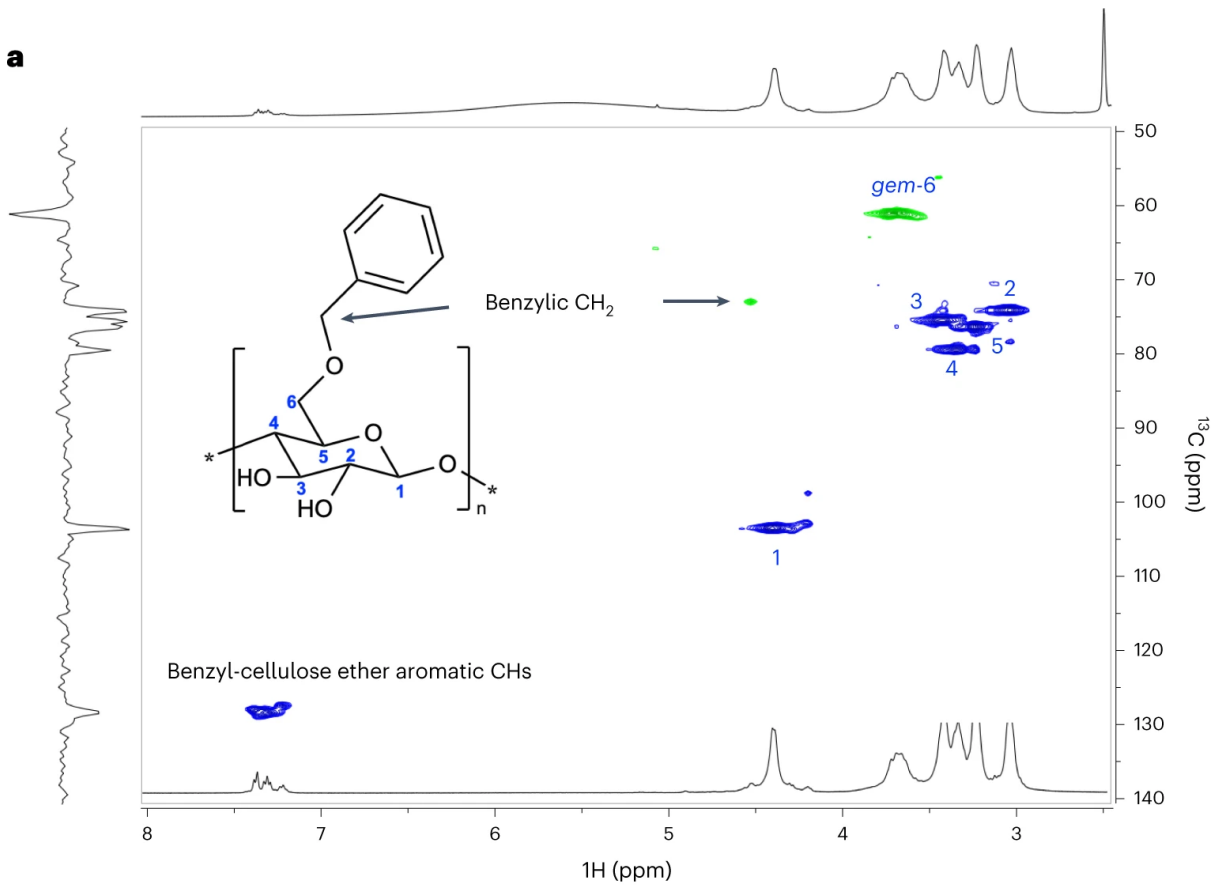
a
gem-6
Benzylic CH2
Benzyl-cellulose ether aromatic CHs
1H (ppm)
13C (ppm)

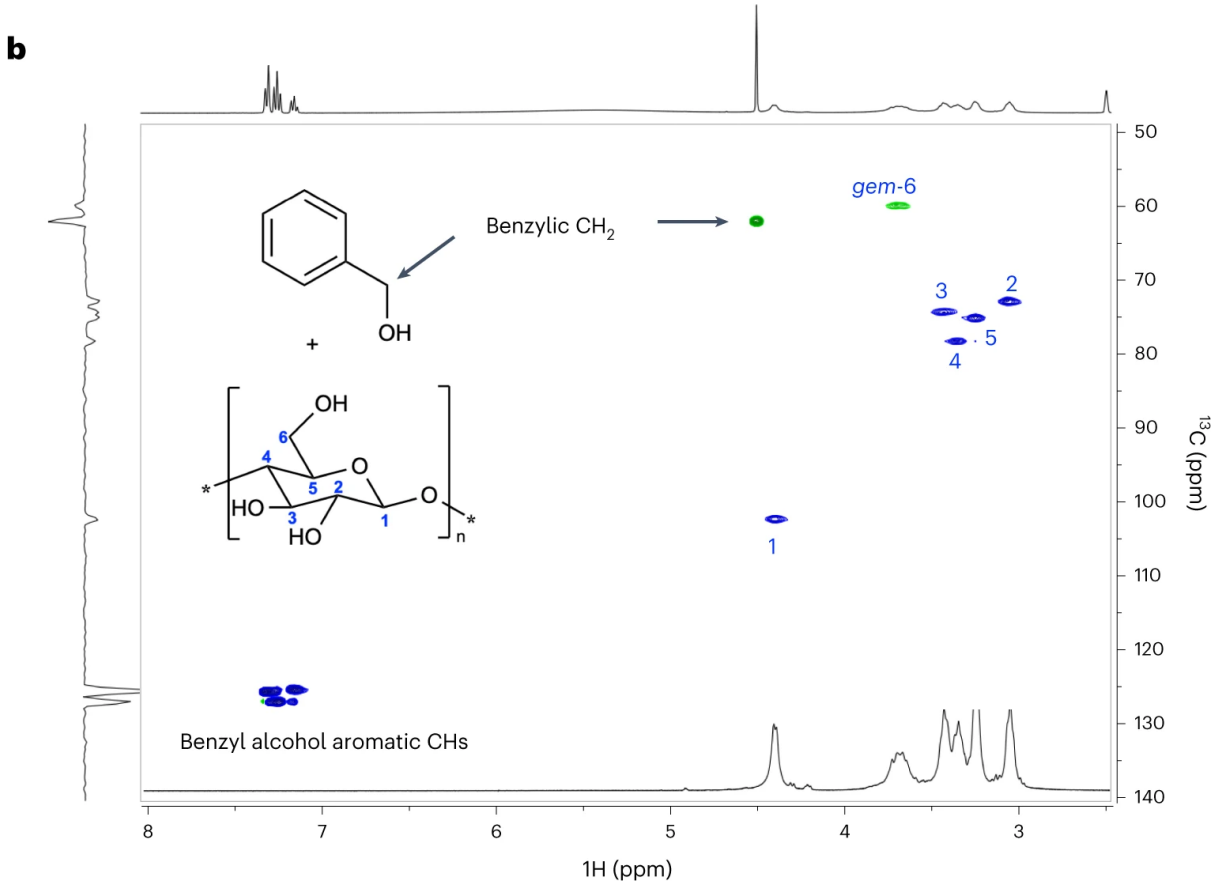
b
gem-6
Benzylic CH2
Benzyl alcohol aromatic CHs
1H (ppm)
13C (ppm)

2083

2084 **Fig. 12.** Application of the initial NMR experiments to distinguish between covalent
2085 modifications and impurities in cellulose chemistry. Multiplicity-edited HSQC with ^{1}H
2086 trace (top trace) and diffusion-edited ^{1}H trace (bottom trace) for (**a**) MCC (Avicel® PH-
2087 101) covalently modified through surface grafting with benzylbromide and (**b**) MCC
2088 doped with benzyl alcohol (Spectra obtained using: $[P_{4444}]$[OAc]:DMSO-d_6 1:4 wt%, 65
2089 °C, 5 wt%; 400 MHz ^{1}H frequency).
2090

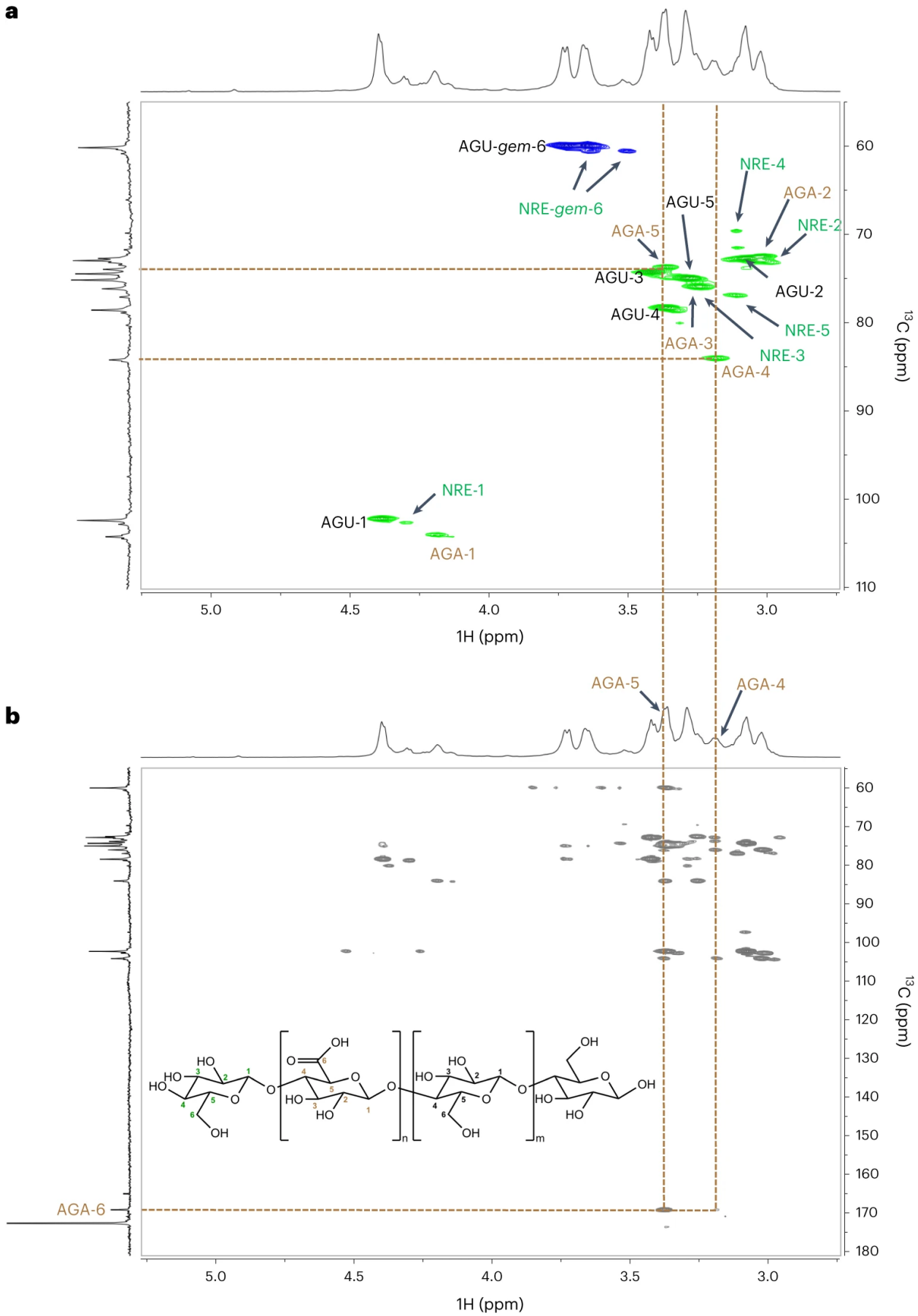
a
AGU-gem-6
NRE-gem-6
NRE-4
AGA-2
AGU-5
NRE-2
AGA-5
AGU-3
AGU-2
AGU-4
NRE-5
AGA-3
NRE-3
AGA-4
NRE-1
AGU-1
AGA-1
1H (ppm)
13C (ppm)
b
AGA-5
AGA-4
AGA-6
1H (ppm)
13C (ppm)

2091

2092 **Fig. 13.** Utility of single and multiple bond 2D heteronuclear correlated spectroscopy
2093 (HSQC & HMBC) in the assignment of a TEMPO-oxidised cellulose nanocrystal
2094 ([P_{4444}][OAc]:DMSO-d_6 1:4 wt%, 65 °C, 5 wt%, 600 MHz ^{1}H frequency):[26] (**a**) After
2095 modification of the CNC a new spin system in the multiplicity-edited HSQC becomes
2096 visible. However, as the introduced carboxylate functionality does not show a
2097 resonance in the HSQC experiment, the new peaks cannot ultimately be assigned to
2098 the AGA structure. (**b**) In the HMBC experiment clear interactions between the new
2099 spin system and a characteristic carboxylate peak become visible, allowing to assign
2100 the structure.Spectra shown with diffusion-edited ^{1}H trace (top trace) and ^{13}C trace
2101 (left trace). AGU = anhydroglucose unit; AGA = anhydroglucopyranosiduronic acid
2102 unit; NRE = non-reducing end; RE = reducing end. In the spectra HSQC correlations
2103 are shown in green (CH) and blue (CH_2).
2104

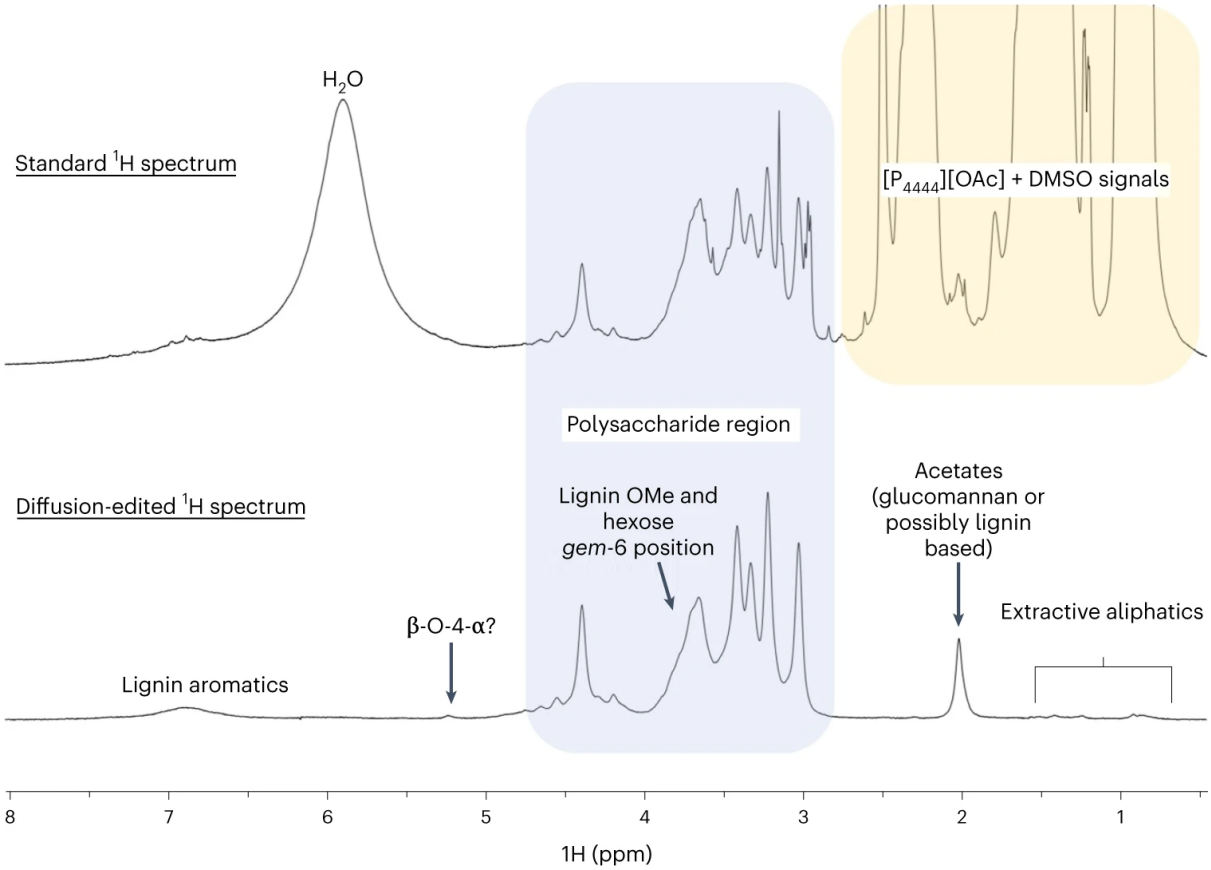

Fig. 14 ^{1}H and diffusion-edited ^{1}H spectra ([P_{4444}][OAc]:DMSO-d_6 1:4 wt%, 65 °C ,2.5 wt%, 600 MHz) for 'Asplund' wood (spruce fibres produced through low-energy thermomechanical refining).

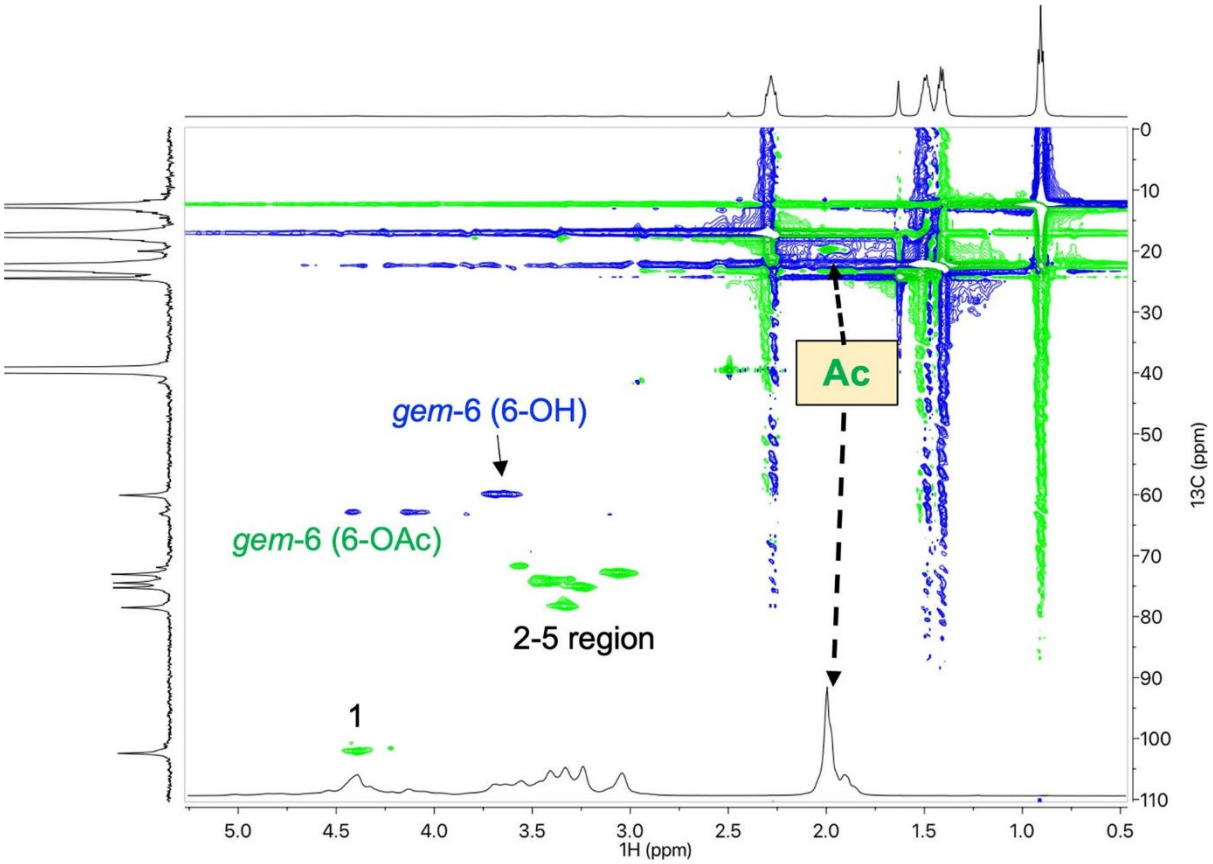

Extended Data Figure 1: Multiplicity-edited HSQC of acetylated MCC showing strong peak superposition ([P_{4444}][OAc]:DMSO-d_6 1:4 wt%, 65 °C, 5 wt%; 600 MHz ^{1}H frequency. For multiplicity edited HSQC green = CH, blue = CH_2).

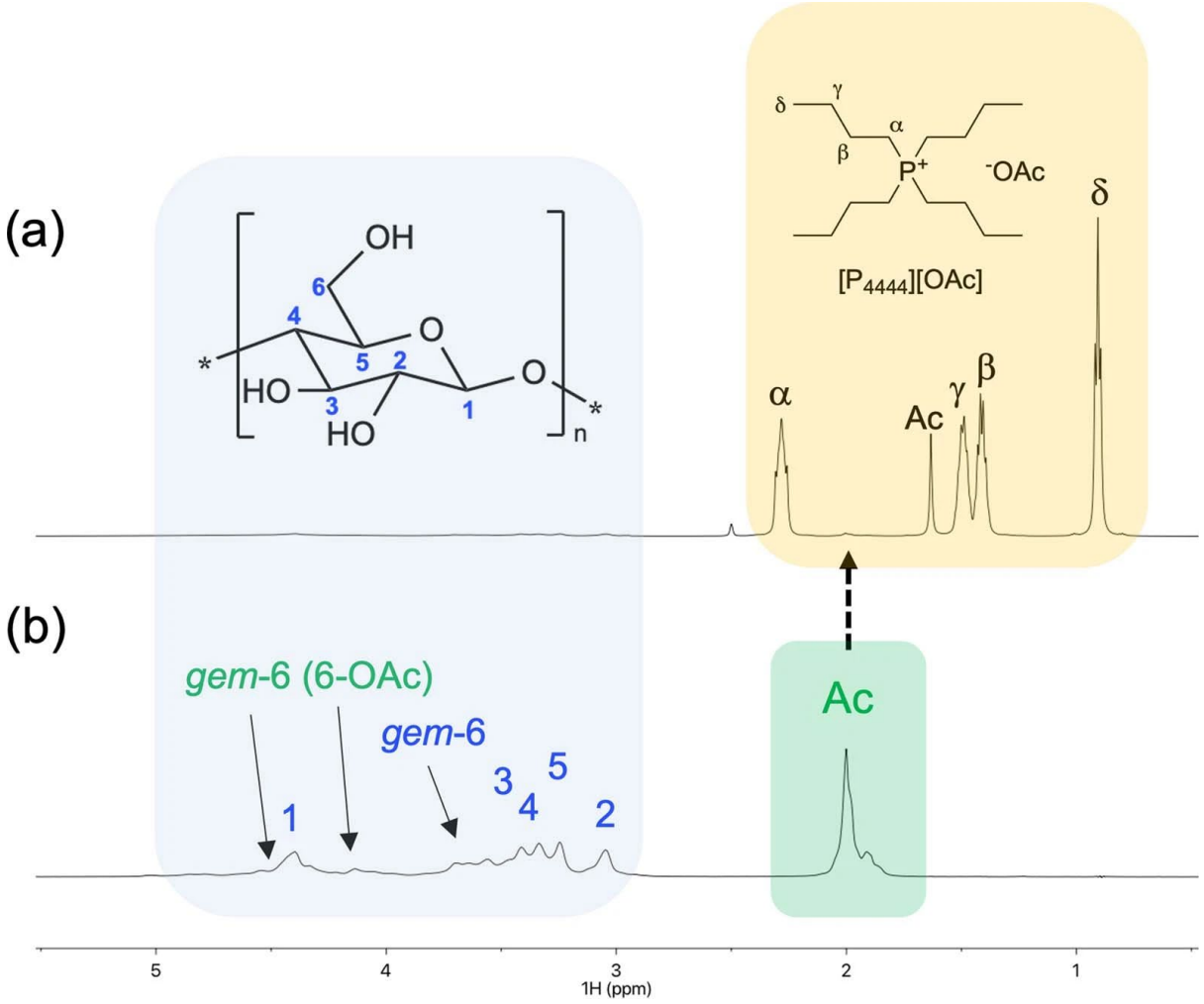

Extended Data Figure 2: Effect of diffusing-editing on the ^{1}H 1D data for surface acetylated MCC. Comparison of the quantitative ^{1}H spectrum (**a**) with the diffusion edited ^{1}H spectrum (**b**) allows to quickly assess the introduction of functionalities of species exhibiting resonances in the heavily crowded IL spectral region ([P_{4444}][OAc]:DMSO-d_6 1:4 wt%, 65 °C, 5 wt%; 600 MHz ^{1}H frequency).

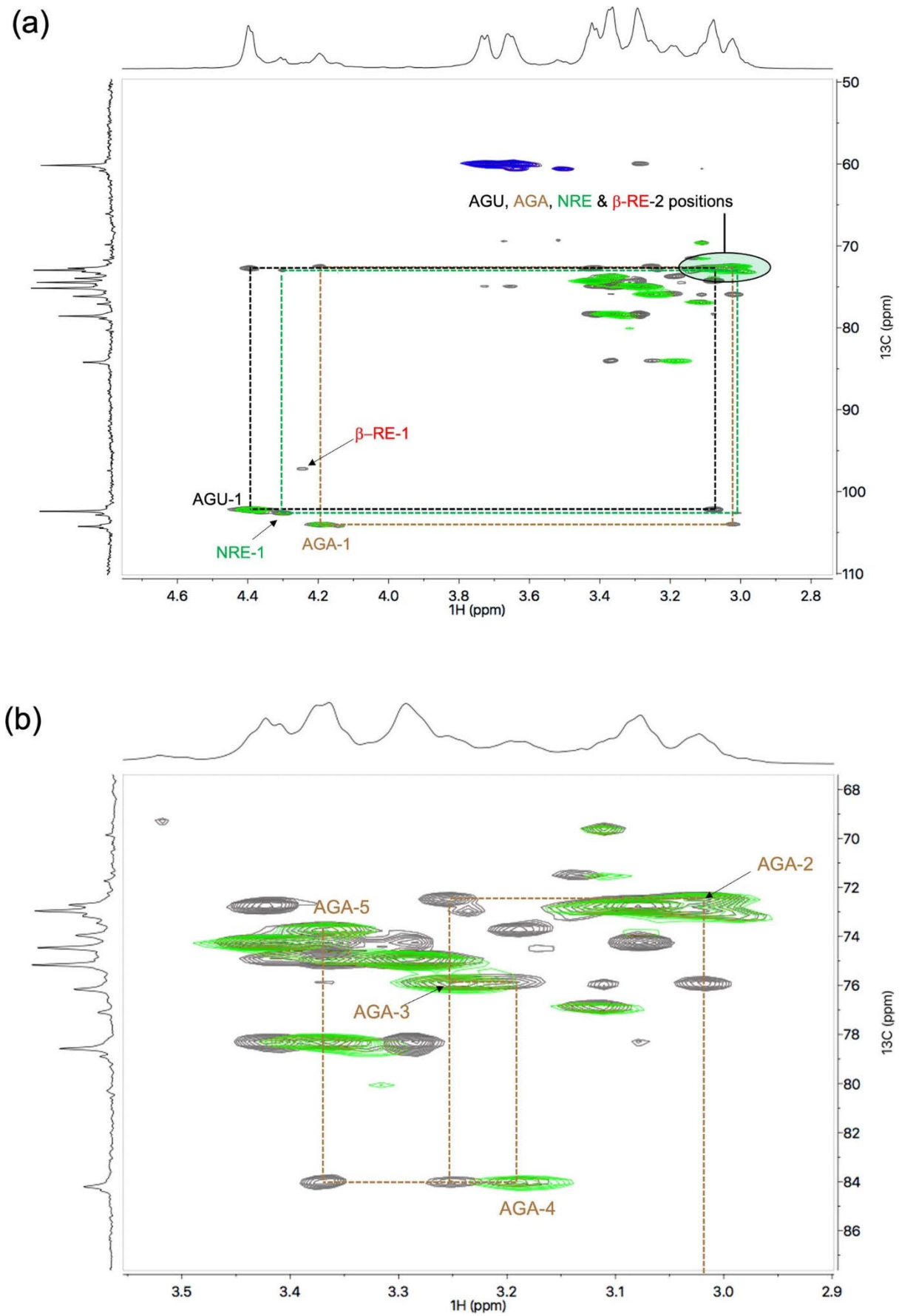
(a)
AGU, AGA, NRE & β-RE-2 positions
β–RE-1
AGU-1
NRE-1
AGA-1
13C (ppm)
1H (ppm)
(b)
AGA-2
AGA-5
AGA-3
AGA-4
13C (ppm)
1H (ppm)

2123

2124 **Extended Data Figure 3:** Utility of the 2D HSQC-TOCSY experiment for further peak
2125 assignment of cellulose derivatives. (**a**) HSQC-TOCSY in the full view allows to further
2126 assign the AGA moiety over interactions of the C1 signal with peaks in the crowded
2127 areas., (**b**) HSQC-TOCSY with zoom into the C2 - C5 region shows that full
2128 characterisation of the spin system can be possible. However, owing to strong
2129 superpositions with the AGU, NRE and RE moieties the peak assignments can
2130 become tedious. Spectra shown with diffusion-edited ^{1}H trace (top trace) and ^{13}C trace
2131 (left trace). AGU = anhydroglucose unit; AGA = anhydroglucopyranosiduronic acid
2132 unit; NRE = non-reducing end; RE = reducing end. In the spectra HSQC correlations
2133 are shown in green (CH) and blue (CH_2) and TOCSY correlations are shown in grey.
2134
2135

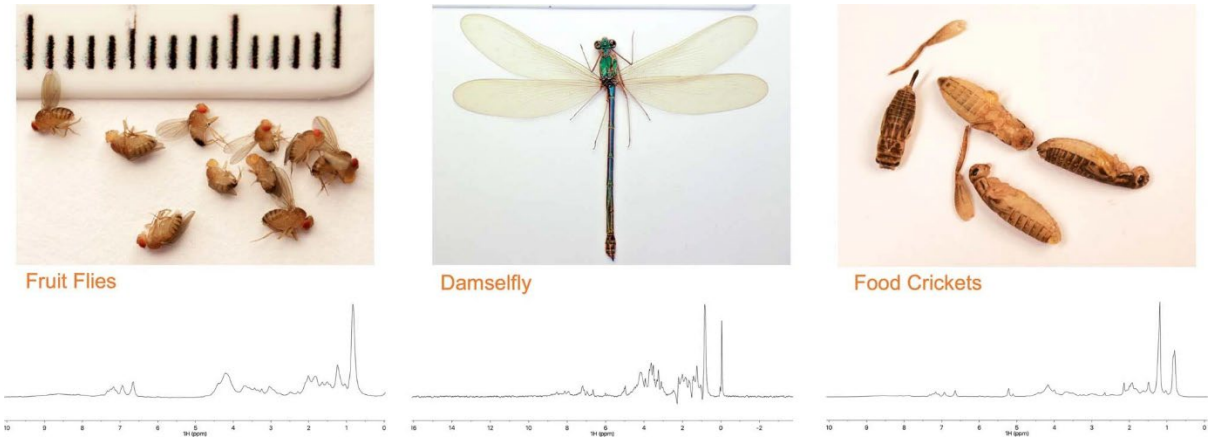

Extended Data Figure 4: Diffusion-edited ^{1}H spectra ([P_{4444}][OAc]:DMSO-d_6 1:4 wt%, 65 °C, 5 wt%, 600 MHz) for fruit flies, damselfly tail and whole food crickets, after Wiley milling and dissolution.